

This dissertation has been 62-3212
microfilmed exactly as received

DENISON, Gilbert W., 1929-
A STUDY OF THE VAPOR ATOMICITY
OF SOME METALS.

The University of Oklahoma, Ph.D., 1962
Chemistry, physical

University Microfilms, Inc., Ann Arbor, Michigan

THE UNIVERSITY OF OKLAHOMA

GRADUATE COLLEGE

A STUDY OF THE VAPOR ATOMICITY OF SOME METALS

A DISSERTATION

SUBMITTED TO THE GRADUATE FACULTY

in partial fulfillment of the requirements for the

degree of

DOCTOR OF PHILOSOPHY

BY

GILBERT W. DENISON

Norman, Oklahoma

1962

A STUDY OF THE VAPOR ATOMICITY OF SOME METALS

APPROVED BY

Andrew Coopers Jr.

J. Rud Nilsson

R.P. Hurst

C.M. Shepwick

W.R. Upton

DISSERTATION COMMITTEE

Abstract

The total vapor pressures and molecular weights of bismuth, antimony, sodium, lead, selenium, and indium vapors were determined by simultaneous measurements using the torsion-effusion and Knudsen mass loss methods. The vapors of bismuth, antimony, sodium, and selenium were found to contain more than one species in the vapor phase over the range of the measurements taken. The vapors of lead and indium were found to be monatomic. In the vapors where more than one species is present, the molecular weight was determined as a function of temperature thus allowing calculation of the vapor pressures of each species and the equilibrium constant K for the equilibrium between species.

The experimental measurements yielded: (1) total heats of vaporization, (2) the heats of vaporization of each species (where more than one was present), and (3) the heats of dissociation of the higher species; in addition to the total vapor pressures, molecular weights, vapor pressures of each species, and the equilibrium constants already mentioned.

A comparison of the equilibrium constants calculated from the experimental data with the values predicted by statistical mechanics using spectroscopic data is presented where the spectroscopic data is sufficient for the comparison.

ACKNOWLEDGEMENTS

The author expresses his sincere appreciation to Professor Andrew Cosgarea, Jr. for his interest, valuable suggestions, and contribution of time: and to the other members of the doctoral committee, Associate Dean C. M. Slipevich, Professor W. R. Upthegrove, Professor J. R. Nielsen, and Professor R. P. Hurst for their contributions.

The author is indebted to Mr. Albert Wilson for his guidance and liberal contribution of time in the development of the circuitry for the automatic recording and controlling microbalance system.

The author expresses his gratitude to Professor Sherril Christian for his assistance in teaching the author how to work quartz rods and fibers used in constructing the microbalance.

The author also acknowledges the contributions of Messrs. Harvey Doering and Thomas Woods for their aid and advice on equipment problems.

The author also wishes to acknowledge the financial support of the National Science Foundation whose grant made this work possible.

TABLE OF CONTENTS

	Page
LIST OF TABLES.....	vi
LIST OF ILLUSTRATIONS.....	vii
Chapter	
I. INTRODUCTION.....	1
II. THEORETICAL.....	13
III. EXPERIMENTAL.....	20
IV. RESULTS.....	43
V. DISCUSSION.....	78
VI. CONCLUSIONS.....	90
BIBLIOGRAPHY.....	92
APPENDICES.....	94

LIST OF TABLES

Table	Page
I. Calibration of Mass Effusion Rate.....	37
II. Calculation of the Torsion Constant from Data.	38
III. Comparison of K_p Values for Bismuth.....	51
IV. Comparison of K_p Values for Sodium.....	66
V. Heats of Vaporization and Dissociation of Bismuth.....	80
VI. Heats of Vaporization and Dissociation of Antimony.....	82
VII. Heat of Vaporization of Lead.....	84
VIII. Heats of Vaporization and Dissociation of Sodium.....	87
IX. Heats of Vaporization and Dissociation of Selenium.....	87

LIST OF ILLUSTRATIONS

Figure	Page
1. Experimental Apparatus.....	26
2. Effusion Cell.....	27
3. Quartz Microbalance.....	27
4. Flow Diagram of the Microbalance System.....	30
5. Detector Unit.....	32
6. Controller Unit.....	33
7. Total Vapor Pressure of Bismuth.....	44
8. Vapor Pressure of Bi.....	46
9. Vapor Pressure of Bi ₂	47
10. Equilibrium Constant Bi - Bi ₂	48
11. Correlation of K _p for Bismuth.....	50
12. Total Vapor Pressure of Antimony.....	52
13. Vapor Pressure of Sb ₂	53
14. Vapor Pressure of Sb ₄	54
15. Equilibrium Constant Sb ₂ - Sb ₄	56
16. Correlation of K _p for Antimony.....	57
17. Total Vapor Pressure of Lead.....	59
18. Total Vapor Pressure of Sodium.....	60
19. Vapor Pressure of Na.....	62
20. Vapor Pressure of Na ₂	63
21. Equilibrium Constant Na - Na ₂	64
22. Correlation of K _p for Sodium.....	65

LIST OF ILLUSTRATIONS

Figure		Page
23.	Total Vapor Pressure of Selenium.....	67
24.	Vapor Pressure of Se_2	69
25.	Vapor Pressure of Se_6	70
26.	Equilibrium Constant $\text{Se}_2 - \text{Se}_6$	72
27.	Total Vapor Pressure of Indium.....	74
28.	Measured Pressure vs. Orifice Diameter.....	76
29.	Measured Pressure vs. Orifice Length.....	77
30.	Comparison of Bismuth Vapor Pressures.....	79
31.	Comparison of Antimony Vapor Pressures.....	81
32.	Comparison of Lead Vapor Pressures.....	83
33.	Comparison of Sodium Vapor Pressures.....	85
34.	Comparison of Selenium Vapor Pressures.....	86
35.	Comparison of Indium Vapor Pressures.....	89

A STUDY OF THE VAPOR ATOMICITY OF SOME METALS

CHAPTER I

INTRODUCTION

Measurement of Vapor Pressure

The experimental techniques which have been used to determine the vapor pressure of metals can be divided into two classes according to the pressure range being investigated:

(a) High vapor pressures in the range of 10^{-1} to 10^3 mm Hg have been determined by direct manometric methods, by observance of condensation points of vapors mixed with inert gases at various pressures, and by vapor-transport techniques.

(b) Low pressure methods that are valid in the pressure range of 10^{-8} to 10^{-2} mm Hg include rate of sublimation, rate of evaporation, rate of effusion, and torsion-effusion.

The high pressure methods are only applicable at comparatively high temperatures in the case of metals; thus the low pressure methods are the most frequently used to investigate the vapor pressures of metals.

Most low pressure methods require a knowledge of the atomicity of the vapor in order to calculate the vapor pressure since a mass loss is measured and not a force.

Thus, the requirement of knowing the molecular weight of the vapor as a function of temperature is inevitable. A different approach to measuring the rate of effusion of vapors has been utilized successfully by several investigators (20, 29, 32). This approach consists of measuring the force exerted by effusing vapors and is known as the torsion effusion method. In order to determine this force the sample is enclosed in an effusion cell which is suspended on a torsion fiber and the vapor is allowed to effuse in a horizontal direction from two eccentrically located holes in the cell, thus exerting a torque. The angle through which the cell is deflected is observed and the vapor pressure is calculated from the equation:

$$P = \frac{2\tau\alpha}{(a_1q_1 + a_2q_2)} \quad (1)$$

where P is the total vapor pressure (dynes/cm²), τ is the torsion constant of the fiber (dyne-cm/rad), α is the angle of deflection (rad.), a_1 and a_2 are the cross-sectional areas of the holes (cm²), and q_1 and q_2 are the horizontal distances of the holes from the suspension point (cm).

Vapor Atomicity

There are a number of metals which are known to have more than one species in the vapor state. It is observed that the atomicity or molecular weight of these vapors is a function of temperature. One is thus led to the conclusion that there is an equilibrium between the various species present in the vapor. In the case where monatomic and diatomic species are present

in the vapor the equilibrium can be expressed by the equation: $2A_1 \rightleftharpoons A_2$. The equilibrium constant for this reaction could be written as $K = f_2/(f_1)^2$; where f_2 is the fugacity of A_2 and f_1 is the fugacity of A_1 . However at very low pressures the fugacity is very nearly equal to pressure and the equilibrium constant can be expressed in terms of partial pressures.

The atomicity of the vapor is the average number of atoms per molecule and is equal to a ratio of molecular weight to atomic weight of the vapor, i.e. $\Gamma = \text{vapor atomicity} = M/M_1$ ($M_1 = \text{atomic weight}$).

In order to determine the partial pressures of each species present in a vapor, one must determine both the total vapor pressure (P) and the molecular weight of the vapor as a function of temperature. In this study the total vapor pressure is measured using the torsion effusion method and the molecular weight is determined by measuring the mass rate of effusion, using the following relation:

$$P = \frac{(2\pi RT)^{\frac{1}{2}} (G)}{(M)^{\frac{1}{2}} (t) (a)} \quad (2)$$

where M is the molecular weight, G is the mass of vapor effusing from the sample in time t, a is the area through which the effusion takes place, T is the absolute temperature, and R is the gas constant.

Perhaps a better measure of the relative amount of each species present is the ratio of the vapor pressures. This ratio can be derived by combining equation (2) with the relationship between total vapor pressure and the vapor pressures

of each species ($P = p_1 + p_2$). The result is stated as equation (3):

$$\frac{p_1}{p_2} = \frac{(2^{\frac{1}{2}} - 1^{\frac{1}{2}})}{(1^{\frac{1}{2}} - 1)} \quad (3)$$

where p_1 is the vapor pressure of the monatomic species and p_2 is the vapor pressure of the diatomic species.

Review of the Literature on Vapor Pressure Measurements

Since most metals have an extremely small vapor pressure at temperatures below 1000°C the majority of vapor pressure measurements has been done on low boiling point metals such as bismuth, antimony, and selenium. Of these metals by far the greatest amount of work has been done on bismuth.

Bismuth Vapor Pressure

An investigation of the heat of dissociation of Bi_2 was carried out by Ko⁽¹⁶⁾, using the method of molecular beams to determine the combined velocity spectrum of Bi atoms and Bi_2 molecules. The degree of dissociation of Bi_2 molecules was computed from the velocity spectrum and combined with vapor pressure measurements made using the rate of effusion method in order to obtain the heat of dissociation. The heat of dissociation determined by Ko was 77.1 ± 1.2 kcal/gram mole over a temperature range of 827-947°C.

Examination of Ko's method of calculating the heat of dissociation shows that the equilibrium temperature used in this calculation was that of the slit chamber of the effusion

cell, which was 24°C above the temperature of the melt from which the vapor was effusing. The vapor pressures which were used in these calculations were determined at the lower temperature of the melt in the crucible. Thus a large error is introduced in the calculations due to the necessity of keeping the slit temperature above the crucible temperature in order to avoid condensation.

Yoshiyama⁽³²⁾ made a determination of the vapor pressure of bismuth and the molecular weight of the vapor using a torsion-effusion technique combined with a mass rate of effusion measurement. From this work Yoshiyama derived an equation for the variation of the molecular weight of the vapor with change in absolute temperature. Yoshiyama reported the total heat of vaporization as 47.3 kcal/gram mole at 943.1°K and the heat of dissociation as 69.9 kcal/gram mole.

There are some possible sources of error in Yoshiyama's work. The thermocouple in the cell was not shielded from outside radiation which could cause an error in the temperature measurement. Yoshiyama's calculation of the orifice coefficient is probably in error since the value reported implies that the wall thickness at the orifice is approximately 0.04 mm. Also, precautions were not taken for preventing the formation of bismuth oxide on the sample. The presence of bismuth oxide will decrease the evaporation rate from the surface of the sample.

Weber and Kirsch⁽³⁰⁾ used a small open end tube as an "effusion" cell to measure the vapor pressure of bismuth.

Whitman⁽³¹⁾, in a theoretical paper written in 1952, showed that equilibrium could not be established in a cell of this type. The results obtained could be as low as 22 per cent of actual values but were probably higher than this, by an undeterminable amount, due to the volume occupied by the sample in the cell.

Granovskaya and Lubimov⁽¹³⁾ measured the vapor pressure of bismuth using the Langmuir evaporation technique. In this method the vapor pressure is determined by the quantity of material which evaporates (under vacuum) per unit time from a constant surface area. The quantity that is measured is the mass of material striking a given area in a specified time interval. Granovskaya and Lubimov correlated the quantity of material vaporized per unit time from the entire surface area of the sample with the vapor pressure of bismuth and reported the heat of vaporization of bismuth as 38.61 kcal/gram atom. No mention of the molecular weight of the vapor was made.

O'Donnell⁽²²⁾ made an investigation of the vapor pressure of bismuth using the Knudsen effusion method. Radioactive bismuth 210 was used to increase the sensitivity of the method. The small weight of vapor which condensed on the cold target of the effusion cell was determined by measuring the radioactivity of the condensed material compared to that of the isotopic mixture in the cell. Using this ratio of activities the weight of the condensed material and the vapor pressure were calculated at the temperature of measurement.

Since O'Donnell's measurements were made by the Knudsen effusion technique it was necessary to know the molecular weight of the vapor in order to calculate the vapor pressure. After reviewing the work of previous investigators, O'Donnell concluded that there was no reliable information on the molecular weight of bismuth vapor. Hence, a molecular weight of 418 corresponding to undissociated Bi_2 was assumed for calculations. Since the vapor pressure of Bi is small in the temperature range of the investigation (400-500°C), this is a reasonable assumption but may not be an accurate one. O'Donnell reported that the heat of vaporization of bismuth is 48.1 ± 0.6 kcal/gram mole.

Brackett and Brewer⁽³⁾, in a recent study of the heat of dissociation of Bi_2 , have noted that the usual method of determining the heat of dissociation from the slope of a plot of $\log K_p$ versus $1/T$ can lead to considerable error due to small temperature-dependent errors in the data (particularly if the data is over a small temperature range). In an attempt to avoid these errors, Brackett and Brewer correlated previous experimental data using the Third Law method. A table of values of $(F_T - H_{298})/T$ for monatomic, diatomic, liquid, and solid bismuth are required for their correlation. Brackett and Brewer evaluated the work of Yoshiyama, Ko and Leu using some supplementary data obtained from the compilation of Stull and Sinke⁽²⁷⁾, and calculated the heat of dissociation of Bi_2 to be 46.5 ± 1.0 kcal/gram mole. Brackett and

Brewer tabulated the vapor pressure of both Bi and Bi₂ and concluded that both species are equally important in the temperature range of 700-1200°C. It may also be noted from their tabulation that Bi₂ is a substantial part of the total vapor pressure of bismuth at the boiling point.

Cosgarea⁽⁶⁾, in his study of thermodynamic properties of uranium-bismuth alloys, determined the heat of vaporization of Bi and Bi₂, and the heat of dissociation of Bi₂. An optical absorption technique was used to determine the abundance of each species present. The method consists of measuring concentrations in a vapor by the quantity of light absorbed at characteristic frequencies by each species. The quantity of light absorbed by each species is proportional to the vapor pressure and when plotted versus 1/T yields the heat of vaporization. Cosgarea calculated the heat of vaporization of Bi to be 37.3 kcal/gram mole, the heat of vaporization of Bi₂ as 39.5 kcal/gram mole, and the heat of dissociation of Bi₂ as 35.0 kcal/gram mole.

A tabulation of the previously reported results, comparing them with the results of this study is presented later in the text.

Antimony Vapor Pressure

Yoshiyama and Niwa⁽³³⁾ made a determination of the vapor pressure and atomicity of antimony utilizing the same apparatus that was used in determining the vapor pressure of bismuth. This determination thus has the same possible sources of error

as those discussed in the section on bismuth vapor pressures. A heat of vaporization of 46.2 kcal/gram mole for Sb_4 and the heat of dissociation of Sb_4 to Sb_2 of 62.0 kcal/gram mole were reported.

In a recent study of lead-antimony alloys, Richards⁽²³⁾ measured the vapor pressure of antimony over the alloys and the vapor pressure of pure antimony by a transpiration method. The method consists of passing a stream of gas ($\text{N}_2\text{-H}_2$ mixture) over a pool of the liquid metal at a low flow rate and measuring the amount of metal vapor transported by the gas to a condenser. The vapor pressure can be calculated knowing the amount of metal condensed from the measured amount of gas and the working pressure of the cell. Precautions were taken to assure equilibrium by carrying out experiments at different gas flow rates until a range of rates was found where no change in measured vapor pressures occurred. The dynamic nature of the method however may cause a non-equilibrium situation which is not detectable by the method of varying the flow rate of the gas. Richards calculated the heat of vaporization of Sb_2 to be 45.5 kcal/gram mole and the heat of vaporization of Sb_4 to be 28.4 kcal/gram mole.

Vapor Pressures of Other Metals

Neumann and Lichtenberg⁽¹⁹⁾ made an early study of the vapor pressure and molecular weight of selenium. A torsion-effusion measurement of the total vapor pressure was combined with mass rate of effusion data taken with a microbalance to

determine the molecular weight of selenium. Neumann and Lichtenberg calculated the heat of vaporization of selenium to be 24.58 kcal/gram mole. No calculations were made for the heat of dissociation.

A study of the vapor pressure and molecular weight of selenium was made by Niwa and Sibata⁽²¹⁾ using the same method and nearly the same apparatus as that described in Yoshiyama's article on bismuth vapor pressure and atomicity. The heat of vaporization of selenium was reported to be 26.8 kcal/gram mole, and the heat of dissociation of Se_6 ($\text{Se}_6 \rightleftharpoons 3\text{Se}_2$) as 58.4 kcal/gram mole.

Neumann and Volker⁽²⁰⁾ made the first vapor pressure determinations on metals employing the torsion-effusion cell technique developed by Volmer⁽²⁹⁾ to measure vapor pressures of organic solids. A modification of this technique combined with mass rate of effusion data was used by Neumann and Lichtenberg on selenium. Neumann and Volker measured the total vapor pressure of mercury and potassium and calculated the heats of vaporization to be 14.71 kcal/gram mole (at 300°K) for mercury and 20.82 kcal/gram mole (at 336.6°K) for potassium.

A thorough analysis of thermophysical and thermochemical data on sodium was compiled by Thomson and Garellis⁽²⁸⁾. Vapor pressure data and thermodynamic functions were used to calculate the heat of vaporization and dissociation of sodium. The most consistent values were reported to be: heat of vaporiza-

tion, 26.366 kcal/gram mole; heat of dissociation of Na_2 , 18.200 kcal/gram mole.

Spectroscopic Data

Another source of data of the heat of dissociation of metals is spectroscopic data from absorption or emission spectra.

The absorption spectrum of diatomic bismuth was analyzed by Almy and Sparks⁽²⁾. The data was obtained by heating pure bismuth in an atmosphere of nitrogen within a carbon-tube resistance furnace at temperatures of 850 to 1500°C. Band systems in the visible, the ultraviolet, the far ultraviolet, and the violet range were analyzed. Almy and Sparks analyzed and correlated the several hundred bands in the bismuth system into a set of potential energy curves for the molecular states. From these potential energy curves it was estimated that the heat of dissociation of the ground state of Bi_2 was 1.71 electron volts (39.6 kcal/gram mole).

Naude⁽¹⁸⁾ made a study of the absorption spectrum of antimony. The apparatus consisted of a quartz tube enclosed in a resistance furnace into which a sample of pure antimony is distilled through a side arm tube. The side arm tube was sealed off after placing the sample in the main tube and was kept heated by an auxiliary furnace. Maximum temperature reached in the main tube was 1100°C. Naude found absorption in two different wave length ranges but analyzed only one of these regions; the one of longest wave length (2840-3350Å)

which corresponds to the transition of Sb_2 from the ground state to an excited state. The upper energy level had no regular energy differences between vibrational levels, thus preventing the determination of the heat of dissociation by extrapolation. A partial explanation of the irregularities in the upper state was given by attributing the irregularity to different isotope combinations of Sb_2 (Sb^{121} and Sb^{123} isotopes).

An extensive treatise on the spectra of diatomic molecules together with a large compilation of spectroscopic data on diatomic molecules was published by Herzberg⁽¹⁵⁾. This book contains such data as heats of dissociation, energy level diagrams and molecular constants determined by vibrational and rotational analysis of diatomic spectra. This book contains without a doubt the largest collection of spectroscopic data on diatomic molecules.

CHAPTER II

THEORETICAL

In any system where more than one molecular species is present and the relative amounts of the species change as the environmental conditions of the system are changed, there must be an equilibrium between the species. The equilibrium which is established between the species can be determined by calculation of the equilibrium constant K , using the concepts of statistical mechanics.

Equilibrium in the Vapor State

For the equilibrium $A + A \rightleftharpoons A_2$, the equilibrium constant K is given by the expression:

$$K = V \frac{Q_{A_2}}{Q_A^2} \quad (4)$$

where V is the volume of the system, and the Q 's are the partition functions. The explicit forms of the partition functions are:

$$Q_{A_2} = \frac{\left[\frac{V [2\pi(2m_A)k_B T]^{3/2}}{h^3} \right] \left[\frac{8\pi^2 k_B T}{2h^2} \right] \left[\frac{\sigma^2 m_A e^{-hv/2k_B T}}{2} \right] \left[\frac{\omega_{A_2} e^{D_e/k_B T}}{(1 - e^{-hv/k_B T})} \right]}{(5)}$$

$$Q_A = \frac{V(2\pi m_A k_B T)^{3/2}}{h^3} (\omega_A) \quad (6)$$

where ν is the vibrational frequency of the molecular ground state, D_e is the electronic energy at the equilibrium distance, m_A is the mass of the atom A, ω is the multiplicity or number of slightly different energy states in the particular electronic level of the atom or molecule, and σ is the effective internuclear distance in the molecule.

The dissociation energy of the molecule at 0°K , D_0 , is given by the following expression:

$$D_0 = D_e - \frac{h\nu}{2} \quad (7)$$

The equilibrium constant K for the equilibrium $A + A \rightleftharpoons A_2$ can now be obtained by substituting equations (5), (6), and (7) into equation (4); after rearranging equation (4) becomes:

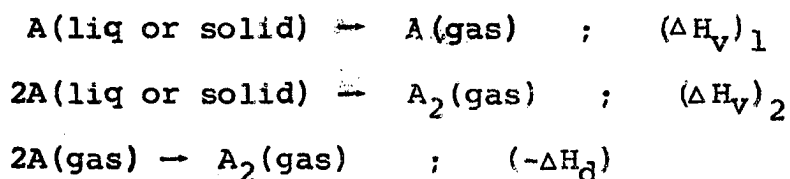
$$K = \frac{\sigma^2 (4\pi)^{\frac{1}{2}} h}{(m_A k_B T)^{\frac{1}{2}}} \frac{\omega_{A_2}}{\omega_A^2} \frac{e^{D_0/RT}}{(1 - e^{-h\nu/k_B T})} \quad (8)$$

(The assumption that only the first term in the electronic partition functions for A and A_2 (ω) need be considered is justified since where equation (8) is used the higher electronic levels are far enough above the ground state so that the succeeding terms are negligible compared to the first term.) The dissociation energy, the vibrational frequency of the molecular ground state (ν), σ the internuclear distance in the molecule, and the multiplicities of the electronic states (ω) of the atom and molecule must be determined from analysis of the spectra of the atom and the molecule.

Atomicity in the Vapor State

For a number of elements it has been shown experimentally that there exists two or more molecular species in the vapor state. It is observed that the atomicity or relative amounts of each species present is a function of temperature. It has also been observed experimentally that in some elements the relative amount of the highest molecular species increases as temperature is increased (in the vapor which is in equilibrium with the condensed phase) while in other elements the relative amount decreases as temperature is increased. Rationalization of this experimental observation can be accomplished as follows: $(\Delta H_V)_1$ = heat of vaporization of the monomer
 $(\Delta H_V)_2$ = heat of vaporization of the dimer
 (1) if $(\Delta H_V)_1 > (\Delta H_V)_2$, the partial pressure of the monomer will increase faster than the partial pressure of the dimer in the equilibrium vapor above the condensed phase as the temperature is increased; (2) if $(\Delta H_V)_2 > (\Delta H_V)_1$, the partial pressure of the dimer will increase faster than that of the monomer as the temperature is increased.

Further, if we consider the following processes (without regard as to how they take place or whether polyatomic species exist in the liquid and solid states) and the energies required to produce them:



(ΔH_d = heat of dissociation of the dimer) the energies may be related to each other by addition and subtraction of the equations to obtain the following expression:

$$\Delta H_d = 2(\Delta H_v)_1 - (\Delta H_v)_2 = (\Delta H_v)_1 + (\Delta H_{v_1} - \Delta H_{v_2})$$

Thus in case (1) above, $(\Delta H_v)_1 > (\Delta H_v)_2$ which corresponds to $\Delta H_d > (\Delta H_v)_1$, and case (2), $(\Delta H_v)_2 > (\Delta H_v)_1$ corresponds to $\Delta H_d < (\Delta H_v)_1$.

The difference between case (1) and case (2) can be stated in the following manner: when the dimer is stable to dissociation ΔH_d is greater than the heat of vaporization of the monomer $(\Delta H_v)_1$, case (1) will occur with a high percentage of dimer at low temperatures and the percentage of dimer decreasing as temperature increases. If the dimer is not very stable to dissociation ΔH_d is less than $(\Delta H_v)_1$, case (2) and the concentration of the dimer will be small at low temperatures but will increase as the temperature increases⁽⁴⁾.

The heat of vaporization of a substance to form a gaseous molecule is the cohesive energy of the molecules in the condensed phase. Although the cohesive energy is not absolutely predictable, a general qualitative statement can be made about the relation between the cohesive energy and the boiling point: the higher the boiling point of the substance the larger the heat of vaporization or cohesive energy. Thus we see that the probability of case (1) above becomes smaller for high boiling substances since $(\Delta H_v)_1$ is becoming larger for high boiling materials and the dimer would have to be very stable for ΔH_d

to be larger than $(\Delta H_v)_1$, for a high boiling substance.

Looking at the periodic chart of the elements the following qualitative statements may be made:

Group I - these elements form a diatomic molecule with 1 pair of electrons so that ΔH_d is not too large. For group Ia the boiling points are fairly low so that $(\Delta H_v)_1 > \Delta H_d$, case (2). For group Ib (Cu, Ag, Au) ΔH_d is larger than for the Ia elements but the boiling points are much higher also, so that $(\Delta H_v)_1 > \Delta H_d$ still holds.

Group II - this group of elements can form only a very unstable diatomic molecule by means of weak polarization or van der Waals forces and consequently ΔH_d is extremely small. The boiling points of group IIa are in a moderate range while those of group IIb are fairly low, but for both sub-groups $(\Delta H_v)_1 \gg \Delta H_d$. The excited states of the molecules in this group are much more stable than the ground states since the excited states of the atoms have two unpaired electrons; thus the molecule in the excited state forms a bond with 2 pairs of electrons. While this group should logically be classified as case (2), it seems more likely that at a temperature high enough to observe diatomic molecules in an equilibrium concentration the molecules will be dissociated due to their instability (the molecules cannot exist as excited molecules in an equilibrium concentration).

Group III - these elements form a diatomic molecule with 1 pair of electrons as the bond; thus their ΔH_d is not large.

For this group however the boiling points are fairly high and consequently $(\Delta H_V)_1 > \Delta H_D$, so that case (2) is indicated.

However $(\Delta H_V)_1$ is quite a bit larger than ΔH_D so that appreciable amounts of diatomic molecules should not appear until the temperature is quite high.

Group IV - this group of elements forms a diatomic molecule with 2 pairs of electrons for the bond, so that their ΔH_D is fairly large. However the boiling points in this group are very high (in any period, the group IV element has the highest boiling point); thus $(\Delta H_V)_1 > \Delta H_D$ still holds for this group. Due to the high boiling points in this group a rather high temperature must be reached before the vapor pressure is measurable and consequently only at rather high temperatures do the diatomic molecules (and higher species) become detectable.

Group V - these elements form the most stable diatomic molecules of any group, having 3 pairs of electrons for the bond. The values of ΔH_D are thus quite large in this group. The boiling points in this group are rather low so that case (1) occurs, i.e. $\Delta H_D > (\Delta H_V)_1$. The diatomic molecules are in abundance for this group at fairly low temperatures and only in Bi and Sb does the monatomic species appear at all. In fact, for P, As, and Sb the tetratomic species are quite stable at low temperatures.

Group VI - this group of elements forms a diatomic molecule with a bonding of 2 pairs of electrons giving a fairly large

value of ΔH_d . The boiling points of these elements are fairly low, however, and case (1) occurs, i.e. $\Delta H_d > (\Delta H_v)_1$. Here again, as in group V, the diatomic molecules appear at fairly low temperatures. S and Se, in fact, show a preponderance of sexatomic molecules at the lower temperatures.

Group VII - these elements form the diatomic molecule with a bond of 1 electron pair. Their ΔH_d thus are not large but are much larger than $(\Delta H_v)_1$ since the boiling points are very low in this group. Due to the low boiling points in this group the critical pressure of the vapor is reached quickly and the observance of monatomic molecules is obscured even though the relative values of ΔH_d and $(\Delta H_v)_1$ indicate case (1). Since ΔH_d is so much larger than $(\Delta H_v)_1$ it is indicated that the diatomic molecules would predominate at low vapor pressure.

CHAPTER III

EXPERIMENTAL

Theory of Measurements

The atomicity of a vapor whose molecular weight changes with temperature requires knowledge of the molecular weight of the vapor at the desired temperature. In this study the total vapor pressure is determined by the torsion-effusion method and the molecular weight is then calculated from the proper relation using mass rate of effusion data taken concurrently but independently. A discussion of these methods follows.

Torsion-Effusion Method

The torsion-effusion method was originated by Volmer⁽²⁹⁾ for measuring the vapor pressure of various organic solids. In this method the pressure exerted by the vapor is determined by measuring the force exerted by the vapors effusing from an orifice in the effusion cell. A sample of the metal is placed in an effusion cell suspended from a torsion fiber and the vapor allowed to effuse in a horizontal direction from two holes placed eccentrically in the cell. In the case

of an ideal orifice the total vapor pressure (P) is calculated from the equation:

$$P = \frac{2\tau\alpha}{(a_1q_1 + a_2q_2)} \quad (1)$$

where τ is the torsion constant of the fiber, α is the angle of deflection, a_1 and a_2 are the cross sectional areas of the holes, and q_1 and q_2 are the horizontal distances of the holes from the suspension point.

Since in actual practice the orifice is not ideal and must have finite length, the vapor pressure is calculated using the following relation:

$$P = \frac{2\tau\alpha}{(a_1q_1f_1 + a_2q_2f_2)} \quad (1a)$$

where f_1 and f_2 are correction factors for the effect of the finite length of the orifices and are functions of the angular distribution of the effusing molecules.

A study of the effect of finite orifice length on the angular distribution of effusing molecules was performed by Clausing⁽⁵⁾. Freeman and Searcy⁽¹⁰⁾, in a more recent article, have derived a simplified relation for determining the f factor when orifice dimensions are in the range $0 \leq L/r \leq 2$, where L and r are orifice length and radius respectively. This relation will be used in this study to calculate the f factors. The relation is:

$$\frac{1}{f} = 0.0147 \frac{(L)^2}{(r)^2} + 0.349 \frac{(L)}{(r)} + 0.9982 \quad (4)$$

The pressure calculated by this method is the pressure of the vapor at the orifice exits. As long as the holes are small in comparison to the mean free path of the molecules and the diameter of flow inside the cell, the pressure gradient in the cell between the metal surface and the orifice exits can be neglected⁽²⁰⁾. The primary factor in determining whether the pressure at the orifice exits corresponds to the equilibrium vapor pressure is the ratio of evaporation rate to effusion rate. In pure liquid surfaces every molecule striking the liquid surface is absorbed immediately and therefore the maximum velocity of evaporation is equal to the velocity of effusion. Since the area of the evaporating surface is much larger than the area of the orifices (about 1000 times larger in the apparatus used) the rate of evaporation is completely sufficient to maintain the equilibrium vapor pressure in the cell.

Mass Rate of Effusion Method

This technique is usually referred to as the Knudsen effusion method. The vapor pressure is determined in this method by measuring the mass rate of effusion of a vapor through an orifice of known cross-sectional area. The calculation of the vapor pressure from the effusion rate data requires a knowledge of the molecular weight of the effusing vapor. The vapor pressure is calculated by using the equation:

$$P = \frac{(2\pi RT)^{\frac{1}{2}} (G)}{(M)^{\frac{1}{2}} (t) (a)} \quad (2)$$

where M is the molecular weight, G is the mass of vapor effusing from the cell in time t , a is the cross-sectional area of the effusion orifice, T is the absolute temperature, and R is the gas constant. This relation applies only to an orifice of zero length and for actual use with finite length orifices must be modified by an efficiency factor (f) which is a function of the angular distribution of the effusing molecules. In this study the effusion cell has two orifices and thus the relation for P is modified to:

$$P = \frac{(2\pi RT)^{\frac{1}{2}} (G)}{(M)^{\frac{1}{2}} (t) (a_1 f_1 + a_2 f_2)} \quad (2a)$$

Since the total vapor pressure (P) is determined by the torsion-effusion measurements, equation (2a) is then utilized to determine M , the molecular weight. The value of M is then used to calculate Γ the atomicity in the following relation: $\Gamma = M/M_1$, where M_1 is the atomic weight.

The value of Γ is then substituted into the following relation to determine the ratio of the vapor pressures of the monatomic and diatomic species (β):

$$\beta = \frac{2^{\frac{1}{2}} - \Gamma^{\frac{1}{2}}}{\Gamma^{\frac{1}{2}} - 1} = \frac{P_1}{P_2} \quad (3)$$

(similar relations apply for equilibrium between other pairs of species and the ratio of their vapor pressures). The

equilibrium constant for the dissociation reaction of the diatomic species can now be calculated since both total vapor pressure P and β have been determined, since:

$$K_p = \frac{\beta + 1}{\beta^2 P} \quad (9)$$

K_p as defined here is not numerically equal to the equilibrium constant K defined in Chapter II although it is equivalent to it. The relationship between K_p and K is:

$$K_p = \frac{K}{k_B T} \quad (10)$$

Also the value of K_p depends on the units of pressure used in calculating it.

The heat of dissociation may be determined by a plot of $\ln K_p$ versus $1/T$ since the slope of this plot is $\Delta H_d^\circ/R$. (The temperature range in this study is large enough so that the temperature dependent errors are small.) The heats of vaporization of the monatomic and diatomic species may be determined by plotting $\ln p_1$ versus $1/T$ and $\ln p_2$ versus $1/T$ respectively, since the slopes of these plots are $(\Delta H_v)_1/R$ and $(\Delta H_v)_2/R$ respectively. The values of p_1 and p_2 are also calculated from P and β :

$$p_1 = \frac{P\beta}{\beta + 1} \quad , \quad p_2 = \frac{P}{\beta + 1}$$

Description of Apparatus

The apparatus used in this study consists of an effusion cell with two eccentrically placed holes suspended from a

quartz microbalance by a fine quartz torsion fiber. A diagram of the apparatus is shown in Figure 1.

The effusion cell is illustrated in Figure 2. Three different effusion cells each having different orifice diameters were used. The cells are machined from graphite stock ("Graph-I-Tite", Grade G, Graphite Specialties Corp.). The sample well in the cells is a hole drilled lengthwise through the cell. The sample well is closed at both ends by two small plugs machined from the graphite stock. The effusion orifices are holes drilled perpendicular to the sample well, one at each end of the well on opposite sides from each other. The wall thickness at each orifice is reduced to the order of 0.4 to 0.8 mm by careful polishing with metallographic paper. The length of each orifice was determined by measurement with a metallographic microscope. The distance of each orifice from the axis of rotation of the cell is measured with a travelling stage microscope. The orifice lengths and distances from axis of rotation are corrected for the effect of thermal expansion at each temperature using a value of the coefficient of linear expansion of $7.86 \times 10^{-6}/^{\circ}\text{C}$.

The orifice areas are measured from magnified images (400x) traced onto uniform thickness weighing paper. The images were made on the screen of a micro-projector. The area of the weighing paper could be determined to within 1% and the weight of the paper to within 0.1%. To obtain the area of each orifice, the total weight of the whole paper, the weight

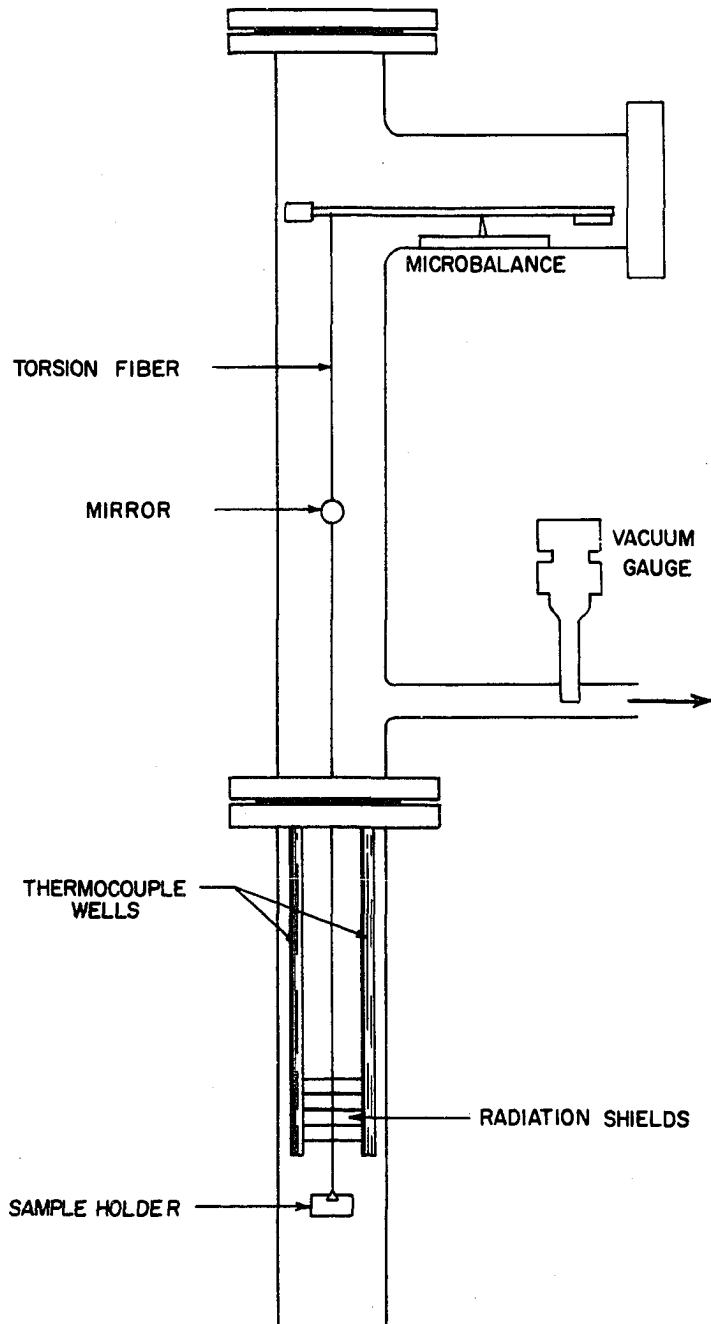


Figure 1. Experimental Apparatus

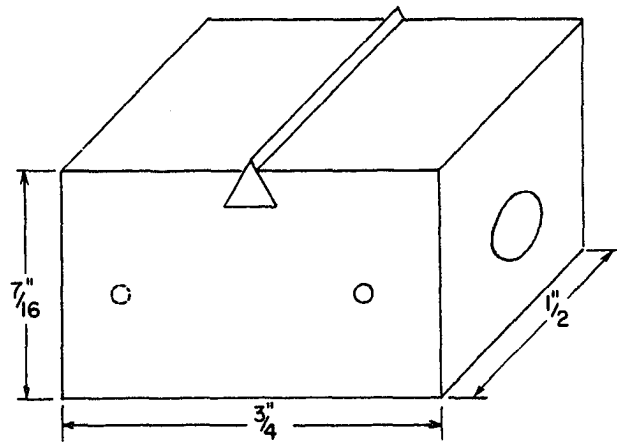


Figure 2. Effusion Cell

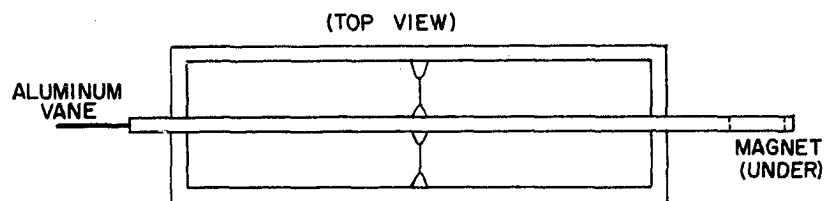


Figure 3. Quartz Microbalance

of the image cut from the whole paper, and the area of the whole paper must be determined. The accuracy of the areas determined are $\pm 10^{-5}\text{cm}^2$ since the area of the weighing paper can be determined to $\pm 4. \times 10^{-3}\text{cm}^2$. The effusion cell is attached to the torsion fiber by means of a machined graphite keyway block which fits into a keyway that is machined into the cell. The keyway block is attached to the torsion fiber with "Sauereisen" refractory cement No. 74.

The torsion fiber is a drawn quartz fiber approximately 0.2 mm in diameter and 26 inches long. A small galvanometer mirror (focal length 0.5 meter) is attached to the fiber with epoxy resin ("Hysol" BRL 2795, Houghton Laboratories, Inc.) 9 inches below its upper end. The purpose of the mirror is to measure the angle of deflection of the cell using a telescope and scale (Leeds and Northrup Co.) made for use with the galvanometer mirror. The divisions on the scale are in millimeters and each scale division is 0.001 radian. The torsion fiber is attached, at its upper end, to the quartz microbalance by means of the epoxy resin.

Before attaching the keyway block to the torsion fiber, it's torsion constant is determined by attaching cylindrical brass balance weights to the fiber with the epoxy resin and measuring the period of oscillation (t). The moment of inertia of each weight is calculated from $I = mr^2/2$, where I is the moment of inertia, m is the mass in grams, and r is the radius of the cylindrical weight. The torsion constant T is

calculated from the relation $\tau = 4\pi^2 I/t^2$. If τ is determined by using two weights having different masses, the moment of inertia of the suspension is canceled if τ is calculated by solving for it simultaneously from two relations as the above. Thus τ is calculated as

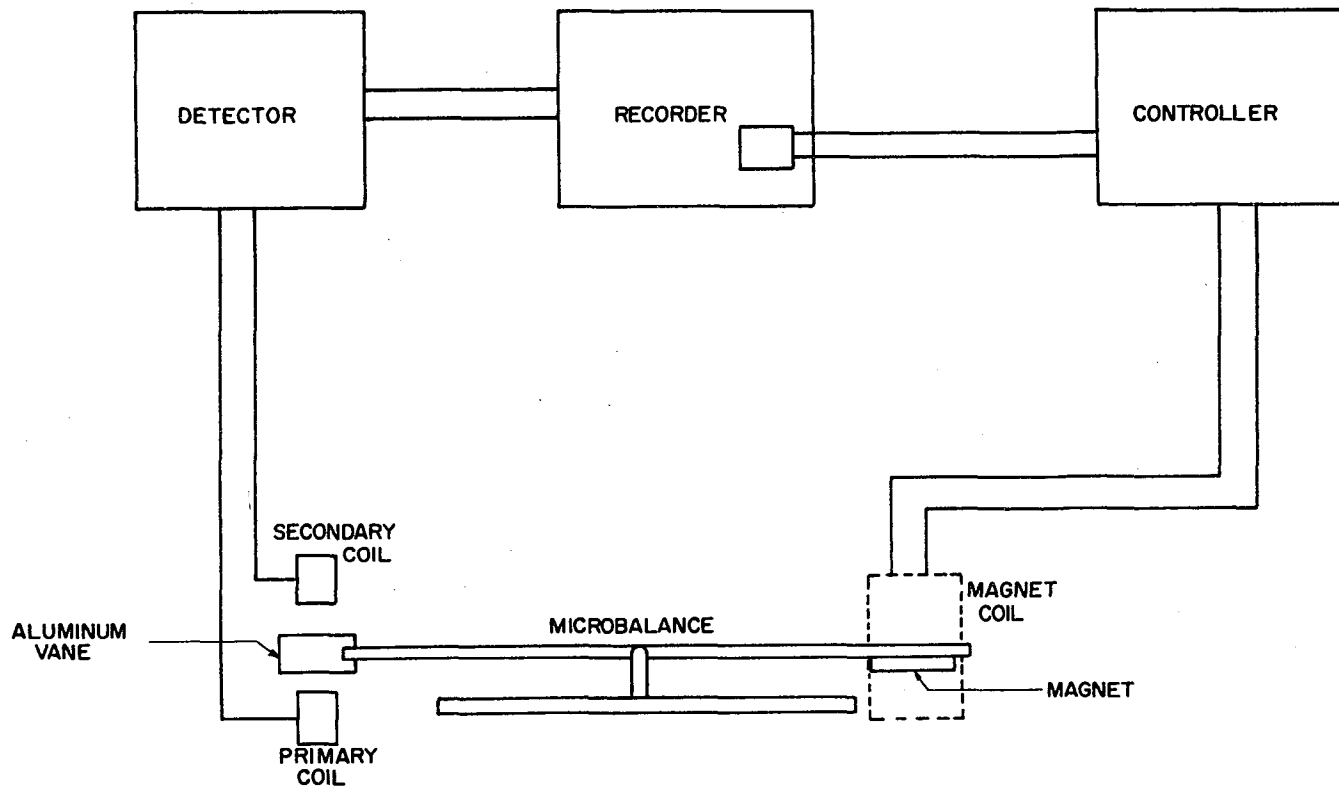
$$\tau = \frac{4\pi^2(I_1 - I_2)}{(t_1^2 - t_2^2)} \quad (11)$$

There is no discernible difference in τ , when using the simultaneous calculation, as compared to the single determination. The value calculated by the foregoing method is checked by calibration against a known effusion rate (see section on Calibration).

The quartz microbalance, shown in Figure 3, is constructed of 3 mm diameter fused quartz rod. The balance arm is attached to the base of the balance at the vertical supports on either side of the base by fusing the quartz. The supporting fibers are carefully thinned with a small flame until the balance has the requisite sensitivity. On one end of the balance arm a small aluminum vane is attached to the arm with the epoxy resin. On the opposite end of the balance arm a small "Alnico" magnet is secured to the arm with the epoxy resin. The vane and the magnet are the detecting and restoring elements in the automatic control circuit of the balance system.

A flow diagram of the components of the automatic controlling and recording microbalance system is shown in Figure 4. The system forms a null-type balance which functions as

Figure 4. Flow Diagram of the Microbalance System



follows: a change in the weight of the effusion cell produces a very slight movement of the balance arm which changes the field between the primary and secondary coils by means of the aluminum vane. The output signal from the secondary is rectified in the detector unit and fed to the recorder (Brown "Elektronik", Model No. Y153X17, Minneapolis Honeywell Co.). The recorder records the signal and controls the setting of a 100K "Helipot" variable resistor by direct drive from the servo motor of the recorder. The "Helipot" resistor is in the circuit with the magnet coil, thus the setting of the resistor determines the current flowing to the magnet coil and the restoring force exerted on the balance arm by the magnet.

The input signal to the primary detector coil is generated in the detector with an oscillator circuit containing high- μ twin triode (12AX7) tubes. The frequency of this signal is 300 kc. The primary and secondary coils are spaced $\frac{1}{2}$ " apart and are located outside the vacuum chamber. The magnet coil is wound on a cardboard form which fits over the outside of the vacuum chamber side arm. The magnet coil has approximately 4000 turns of #32 AWG copper wire and has a resistance of 520 ohms. The circuit diagrams of the detector unit and the controller unit are shown in Figures 5 and 6, respectively.

The apparatus is enclosed within a vertical vacuum chamber. The upper section of the chamber is a pyrex tube 60 mm in diameter and 40 cm long. The side arm which contains the balance is also made of pyrex; this tube is 60 mm in diameter

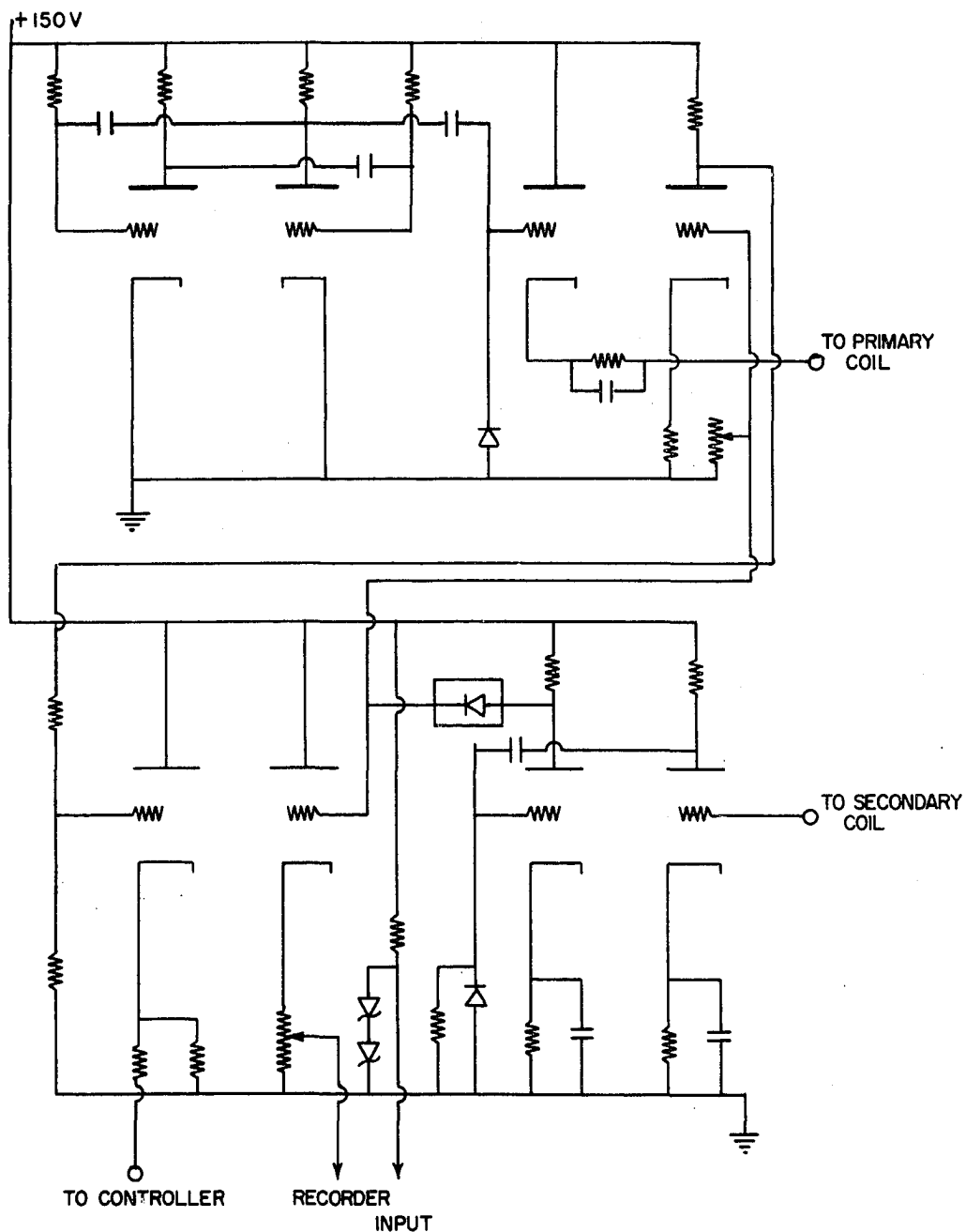


Figure 5. Detector Unit

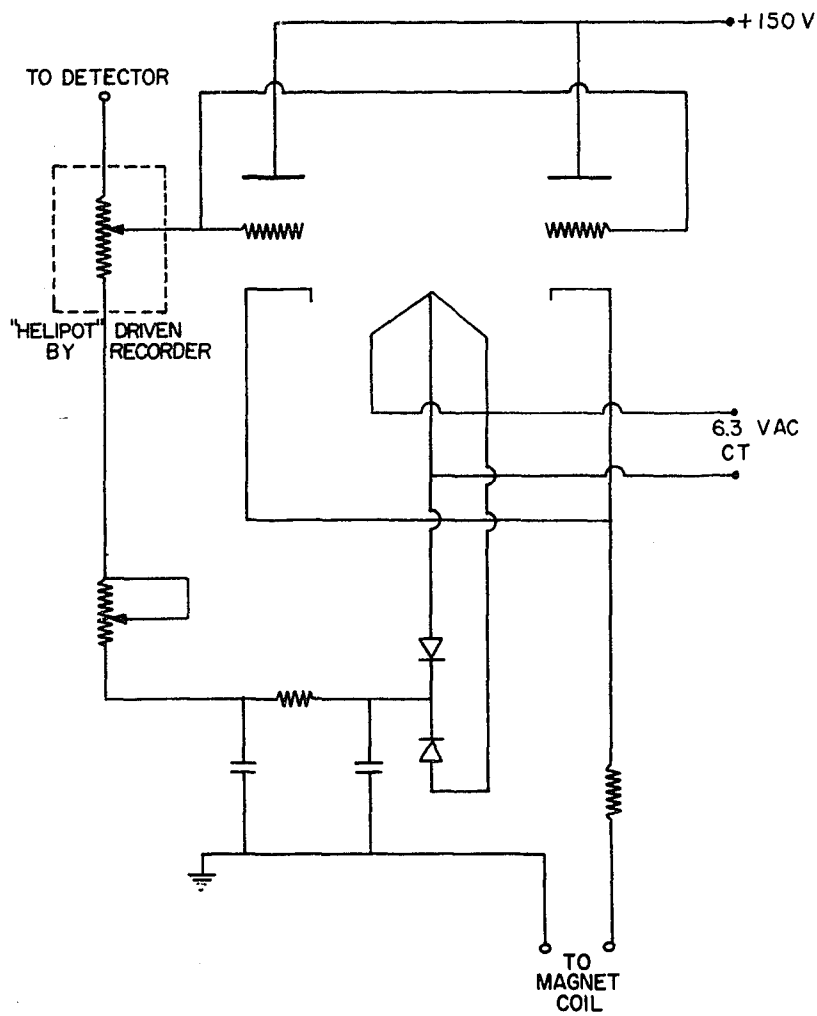


Figure 6. Controller Unit

and 15 cm long. A smaller side arm, through which the system is evacuated, is fused to the main tube near the bottom. The evacuation side arm is a 25 mm diameter pyrex tube. Brass flanges are waxed by means of Apiezon W wax on to the vertical pyrex tube. The upper end of the chamber is closed by a brass plate resting freely on an O-ring.

The lower section of the chamber consists of a fused quartz tube 58 mm in bore and 48 cm long which is closed at the lower end. The upper end is waxed into a brass flange which is a mating flange to the one on the lower end of the upper section of the chamber. The upper and lower halves of the cell are bolted together and the seal is provided by an O-ring. The joint between the sections of the chamber is water cooled so as to keep the upper section of the chamber from becoming too hot.

The vacuum chamber is heated by a split-wound resistance furnace (Type MK-3010-S, Hevi-Duty Electric Co.) which is open at both ends and fits around the lower section of the chamber. The furnace has three split windings; the two end windings are each 3 inches long, and the center winding is 4 inches long giving a total heated length of 10 inches. The space between the lower chamber section and the furnace windings at each end of the furnace is filled with ceramic refractory fiber ("Fiberfrax", The Carborundum Co.) so as to reduce heat losses through the ends.

The power input to the furnace is controlled by a West Model JSB-2 Proportional Controller which controls the furnace

temperature (at the point of measurement) to $\pm 1^{\circ}\text{C}$. The temperature distribution through the heated length of the furnace is further regulated by the rheostats (Type 0656-10 ohm, Allied Radio Corp.) in series with each of the three furnace windings. The furnace is fitted with three chromel-alumel thermocouples; one near the top, one in the center, and one near the bottom. By adjusting the rheostats the maximum variance between the temperatures of the three thermocouples can be reduced to less than 3°C , giving a large zone in the center of the heated length where the maximum temperature variation is $\pm 1^{\circ}\text{C}$.

In addition to the thermocouples in the furnace, there are two chromel-alumel thermocouples which are placed inside the lower vacuum chamber section with their hot junctions about 1 cm from the effusion cell. The thermocouple wells are machined from the same grade of graphite stock from which the effusion cell is made in order to eliminate errors in temperature measurement due to emissivity difference of materials surrounding the sample and the thermocouples. The thermocouples are made from matched chromel and alumel thermocouple wire (3G-170, Hoskins Manufacturing Co.) and their calibration was checked against copper and aluminum melting point standards from the National Bureau of Standards.

The vacuum system consists of a fractionating oil diffusion pump (Type MCF-60, Consolidated Vacuum Company) backed by a Welch "Duo-Seal" No. 1402 B mechanical vacuum pump. The system is capable of evacuation to below 10^{-6} mmHg pressure.

The vacuum gauge used with the system is a Phillips type Cold Cathode ion gauge (Type PHG-010A, Consolidated Vacuum Company).

Calibration

Before using the apparatus the recorder in the micro-balance system was calibrated to determine what mass change corresponded to full scale deflection of the recorder. Since it was necessary to calibrate the recorder for mass effusion rates of the same order to be encountered in this study, it was desirable to use data on a substance with a similar atomic weight at a temperature where its vapor pressure coincided with the vapor pressure range of interest (10^{-4} to 10^{-2} mmHg). Mercury was chosen as the calibrating substance because it met the above stated requirements and because vapor pressure data in the range of 10^{-3} to 10^{-2} mmHg agreed closely from three different determinations^(8, 17, 20) using three different methods. Also mercury has such a small amount of Hg_2 present in the vapor, even at temperatures up to the boiling point⁽²⁷⁾, that its molecular weight may be taken as the atomic weight (within 0.05%).

For the calibration the sample of mercury is brought to the desired temperature and the time required for full scale deflection of the recorder is observed. This time, together with the mass effusion rate calculated from vapor pressure-temperature data, is then used to calculate the total mass loss for full scale deflection. Table I shows calculated

mass effusion rates, observed time for full scale deflection of the recorder, and total mass loss for four different temperatures.

The vapor pressure data of Neumann and Volker⁽²⁰⁾ is used to calculate the mass effusion rates. The choice was made on the basis of the low scatter of data in comparison to other investigations.

TABLE I
Calibration of Mass Effusion Rate

Vapor Pressure (mm Hg)	Temperature °C	Calculated Effusion Rate (gm/min)	Observed Full Deflection of Recorder (min)	Calculated Mass Loss (gm)
2.24×10^{-3}	27.25	8.92×10^{-5}	39.3	3.51×10^{-3}
3.43×10^{-3}	32.5	1.35×10^{-4}	25.9	3.50×10^{-3}
4.52×10^{-3}	36.0	1.75×10^{-4}	19.7	3.45×10^{-3}
9.84×10^{-3}	46.4	3.80×10^{-4}	9.2	3.50×10^{-3}

As a check on the torsion constant (T) of the torsion fiber, the vapor pressure data of Neumann and Volker was used to calculate T by measuring the angle of deflection α at different temperatures. Instead of trying to obtain a "zero point" for the suspension, T was calculated using the vapor pressures at two different temperatures and the corresponding angles of deflection:

$$P_2 - P_1 = \frac{2T(\alpha_2 - \alpha_1)}{(a_1 q_1 f_1 + a_2 q_2 f_2)} \quad (12)$$

$$\tau = \frac{(P_2 - P_1) (a_1 q_1 f_1 + a_2 q_2 f_2)}{2(a_2 - a_1)} \quad (13)$$

Table II shows the values of τ calculated from the vapor pressure data of Neumann and Volker and the measured values of $(a_2 - a_1)$.

TABLE II

Calculation of the Torsion Constant from Data

$\frac{P_2 - P_1}{(\text{mm Hg})}$	$\frac{a_2 - a_1}{(\text{radians})}$	$\frac{\tau}{(\text{dyne-cm/rad})}$
1.19×10^{-3}	0.004	0.533
1.09×10^{-3}	0.004	0.489
5.32×10^{-3}	0.019	0.502

The value of τ determined by the brass balance weights on this same fiber was 0.505 dyne-cm/rad.

Preparation of Metal Samples

The metals used in this study were 99.9999 percent pure bismuth and 99.9996 percent pure antimony supplied by The Consolidated Mining and Smelting Company of Canada Limited; 99.99 percent pure sodium obtained from Mallinckrodt Chemical Company; 99.999 percent pure lead, 99.999 percent pure selenium, and 99.999 percent pure indium supplied by American Smelting and Refining Company.

The bismuth samples were removed from the bar ingot by use of a hacksaw. The small pieces were then immersed in concentrated hydrochloric acid to remove any trace of oxide, then

washed successively with distilled water and acetone. The samples were then dried with warm air from a heat gun and placed in a sample holder which could be evacuated.

The antimony samples were prepared in a manner similar to that of bismuth except that the antimony was obtained mostly as a fine powder (due to the brittleness of the metal) with some small pieces. Only the finely divided powder was used in the samples to give maximum surface area to the sample. The powder was then placed in concentrated hydrochloric acid to remove any oxide then filtered out of the solution and washed with distilled water and acetone. The powdered samples were dried partially with a heat gun then placed on a heated brass plate to complete the drying.

The lead samples were removed from the bar ingot and then immersed in a 1:1 solution of concentrated acetic acid and hydrogen peroxide to remove the surface oxide coating. Upon removing the samples from acetic-peroxide solution they were placed in acetone until ready to be put in the effusion cell.

The sodium samples were prepared by cutting small pieces from the ingot. The samples were stored in a jar filled with kerosene until ready to be used in the cell.

The samples of selenium were prepared as a finely ground powder, from the pellet form supplied by grinding with a mortar and pestle. The finely ground sample was placed immediately in the effusion cell.

The samples of indium were removed from the rod ingot and washed thoroughly with acetone and placed in the sample holder.

Experimental Procedure

After careful preparation, samples of the pure metals are placed in the effusion cell which is then fixed to the torsion suspension. The apparatus is aligned and the vacuum chamber is closed and evacuation is begun. The ends of the furnace between the windings and the vacuum chamber are filled with ceramic insulating fiber and the furnace is turned on. The temperature of the apparatus is raised to 200°C while being evacuated, to help outgassing of the system (except in the runs on sodium and selenium). When a vacuum on the order of 5×10^{-6} mm Hg is achieved the torsion suspension "zero point" is read. The furnace controller is reset to the desired temperature and the power input adjusted for maximum heating rate. After the desired temperature is reached, 20 minutes is allowed for temperature and vapor-liquid equilibration (a period of 45 minutes showed no change in the measured values from those at 20 minutes). The deflection of the torsion fiber is read while the mass loss from the cell is recorded by the recorder in the microbalance system.

Measurements were taken on bismuth, antimony, lead, sodium, selenium, and indium. The readings on the apparatus were taken in both ascending and descending order of temperatures. No difference was observed in the readings on the ascending cycle as compared to those on the descending cycle.

Errors in Experimental Measurements

A. Maximum propagated error for the vapor pressure measurement: from equation (1a) the error (in percent), $\Delta P/P$ is

$$\frac{\Delta P}{P} = \pm \frac{\Delta T}{T} + \frac{\Delta a}{a} + \frac{\Delta(a_1 q_1 f_1 + a_2 q_2 f_2)}{a_1 q_1 f_1 + a_2 q_2 f_2} ;$$

(i) maximum error due to the torsion constant is

$$\frac{\Delta T}{T} = \pm 3.22 \% ;$$

(ii) maximum error due to the angle of deflection is

$$\frac{\Delta a}{a} = \pm 5.0 \% ;$$

(iii) maximum propagated error due to the area of the holes, distance between the suspension point and the holes, and the orifice coefficient is

$$\frac{\Delta(a_1 q_1 f_1 + a_2 q_2 f_2)}{a_1 q_1 f_1 + a_2 q_2 f_2} = \pm 1.36 \% .$$

The maximum propagated error in the vapor pressure measurement is:

$$\frac{\Delta P}{P} = 3.22 + 5.0 + 1.36 = 9.60 \% .$$

B. Maximum error for the molecular weight measurement: from equation (2a) the percent error, $\Delta M/M$ is

$$\frac{\Delta M}{M} = \pm \frac{\Delta T}{T} + 2 \frac{\Delta(G/t)}{G/t} + 2 \frac{\Delta P}{P} + 2 \frac{\Delta(a_1 f_1 + a_2 f_2)}{(a_1 f_1 + a_2 f_2)} ;$$

(i) maximum error due to the temperature is

$$\frac{\Delta T}{T} = \pm 0.2 \% ;$$

(ii) maximum propagated error due to the mass effusion rate is

$$2 \frac{\Delta(G/t)}{G/t} = \pm 3.64 \% ;$$

(iii) maximum propagated error due to total vapor pressure is

$$2\frac{\Delta P}{P} = \pm 19.20 \% ;$$

(iv) maximum propagated error due to the area of the holes and the orifice coefficients is

$$2\frac{\Delta(a_1f_1 + a_2f_2)}{(a_1f_1 + a_2f_2)} = \pm 2.60 \% .$$

The maximum propagated error in the molecular weight measurement is:

$$\frac{\Delta M}{M} = 0.2 + 3.64 + 19.20 + 2.60 = 25.44 \% .$$

The values calculated above are overestimates even if the errors are not compensating. The precision of the data taken in this study is demonstrated by three measurements taken at identical conditions on selenium vapor; the values agree within 1% (see Appendix E). A discussion of the method of determining the errors and some sample calculations are given in Appendix H.

CHAPTER IV

RESULTS

From the experimental data the total vapor pressure and the molecular weight of the vapor are calculated. Using these values, the vapor pressures of each species present and the equilibrium ratio of a pair of species may be determined. The total heat of vaporization, heats of vaporization of each detectable species, and the heat of dissociation of the higher molecular species to the lower species may be determined by plotting the appropriate vapor pressure versus reciprocal absolute temperature and determining the slope (see Appendix G).

Where enough spectroscopic data is available, the equilibrium constant (K) can be calculated from equation (8) and converted to a K_p value for comparison with the experimental value.

Results for Bismuth

The results obtained for the total vapor pressure of bismuth are given in Figure 7. Upon application of the method

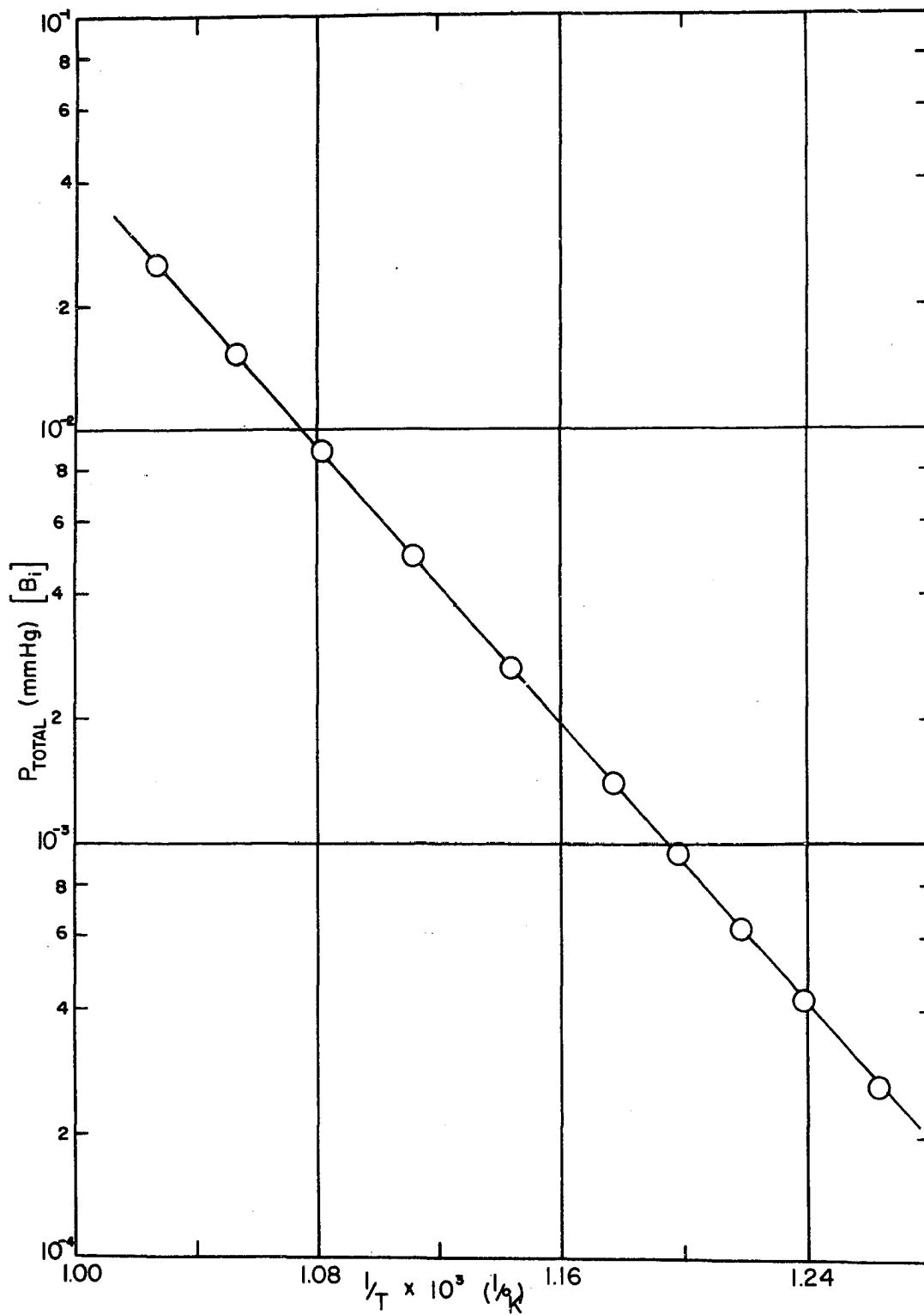


Figure 7. Total Vapor Pressure of Bismuth

of least squares to the data the total vapor pressure is represented by the following relation:

$$\log P(\text{mmHg}) = 7.03 - \frac{8,400}{T}$$

The total heat of vaporization of bismuth is then 38.5 ± 0.1 kcal/gram mole of the liquid as determined from the relation above, over the temperature range of 792-975°K.

The calculated results for the vapor pressures of Bi and Bi₂ are shown in Figures 8 and 9. The application of the least squares method to these plots yields the relations:

$$\begin{aligned} \log p_1(\text{mmHg}) &= 7.12 - \frac{8,780}{T} \\ \log p_2(\text{mmHg}) &= 6.38 - \frac{8,070}{T} \end{aligned}$$

The heat of vaporization of Bi is 40.2 ± 0.1 kcal/gram atom and the heat of vaporization of Bi₂ is 36.9 ± 0.1 kcal/gram mole, over the temperature range of 792-975°K.

The values calculated for the equilibrium constant K_p ($2\text{Bi} \rightleftharpoons \text{Bi}_2$) are shown in Figure 10. The least squares method yields the relation:

$$\log K_p = -4.82 + \frac{9,370}{T}$$

where K_p is in atm^{-1} . The value for the heat of dissociation of Bi₂ is determined as 42.9 ± 0.1 kcal/gram mole of Bi₂, in the temperature range of 792-975°K.

The experimental results show that for bismuth $\Delta H_d > (\Delta H_v)_1$, thus the prediction of the theoretical section is substantiated by the results.

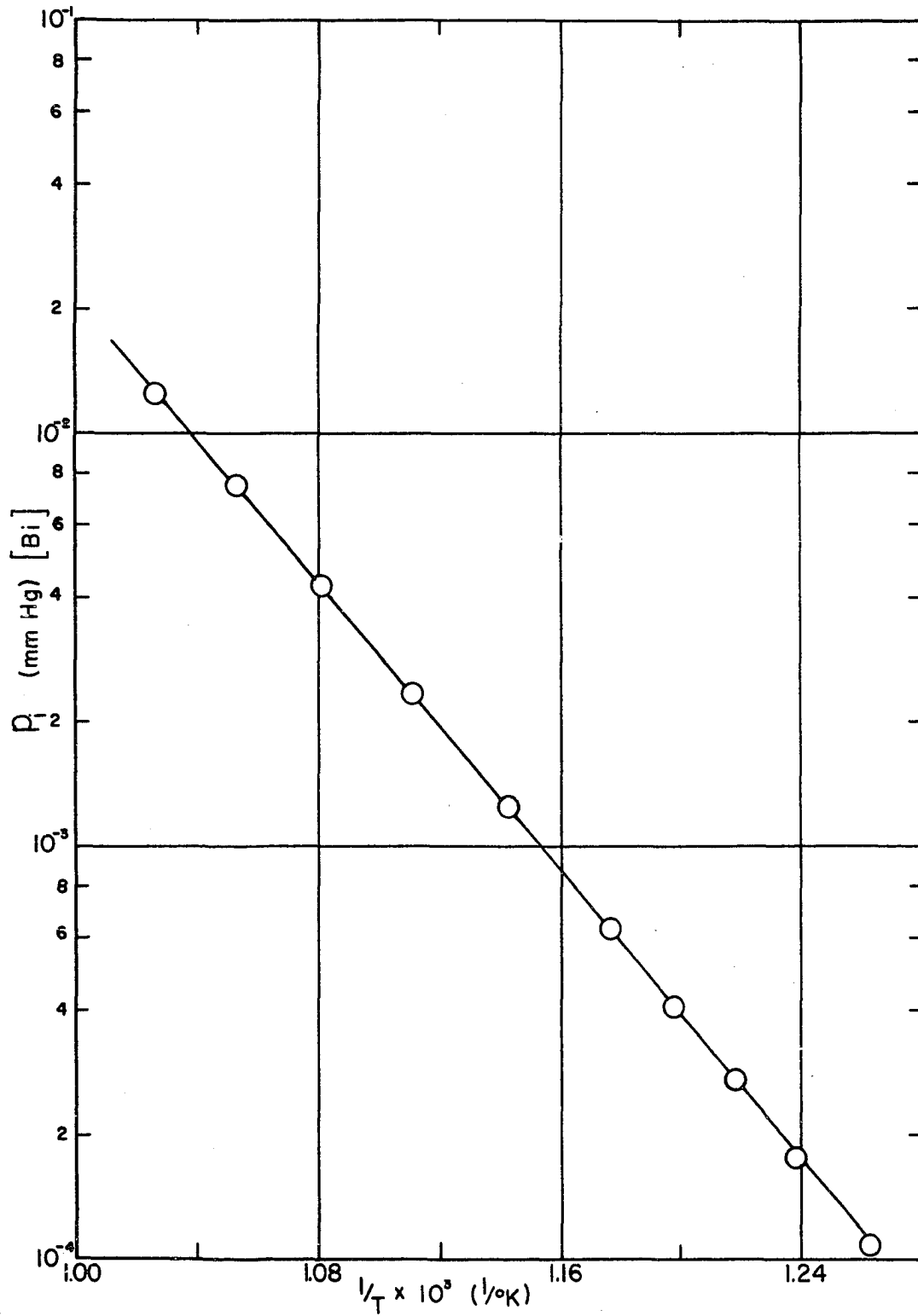


Figure 8. Vapor Pressure of Bi

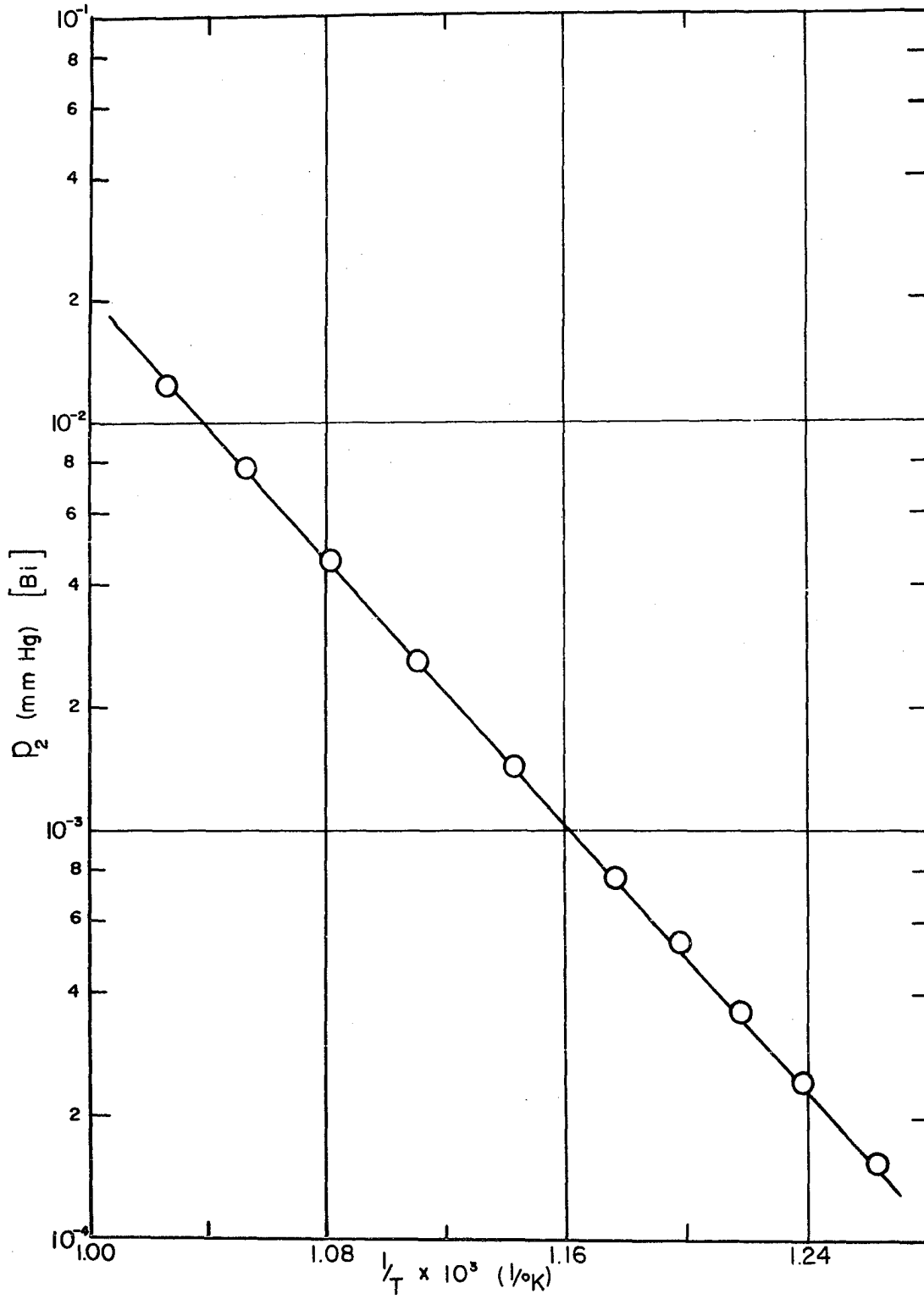


Figure 9. Vapor Pressure of Bi_2

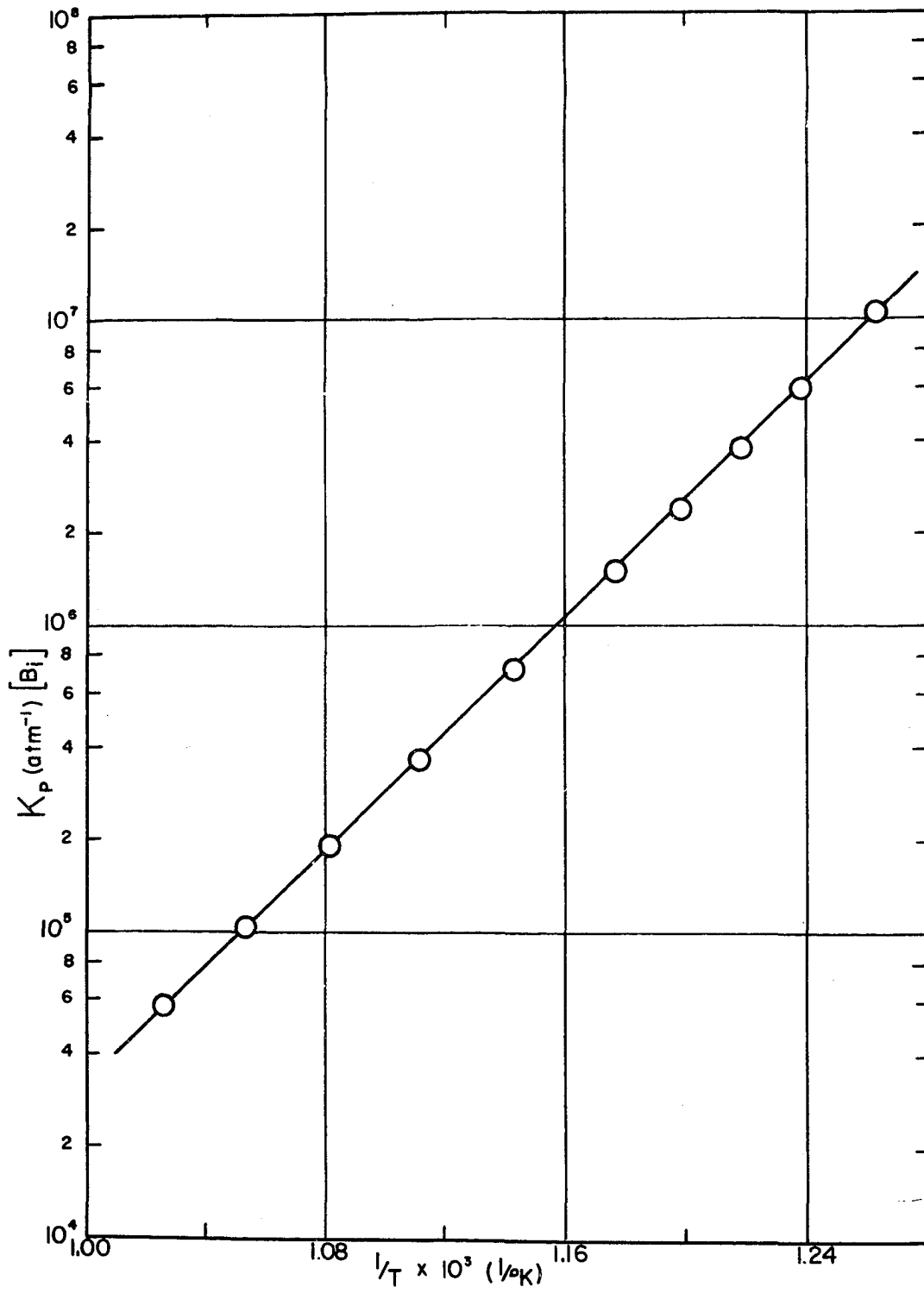


Figure 10. Equilibrium Constant Bi - Bi₂

The calculated values of K_p are correlated by the relation:

$$R \ln K_p - \Delta a \ln T = \frac{[(\Delta H_d^\circ)_{298} - 298]}{T} + C$$

Where Δa is a constant which enters the relation from the integration of C_p values used in deriving the relation. The relation is derived in Appendix I. Figure 11 shows a plot of $(R \ln K_p - \ln T)$ versus $1/T$ for bismuth ($\Delta a = 1$). The slope of this plot is $(\Delta H_d^\circ)_{298} - 298$ and the value of $(\Delta H_d^\circ)_{298}$ obtained for bismuth by the least squares method is 43.51 ± 0.1 kcal/gram mole.

The molecular weight of bismuth vapor as a function of temperature (T) obtained by application of the least squares method is:

$$\log M = 2.3553 + \frac{123.0}{T}$$

The experimental and calculated data which is used to evaluate bismuth vapor pressures by the least squares method is tabulated in Appendix A.

The relation for K developed in the "Theoretical" section (equation 8) was used to calculate values for K over the same temperature range as the experimental data. The K value is then converted to a K_p value by equation (10) and the units are changed to atm^{-1} . A sample calculation of a theoretical K_p value is presented in Appendix J. The theoretical values are compared with the experimental values in Table III. It can be seen from the table that the agreement is quite good.

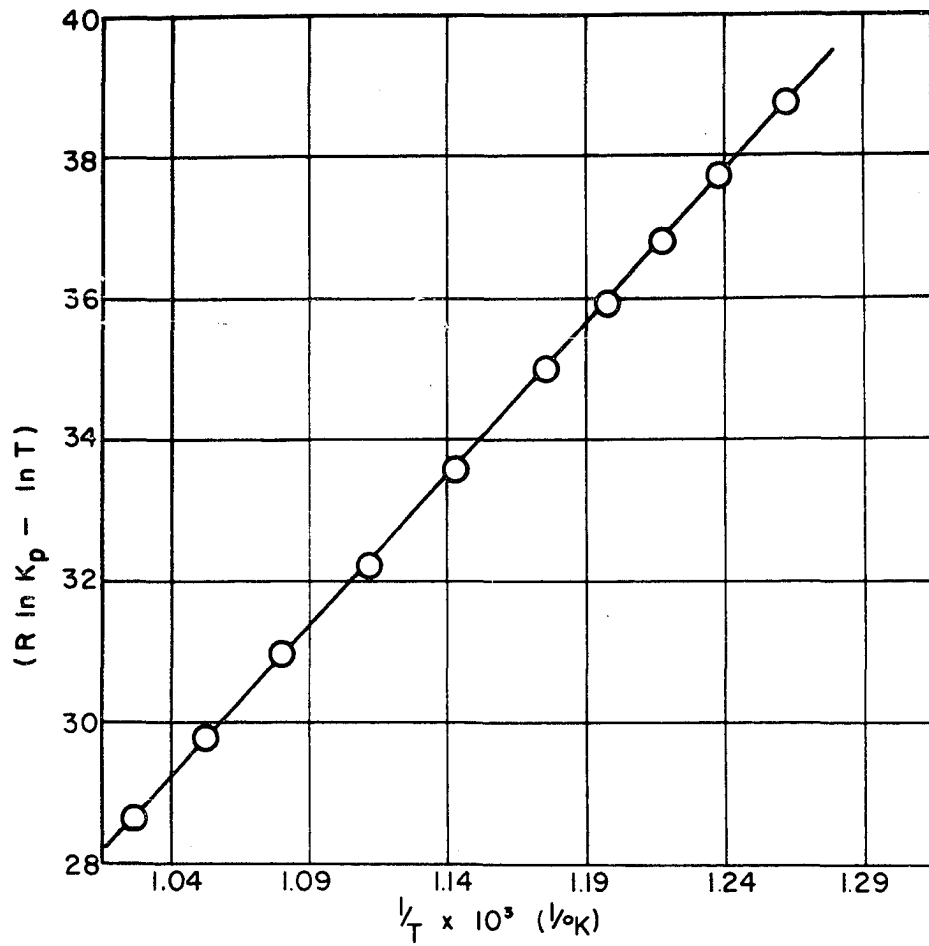


Figure 11. Correlation of K_p for Bismuth

The values of the parameters for the calculation of K from equation (8) are given in Appendix A.

TABLE III

Comparison of K_p Values for Bismuth

$T(^{\circ}\text{K})$	$K_p(\text{atm}^{-1})$ <u>Theoretical</u>	$K_p(\text{atm}^{-1})$ <u>Experimental</u>
850	1.60×10^6	1.51×10^6
875	7.73×10^5	7.26×10^5
900	3.80×10^5	3.62×10^5
925	2.02×10^5	1.89×10^5
950	1.09×10^5	1.03×10^5
975	6.02×10^4	5.76×10^4

Results for Antimony

The results obtained for the total vapor pressure of antimony are given in Figure 12. The least squares method yields an expression for total vapor pressure given by:

$$\log P(\text{mmHg}) = 9.77 - \frac{9,710}{T} .$$

The total heat of vaporization of antimony is calculated as 44.44 ± 0.1 kcal/gram mole of solid from the relation above, over the temperature range of 727-850 $^{\circ}$ K.

The values calculated for the vapor pressures of Sb_2 and Sb_4 are shown in Figures 13 and 14. The least squares method is applied to these values to obtain an expression for the vapor pressures of Sb_2 and Sb_4 :

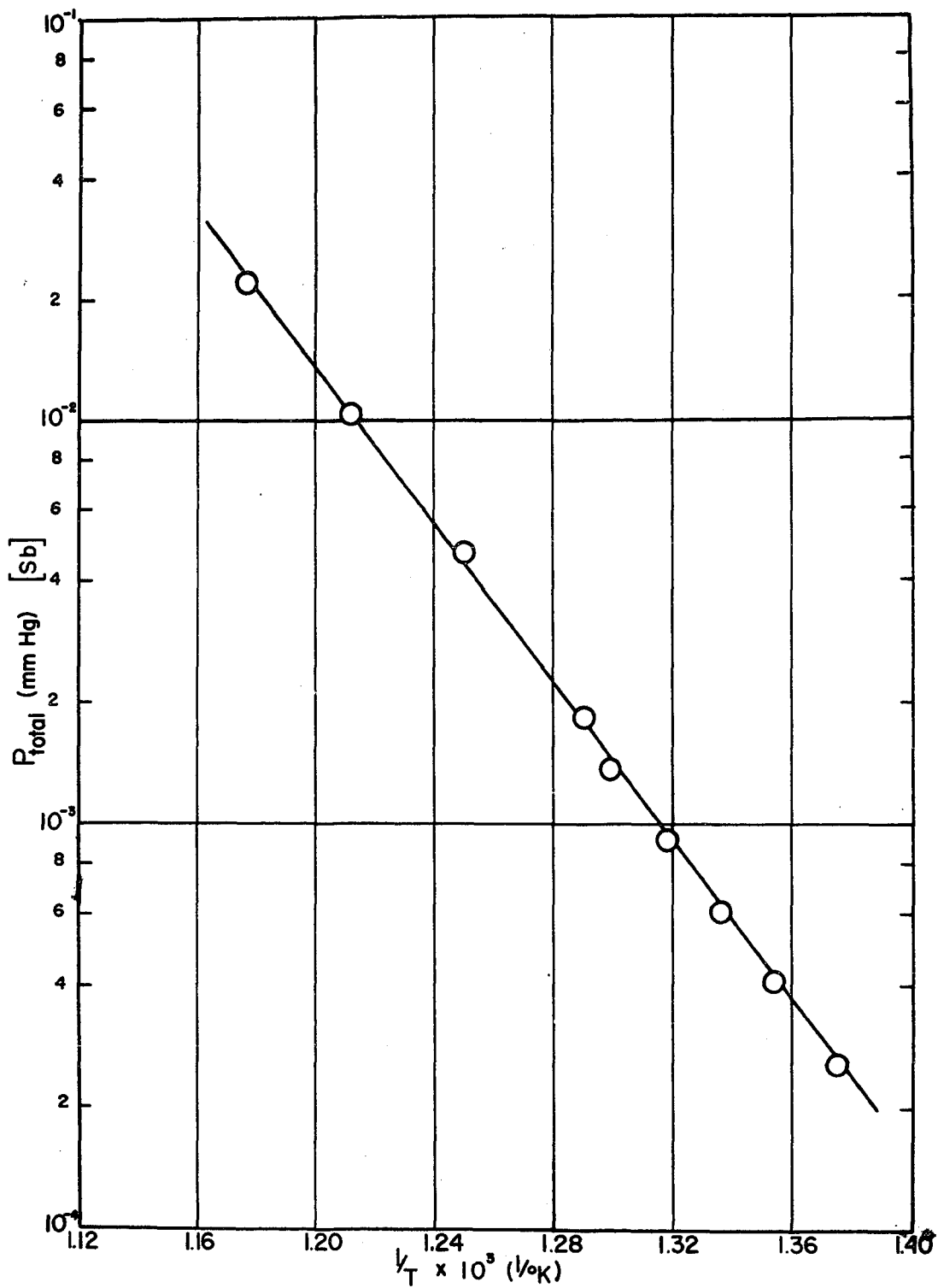


Figure 12. Total Vapor Pressure of Antimony

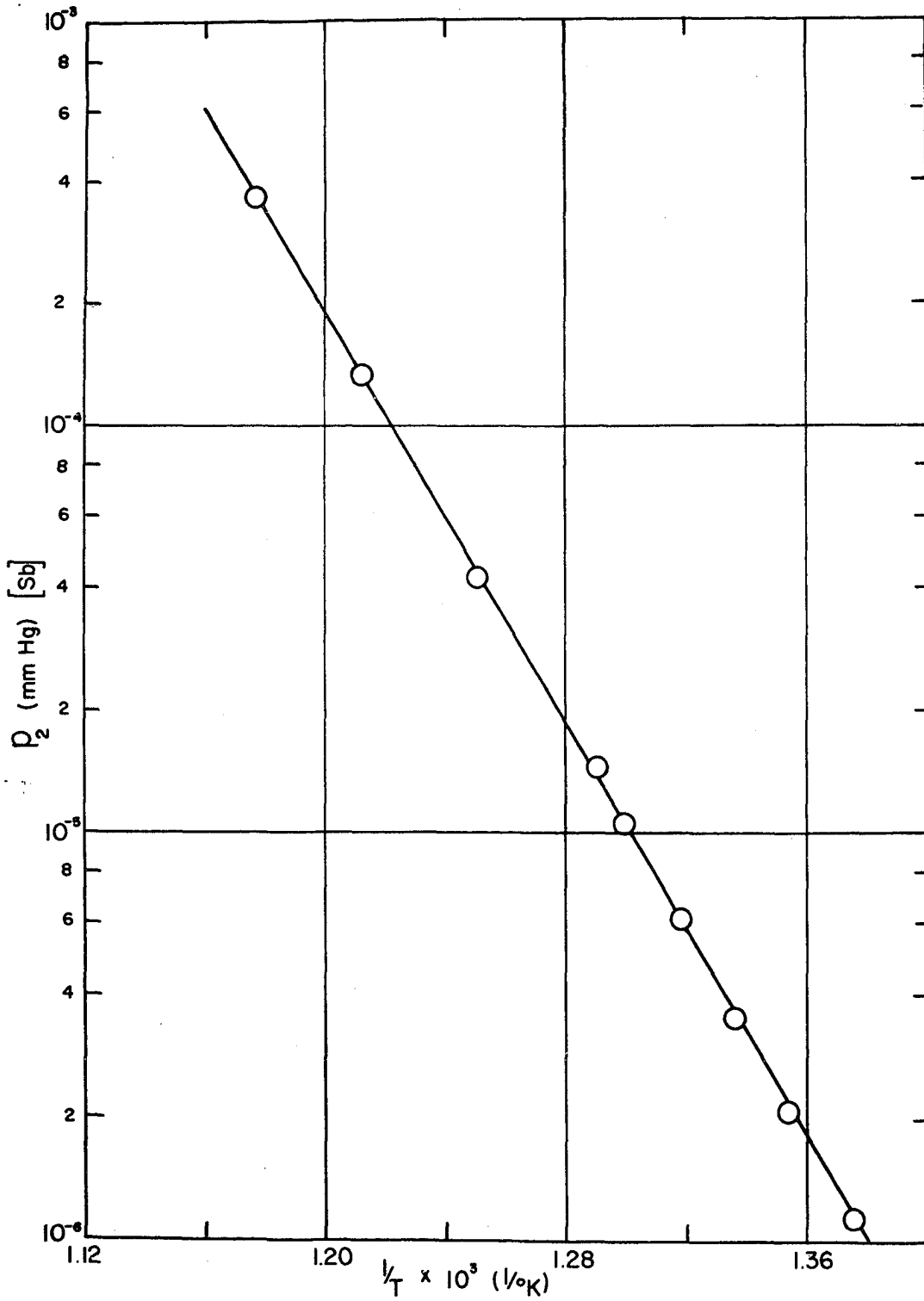
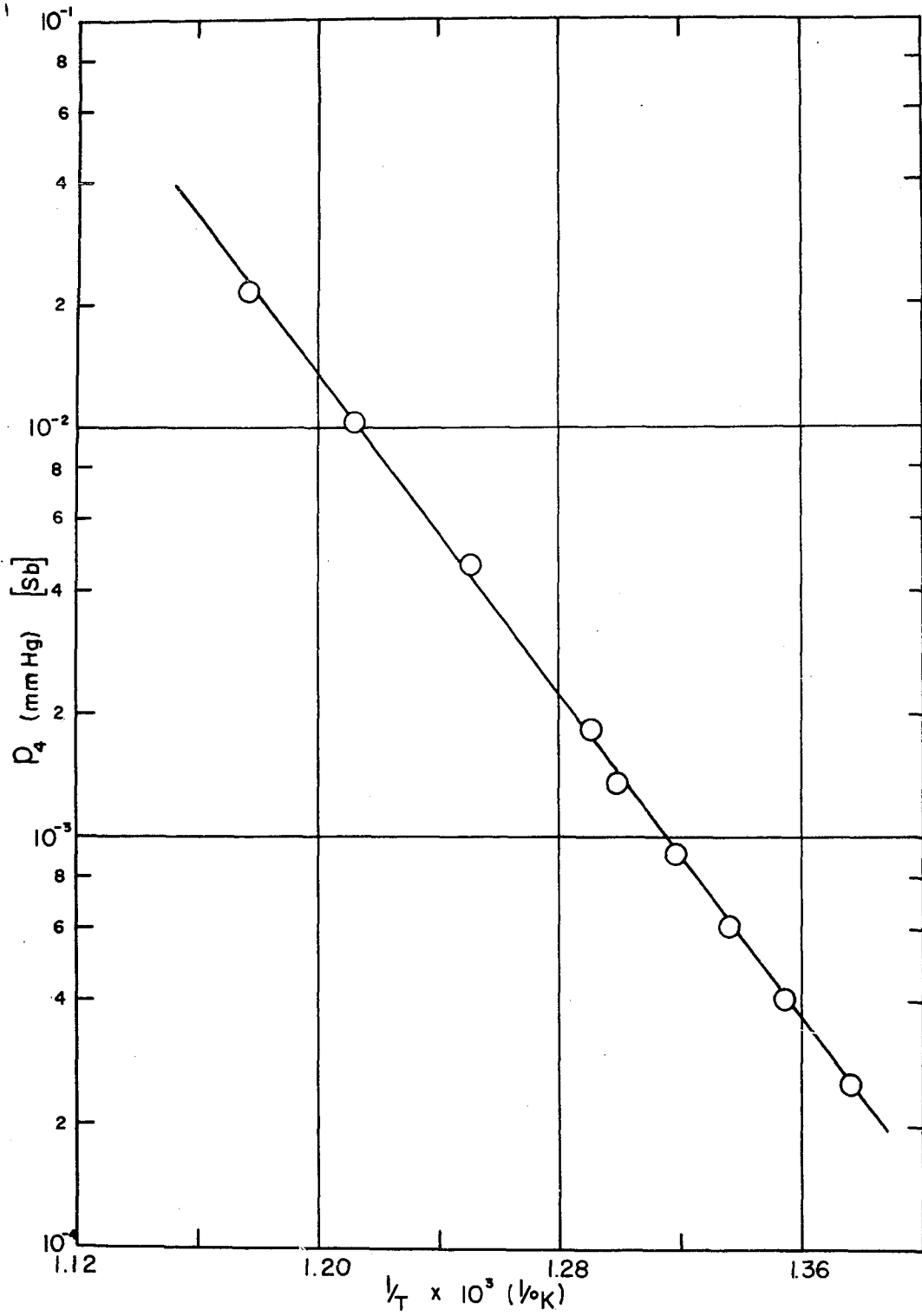


Figure 13. Vapor Pressure of Sb_2

Figure 14. Vapor Pressure of Sb_4

$$\log p_2(\text{mmHg}) = 11.23 - \frac{12,480}{T}$$

$$\log p_4(\text{mmHg}) = 9.75 - \frac{9,700}{T}$$

The heat of vaporization of Sb_4 is 44.4 ± 0.1 kcal/gram mole and the heat of vaporization of Sb_2 is 57.0 ± 2.0 kcal/gram mole, over the temperature range of 727-850°K.

The calculated values of the equilibrium constant K_p ($2\text{Sb}_2 \rightleftharpoons \text{Sb}_4$) are given in Figure 15. The least squares method yields an expression for K_p :

$$\log K_p = -9.82 + \frac{15,230}{T}$$

where K_p is in atm^{-1} . The calculated value of the heat of dissociation of Sb_4 is 69.7 ± 0.1 kcal/gram mole of Sb_4 , over the temperature range of 727-850°K.

The experimental results show that $\Delta H_d > (\Delta H_v)_2$ for antimony, and the theoretical prediction agrees with the results.

A plot of $(R \ln K_p + 2 \ln T)$ versus $1/T$ for antimony ($\Delta a = -2$) is shown in Figure 16. The slope of this plot is $(\Delta H_d^\circ)_{298} - 596$ and the value of $(\Delta H_d^\circ)_{298}$ determined from a least squares analysis of the points is 64.68 ± 0.1 kcal/gram mole.

The molecular weight of antimony vapor as a function of temperature obtained by the least squares method is:

$$\log M = 2.4025 + \frac{219.0}{T}$$

The data given in the figures and the representations of antimony vapor pressure were determined from the experimental

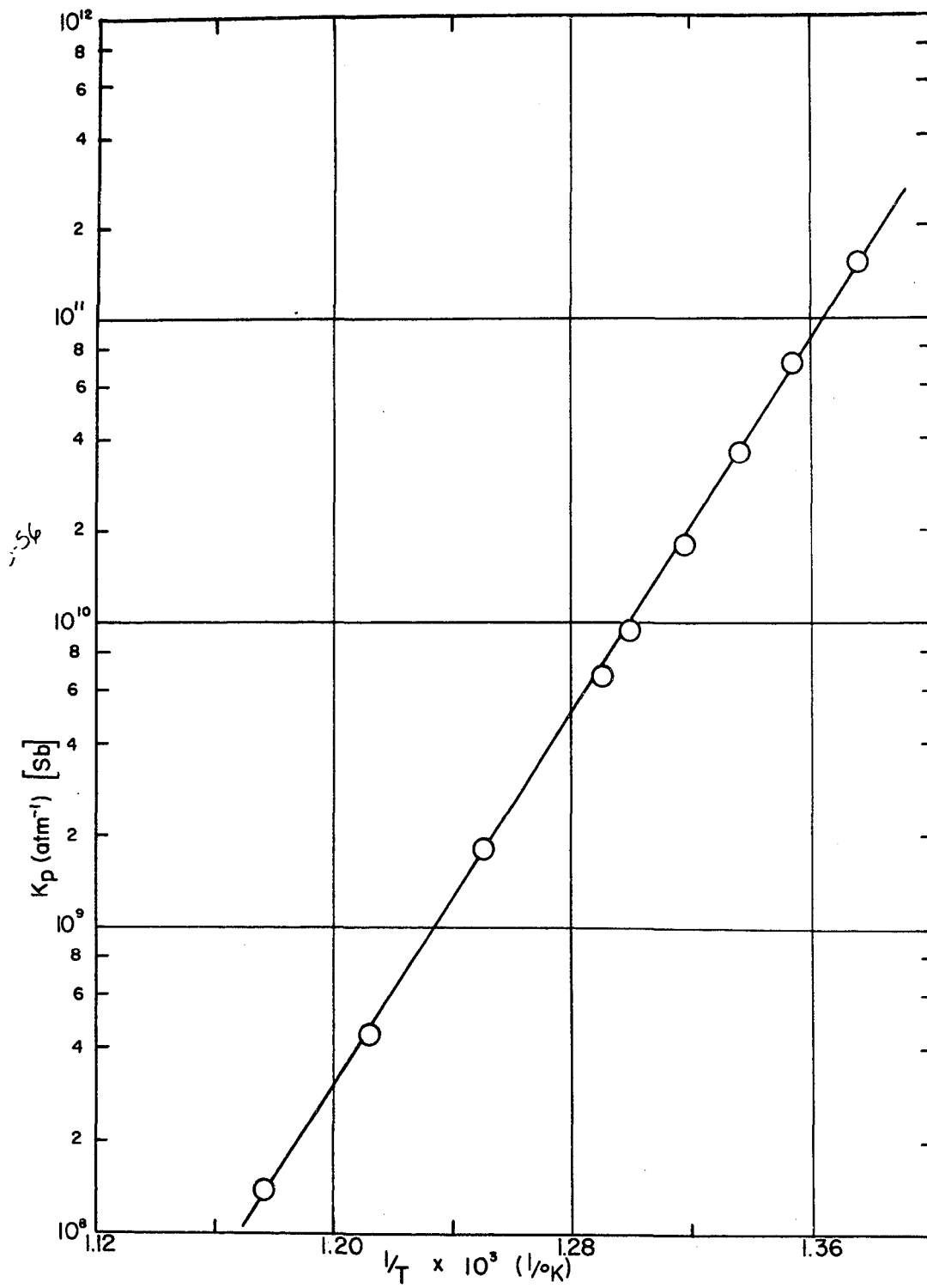


Figure 15. Equilibrium Constant $Sb_2 - Sb_4$

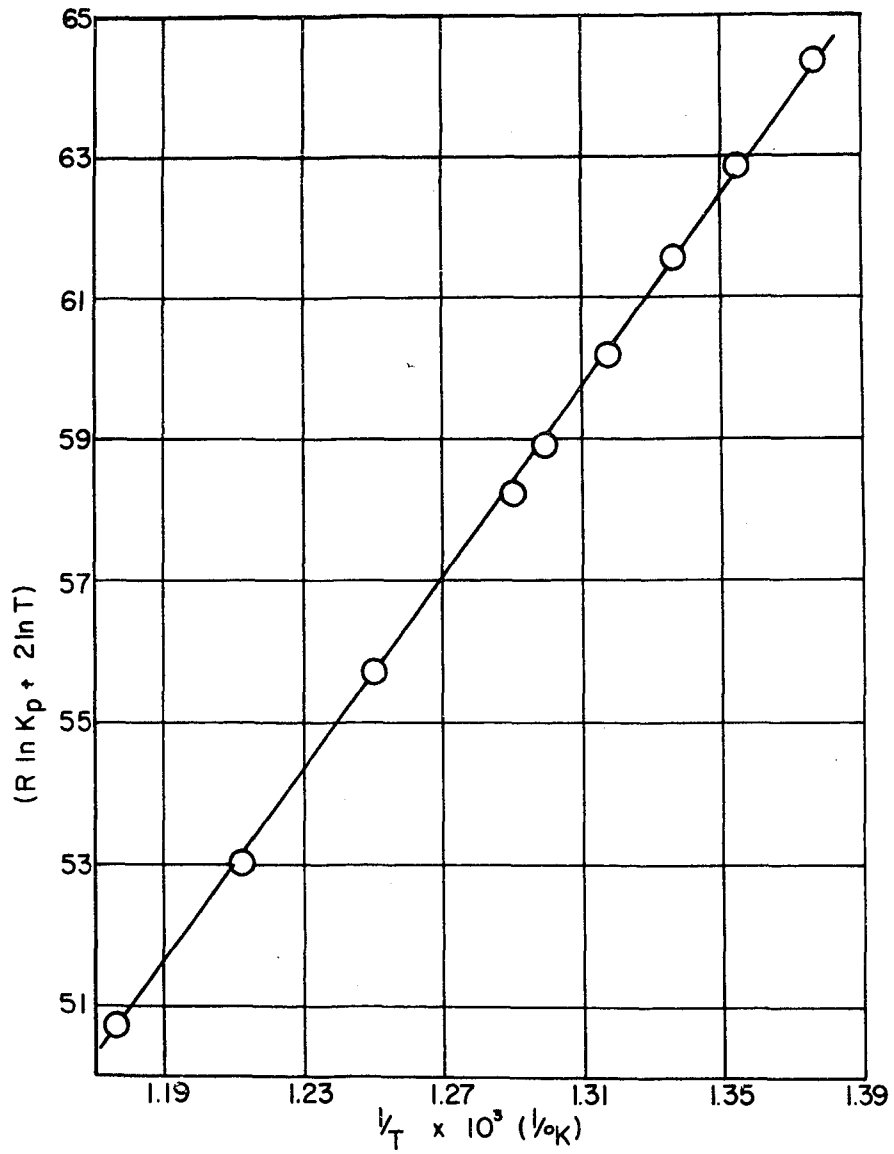


Figure 16. Correlation of K_p for Antimony

and calculated data which is tabulated in Appendix B.

Spectroscopic data on antimony is insufficient to allow calculation of K from equation (8), thus no comparison of experimental K_p with theoretical values are given.

Results for Lead

The results obtained for the total vapor pressure of lead are shown in Figure 17. Application of the least squares method to the data yields the expression:

$$\log P(\text{mmHg}) = 7.74 - \frac{9,570}{T} .$$

The total heat of vaporization as calculated from the relation above is 43.77 ± 0.1 kcal/gram mole of liquid, over the temperature range of 845-1025°K.

Over the range of measurements taken on lead the molecular weight showed no discernible change and was the same value as the atomic weight indicating monatomic vapor molecules were present exclusively.

The experimental data for lead, from which the results above are calculated, is shown in Appendix C.

Results for Sodium

For the total vapor pressure of sodium, the results obtained are given in Figure 18. The least squares analysis of the data yields:

$$\log P(\text{mmHg}) = 7.83 - \frac{5,560}{T} .$$

The total heat of vaporization calculated from the above rela-

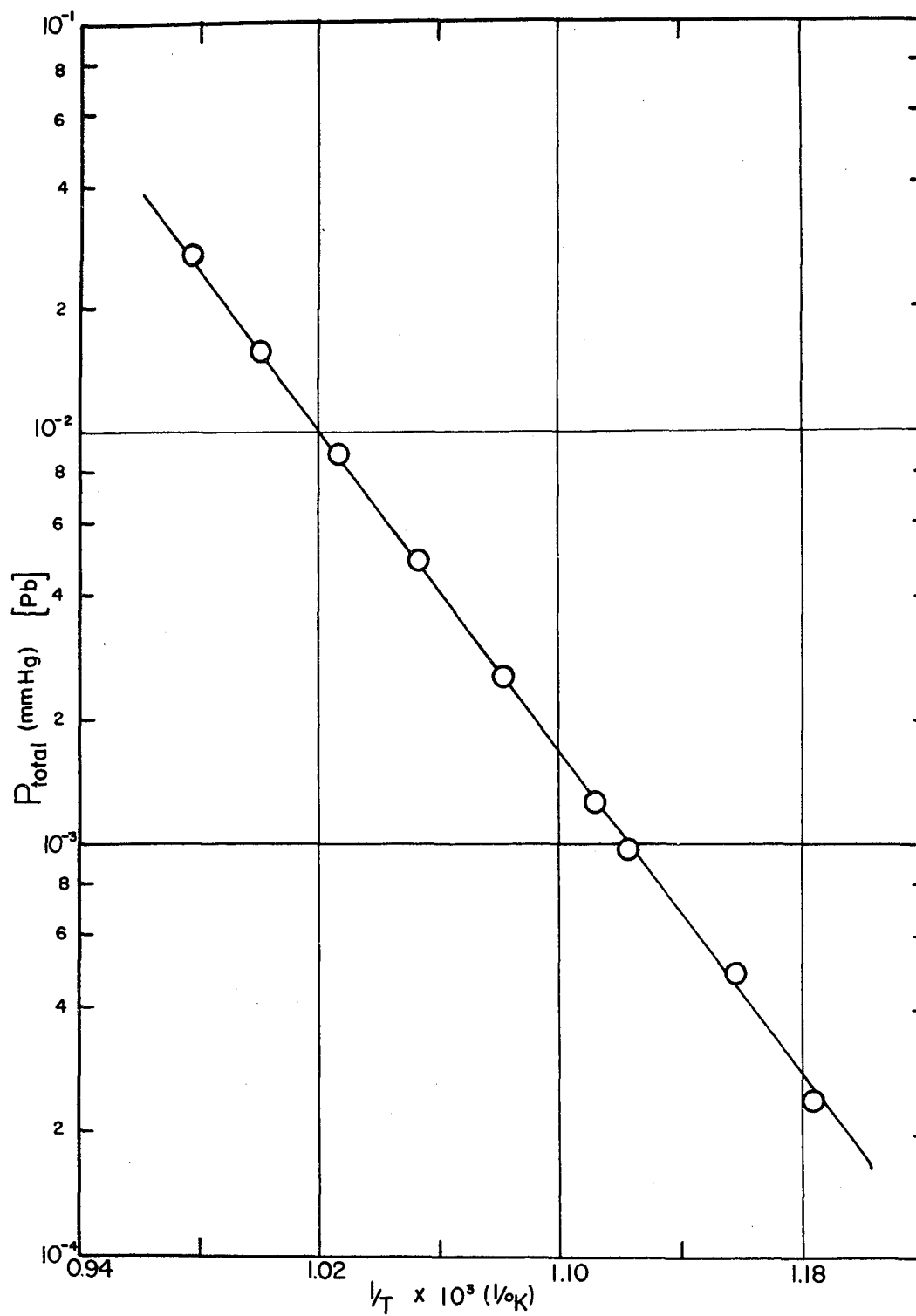


Figure 17. Total Vapor Pressure of Lead

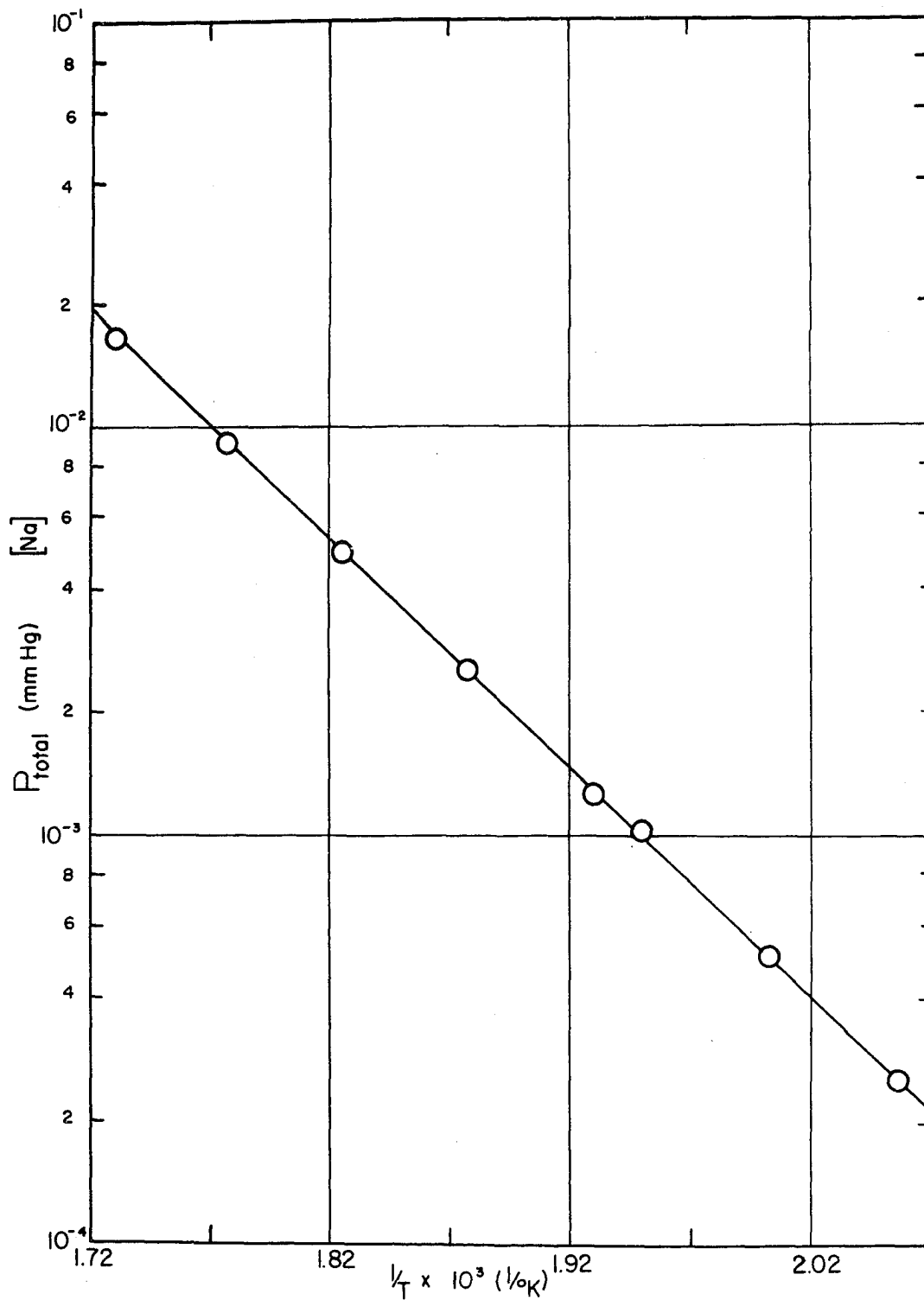


Figure 18. Total Vapor Pressure of Sodium

relationship is 25.43 ± 0.1 kcal/gram mole of liquid, over the temperature range of 486.5-578°K.

The calculated results for the vapor pressures of Na and Na₂ are shown in Figures 19 and 20 respectively. The least squares analysis of the data yields the expressions:

$$\log p_1(\text{mmHg}) = 7.66 - \frac{5,470}{T}$$

$$\log p_2(\text{mmHg}) = 8.63 - \frac{6,960}{T}$$

Thus, the heat of vaporization of Na is calculated as 25.02 ± 0.1 kcal/gram atom and the heat of vaporization of Na₂ as 31.83 ± 0.1 kcal/gram mole, in the temperature range of 486.5-578°K.

The calculated values of the equilibrium constant K_p ($2\text{Na} \rightleftharpoons \text{Na}_2$) are given in Figure 21. The least squares analysis of the K_p values yields:

$$\log K_p = -3.74 + \frac{3,950}{T}$$

where K_p is in atm^{-1} . From the K_p relation above the heat of dissociation of Na₂ is calculated to be 18.06 ± 0.1 kcal/gram mole of Na₂, in the temperature range of 486.5-578°K.

The experimental results show that $\Delta H_D < (\Delta H_V)_1$ for sodium, so that the theoretical prediction is substantiated by the results.

Figure 22 shows a plot of $(R \ln K_p - \ln T)$ versus $1/T$ for sodium ($\Delta a = 1$). The slope of this plot is $(\Delta H_D^\circ)_{298} - 298$ and the value of $(\Delta H_D^\circ)_{298}$ was determined by the least squares method to be 18.30 ± 0.1 kcal/gram mole.

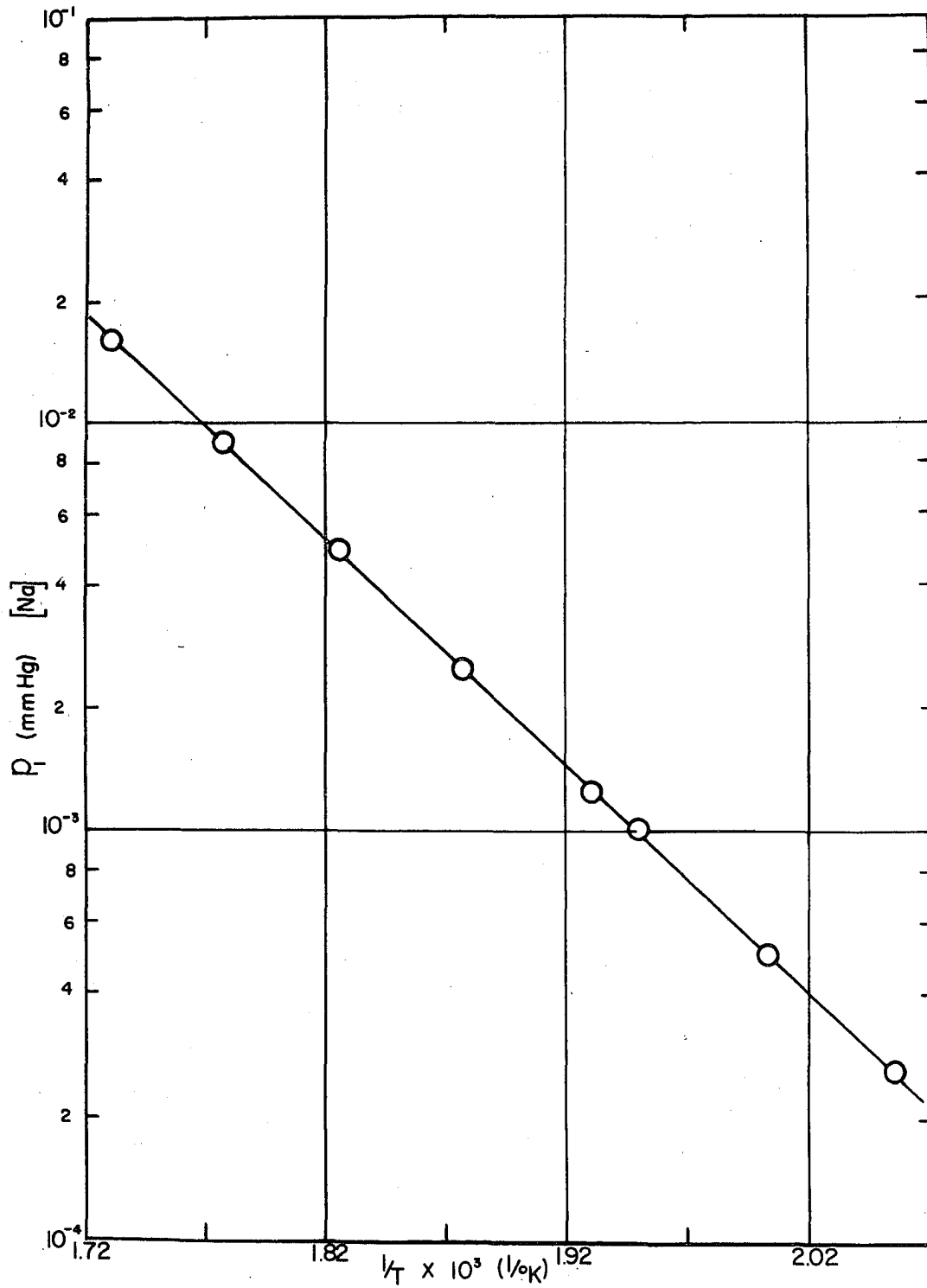


Figure 19. Vapor Pressure of Na

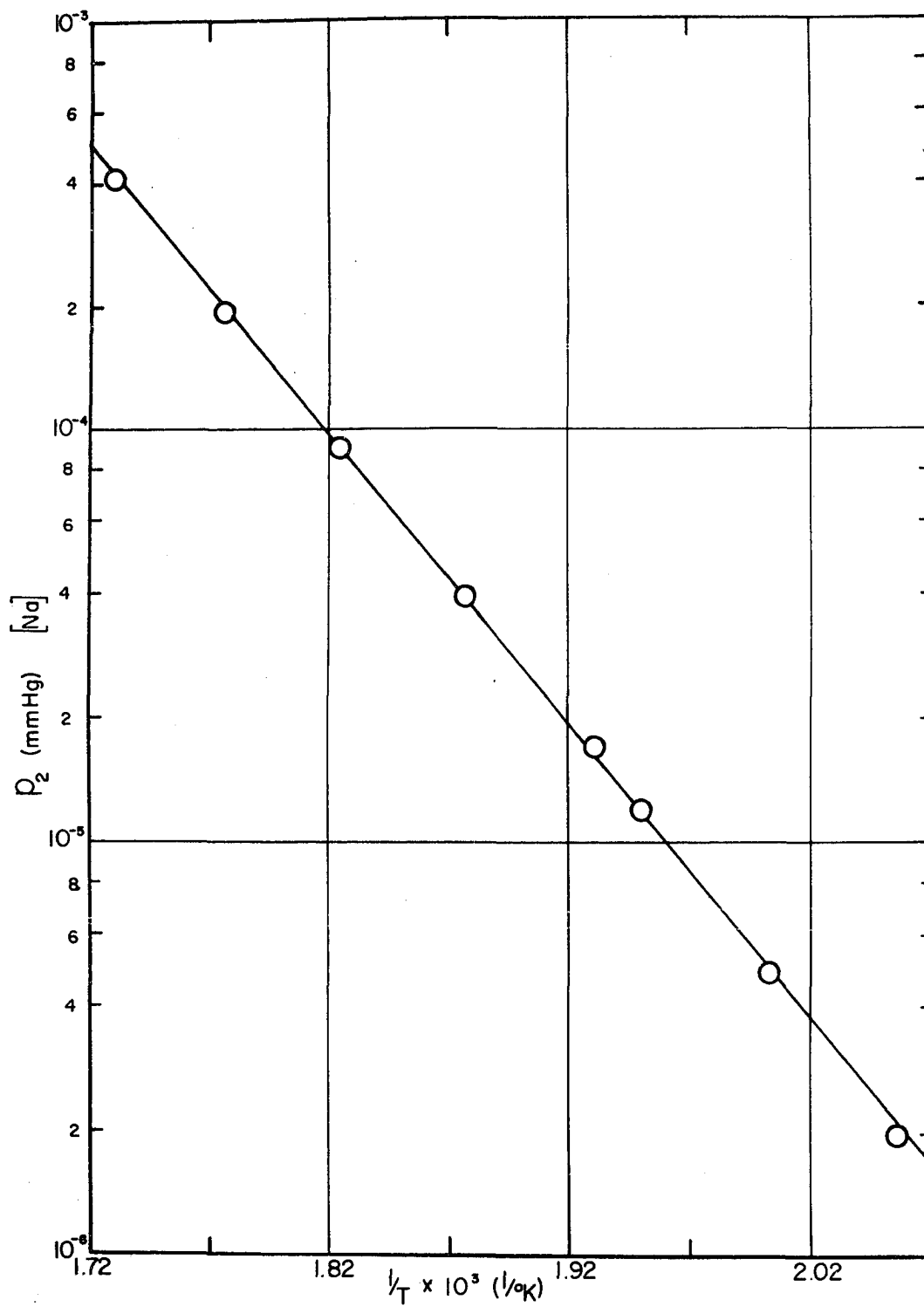


Figure 20. Vapor Pressure of Na_2

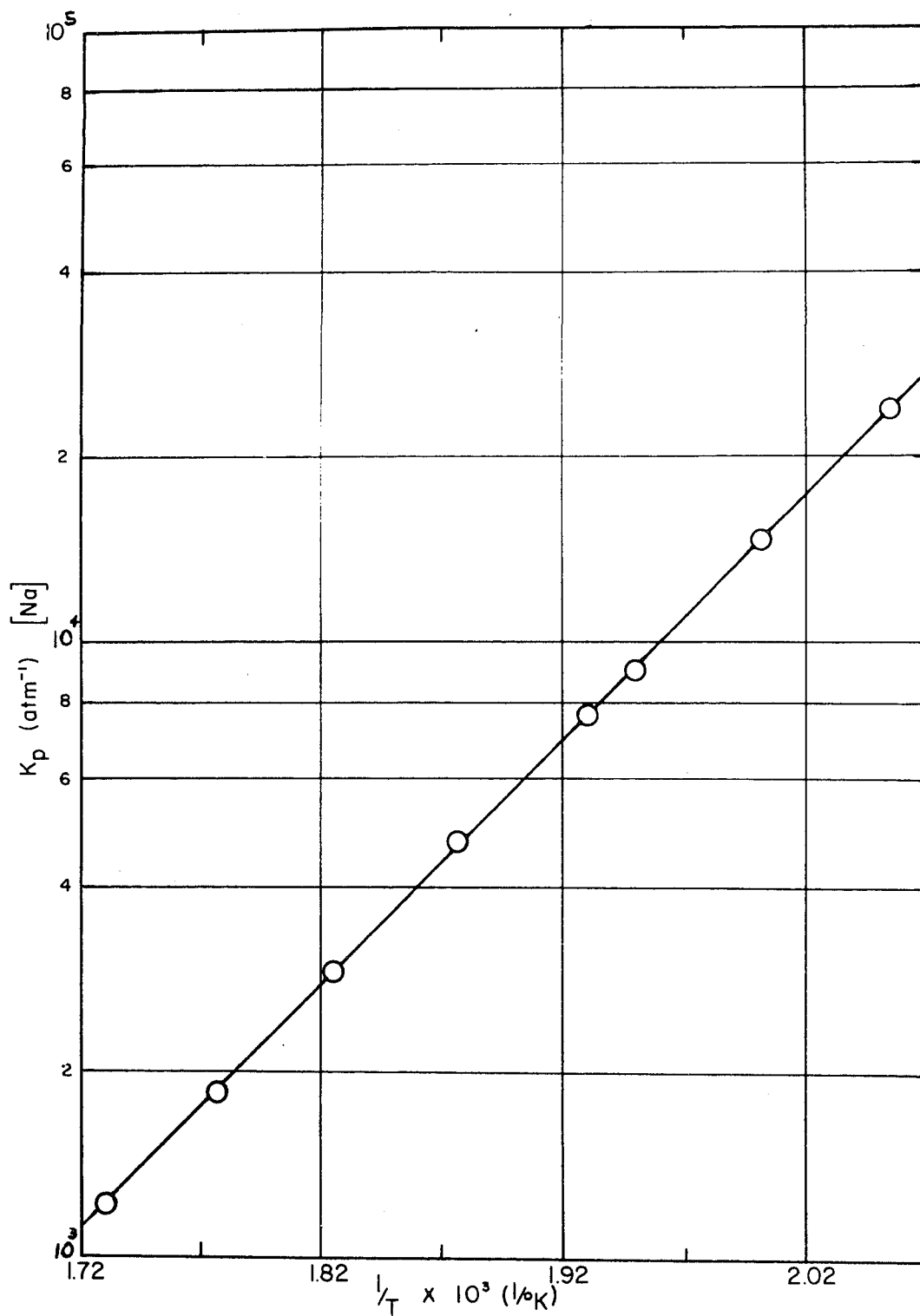


Figure 21. Equilibrium Constant Na - Na₂

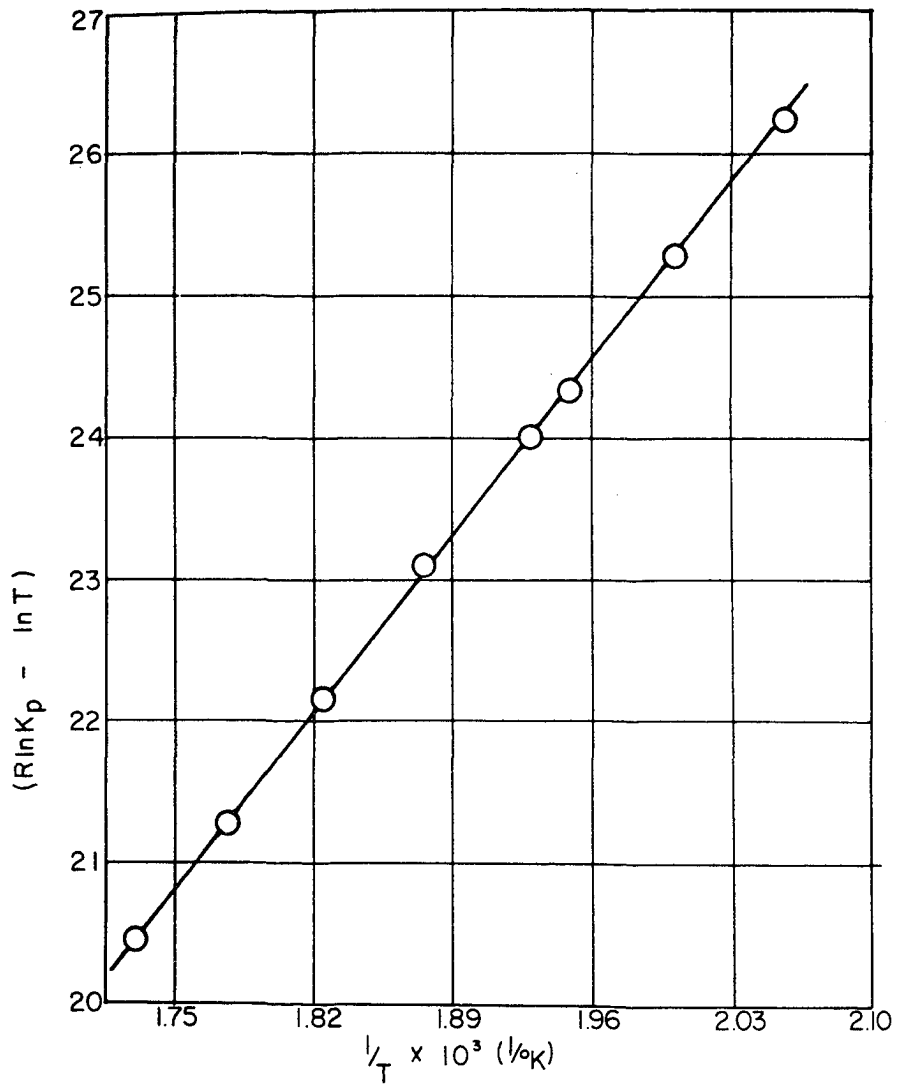


Figure 22. Correlation of K_p for Sodium

The molecular weight of sodium vapor as a function of temperature obtained by the least squares method is:

$$\log M = 1.5099 - \frac{75.74}{T}$$

The experimental and calculated data for sodium is tabulated in Appendix D.

Values of K calculated from equation (8) were determined in the same temperature range as the experimental data. These theoretical values of K_p are compared in Table IV with the values of K_p calculated from the experimental data. The comparison shows good agreement between the theoretical and experimental values. The values of the parameters necessary for calculating the theoretical K values from equation (8) are given in Appendix D.

TABLE IV

Comparison of K Values for Sodium

T(°K)	K_p (atm ⁻¹) <u>Theoretical</u>	K_p (atm ⁻¹) <u>Experimental</u>
513	8.20x10 ³	7.58x10 ³
528	4.93x10 ³	4.76x10 ³
543	3.04x10 ³	2.90x10 ³
558	1.94x10 ³	1.85x10 ³
573	1.25x10 ³	1.21x10 ³

Results for Selenium

The results that were obtained for the total vapor pressure of selenium are shown in Figure 23. Application of the

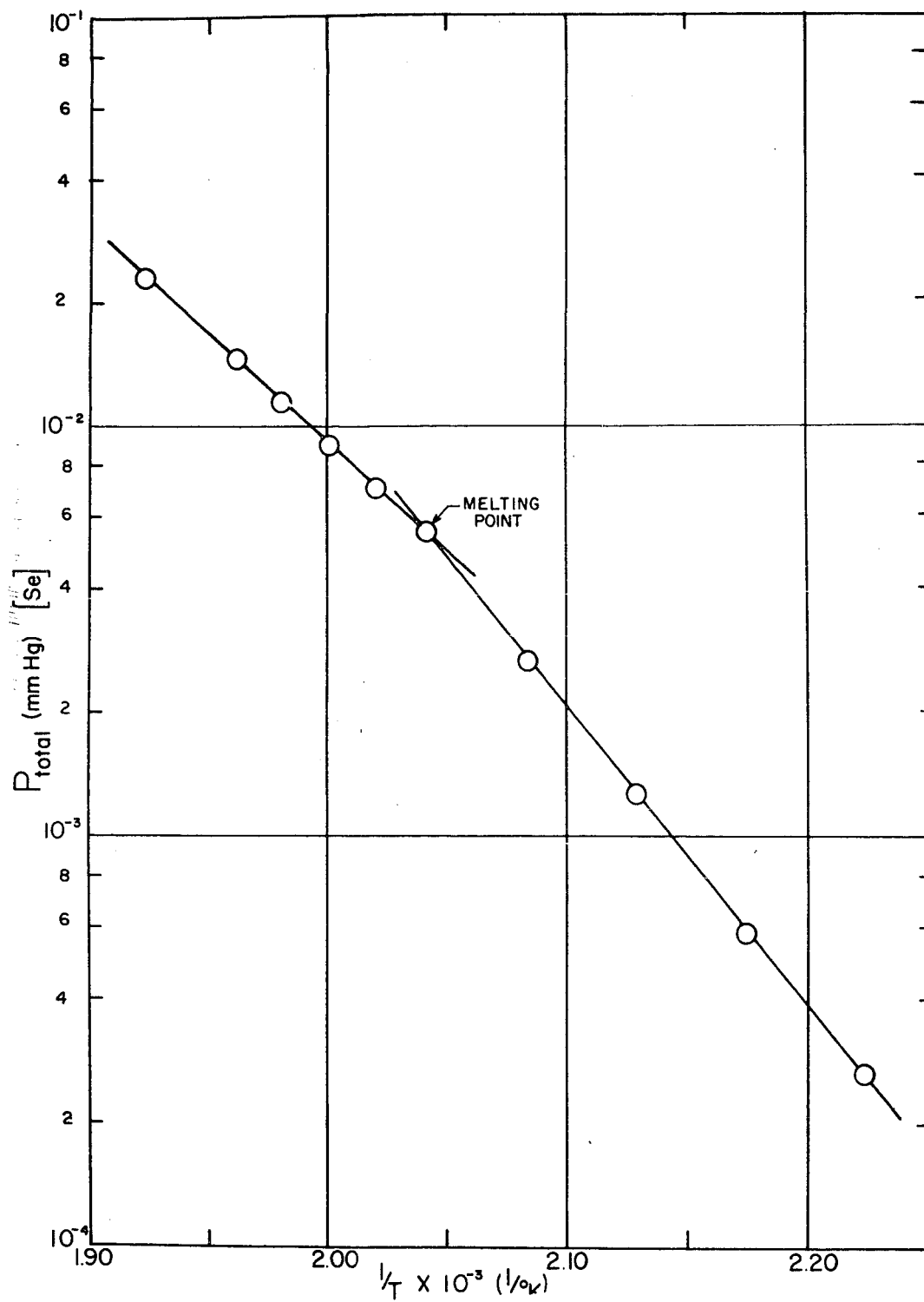


Figure 23. Total Vapor Pressure of Selenium

least squares method to the data yields the expressions:

$$\log P_S(\text{mmHg}) = 12.68 - \frac{7,320}{T}$$

$$\log P_L(\text{mmHg}) = 8.49 - \frac{5,270}{T}$$

where P_S and P_L are the total vapor pressures above the solid and liquid selenium respectively (the melting point occurs at 217°C , which is within the measuring range). From the P_S relation the total heat of sublimation is calculated as 33.50 ± 0.1 kcal/gram mole of solid, and from the P_L relation the total heat of vaporization is 24.12 ± 0.1 kcal/gram mole of liquid. Experimental data was taken over a temperature range of $450\text{--}520^\circ\text{K}$.

The results calculated for the vapor pressures of Se_2 and Se_6 are given in Figures 24 and 25 respectively. The least squares analysis of the vapor pressure data yields for the solid range:

$$\log (p_2)_S(\text{mmHg}) = 13.12 - \frac{7,980}{T}$$

$$\log (p_6)_S(\text{mmHg}) = 12.68 - \frac{7,330}{T}$$

The expressions for the vapor pressures over liquid selenium are:

$$\log (p_2)_L(\text{mmHg}) = 8.48 - \frac{5,850}{T}$$

$$\log (p_6)_L(\text{mmHg}) = 8.32 - \frac{5,220}{T}$$

The heats of sublimation are calculated to be: $\text{Se}_2 - 36.48 \pm 0.1$ kcal/gram mole; $\text{Se}_6 - 33.11 \pm 0.1$ kcal/gram mole. The heats of vaporization are: $\text{Se}_2 - 26.71 \pm 0.1$ kcal/gram mole; $\text{Se}_6 - 23.87 \pm 0.1$ kcal/gram mole.

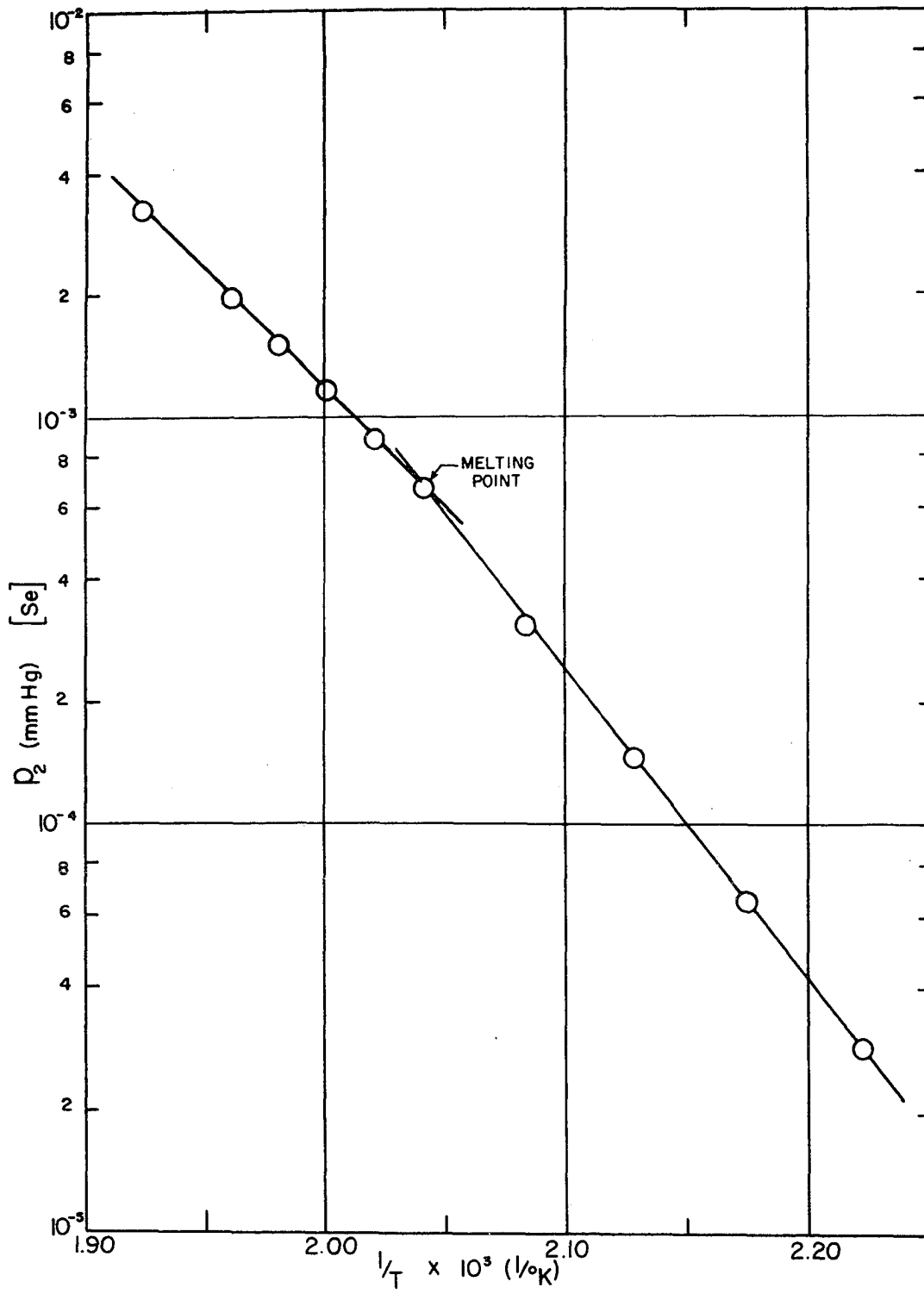


Figure 24. Vapor Pressure of Se₂

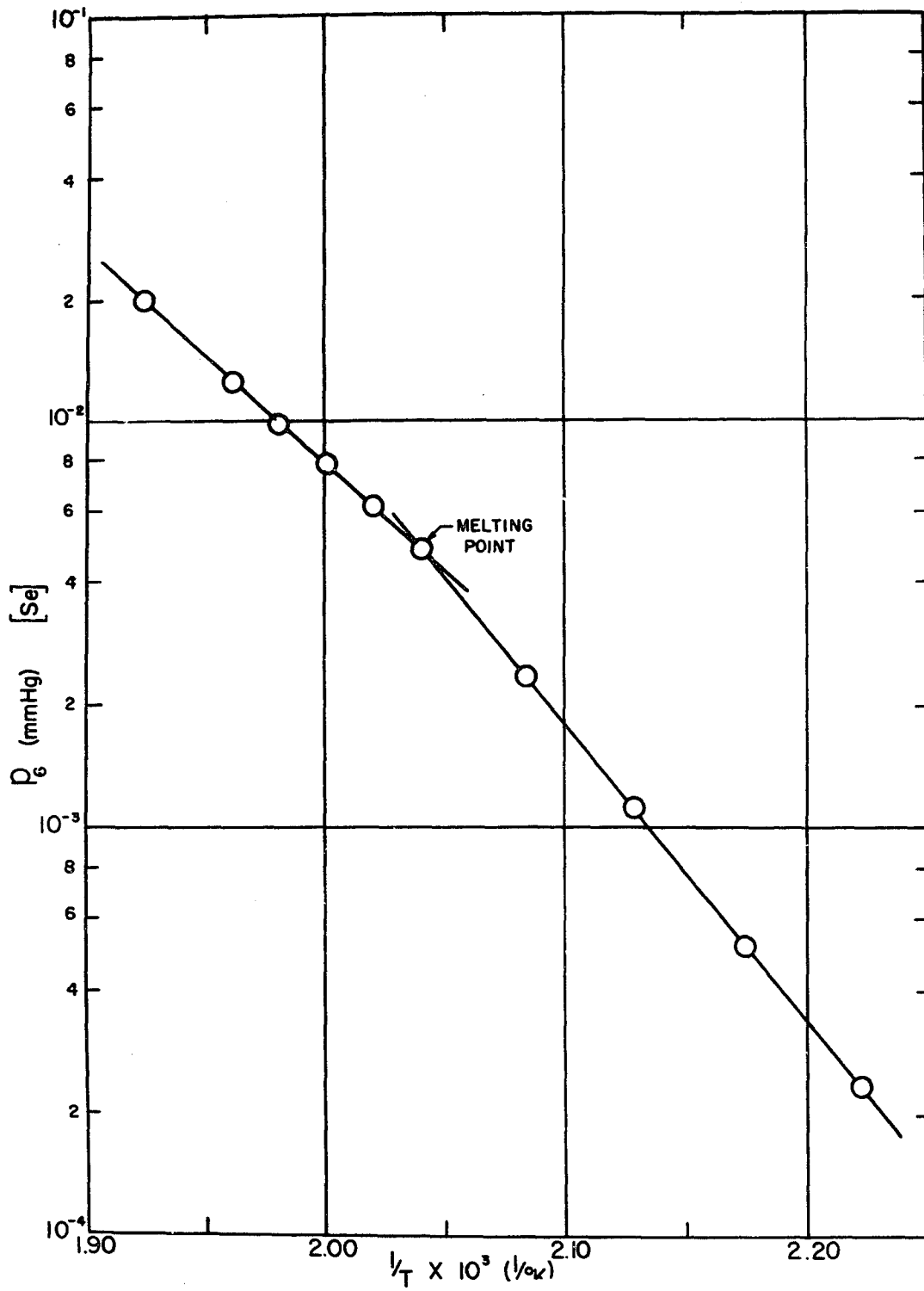


Figure 25. Vapor Pressure of Se_6

The values calculated for the equilibrium constant K_p ($3\text{Se}_2 \rightleftharpoons \text{Se}_6$) are shown in Figure 26. The least squares method yields the expressions:

$$\log K_S = -17.74 + \frac{15,060}{T}$$

$$\log K_L = -11.32 + \frac{12,300}{T}$$

where the K's are in atm^{-1} . From the above relations the values of the heat of dissociation are: above the solid selenium - 68.90 ± 0.1 kcal/gram mole Se_6 ; above the liquid selenium - 56.27 ± 0.1 kcal/gram mole Se_6 (in the temperature range of $450\text{--}520^\circ\text{K}$).

The experimental results show that $\Delta H_d > (\Delta H_v)_2$ for selenium, thus the theoretical prediction agrees with the results.

The molecular weight of selenium vapor as a function of temperature obtained by the least squares method is:

$$\log M_S = 2.5709 + \frac{28.73}{T}$$

$$\log M_L = 2.6061 + \frac{10.50}{T}$$

The experimental and calculated data for selenium are tabulated in Appendix E.

The K_p value for the equilibrium $3\text{Se}_2 \rightleftharpoons \text{Se}_6$ is not calculated from the theoretical considerations for two reasons: (1) the spectroscopic data for Se_6 is questionable, and (2) it is not known whether the mechanism applied in the other equilibrium cases can be applied to the above equilibrium since Se_6 is formed from three molecules instead of two as in the other cases.

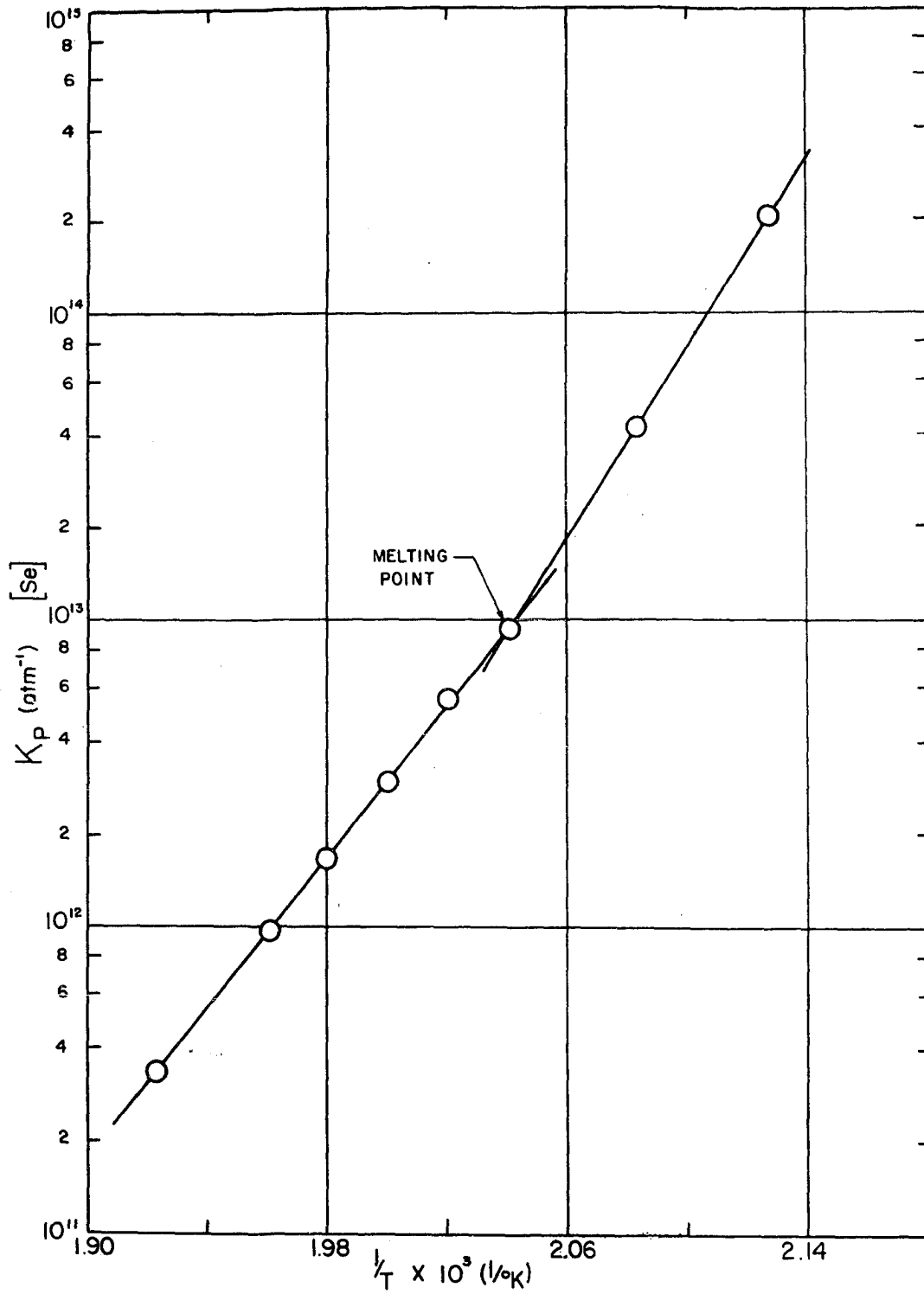


Figure 26. Equilibrium Constant $\text{Se}_2 - \text{Se}_6$

Results for Indium

The values obtained for the total vapor pressure of indium are shown in Figure 27. A least squares analysis of the data gives:

$$\log P(\text{mmHg}) = 8.41 - \frac{12,640}{T}$$

From the above relation the total heat of vaporization is determined as 57.82 ± 0.1 kcal/gram mole, over the temperature range of 1050-1250°K.

The measurements taken on indium showed there was no change in the molecular weight with temperature (except for deviation due to experimental error) and the molecular weight was the same as the atomic weight indicating the predominance of the monatomic species.

The experimental data on indium is tabulated in Appendix F.

Additional Results

As a means of checking the reliability of the experimental results obtained with the apparatus it was felt desirable to answer the following questions: (1) is there any net torque exerted on the torsion suspension due to diffusion through the cell walls, (2) does the diameter of the cell orifices affect the measurements, and (3) does the length of the cell orifices affect the measurements.

In order to answer question (1) a "blank cell" (a cell with no orifices but otherwise unchanged) was made, a sample

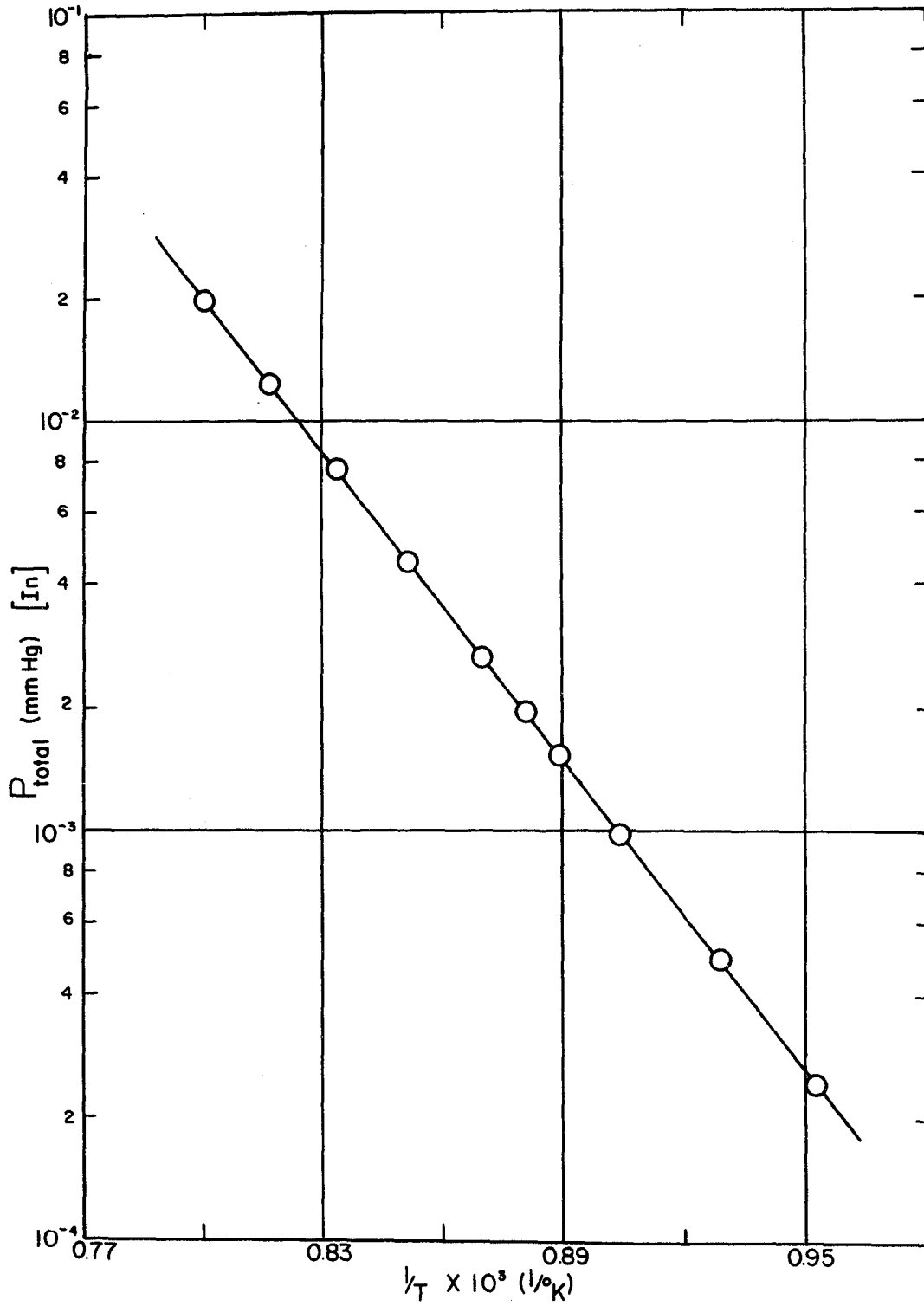


Figure 27. Total Vapor Pressure of Indium

inserted in the cell, and a run was made under experimental conditions. There was no detectable torque exerted on the torsion suspension.

Question (2) was answered by determining the vapor pressure at identical experimental conditions with three cells, each having a different orifice diameter but otherwise identical. The vapor pressure was determined at two different sets of conditions with each of the three cells. The results obtained are shown in Figure 28. The correspondence between the values obtained from the three cells is within the experimental error of the apparatus.

Question (3) was answered by determining the vapor pressure under three sets of experimental conditions which should produce the same vapor pressure with one cell having three different orifice lengths but the same orifice diameter. Cell No. 2 was used in these determinations. The cell is designated as No. 2, No. 2a, or No. 2b to correspond to the different orifice lengths of the cell. The results obtained are shown in Figure 29. The correspondence between the values measured with the three orifice lengths is within the experimental error of the apparatus.

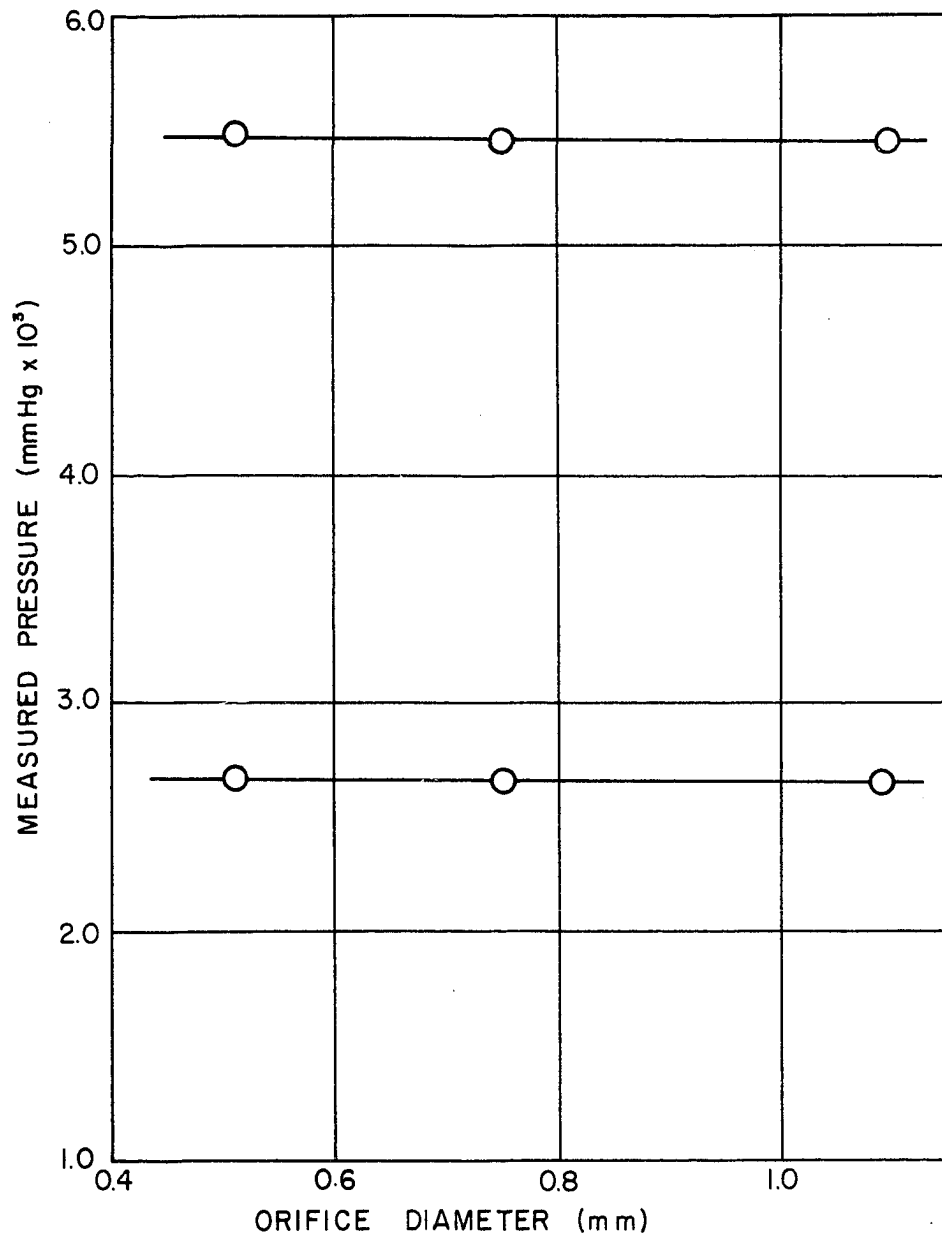


Figure 28. Measured Pressure vs. Orifice Diameter

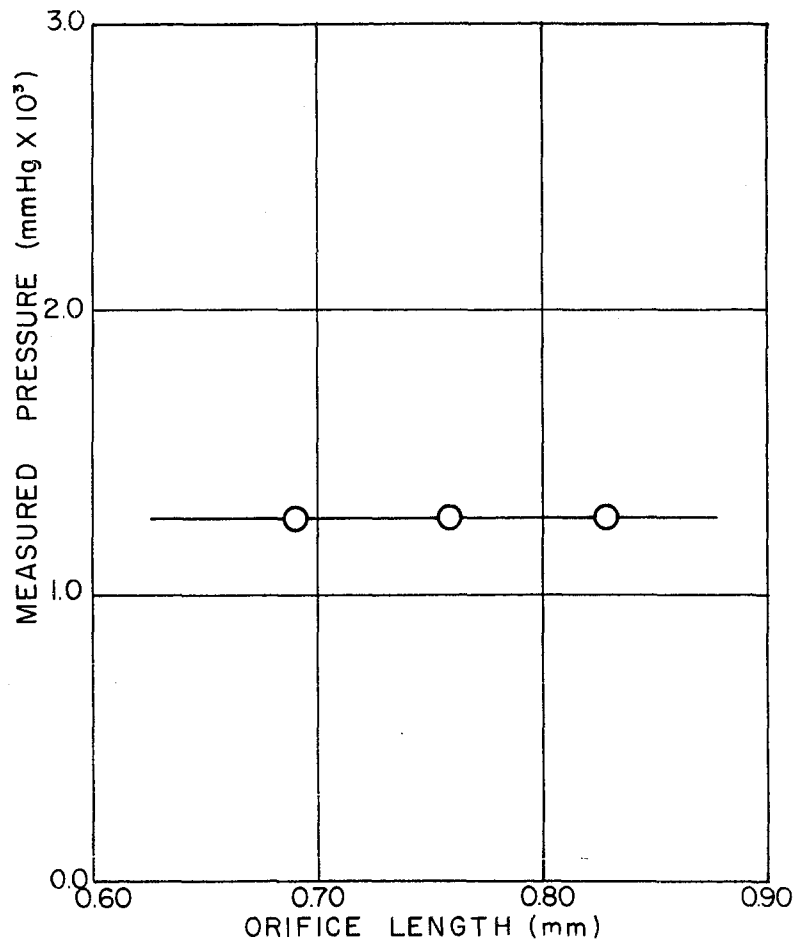


Figure 29. Measured Pressure vs. Orifice Length

CHAPTER V

DISCUSSION

A comparison of previously reported values of the total vapor pressure of bismuth with those determined in this study is shown in Figure 30. As it may be seen in the figure, there is no general agreement between values of the various investigators. However it was pointed out earlier that there are some fairly evident reasons that the values reported by Yoshiyama are lower than they should be. The values reported by O'Donnell would also be expected to be low due to his assumption of a molecular weight of 418 (all Bi_2). The reported values of Granovskaya and Lubimov have been discussed earlier and it is expected that these values should be high. The values given in "Selected Values for the Thermodynamic Properties of Metals and Alloys"⁽²⁶⁾ are calculated from a compilation of the thermodynamic properties of bismuth and may not agree well with measured values.

From the experimental work on bismuth values were calculated for the total heat of vaporization (ΔH_T°), the heats of vaporization of Bi and Bi_2 (ΔH_1° and ΔH_2°), and the heat of

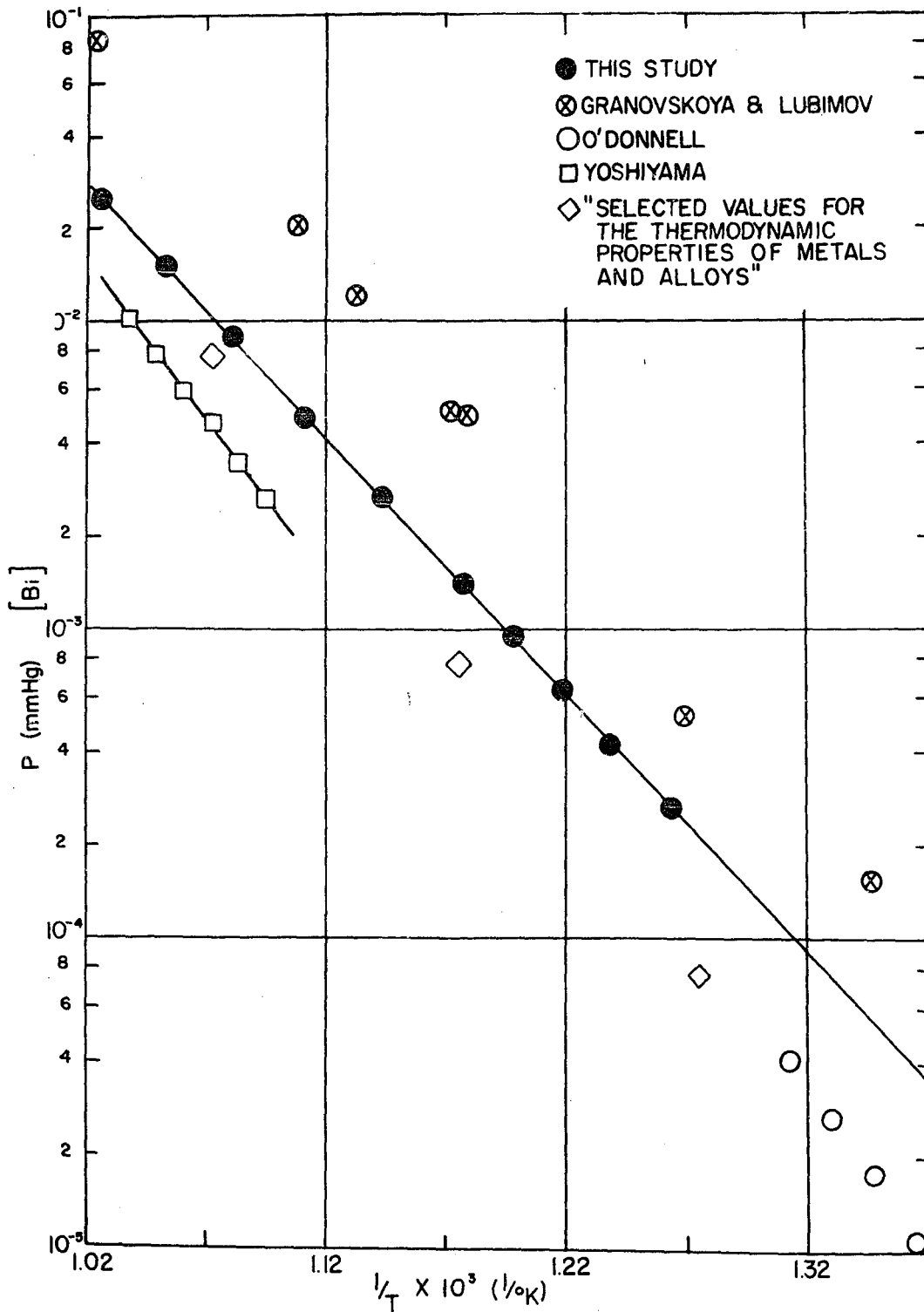


Figure 30. Comparison of Bismuth Vapor Pressures

dissociation of Bi_2 (ΔH_d°). A comparison of the values reported in this study with those previously reported is given in Table V. The values reported by previous investigators are corrected to 298°K by the Third Law method of Brackett and Brewer. All values are in kcal/gram mole.

TABLE V

Heats of Vaporization and Dissociation of Bismuth

Investigator	$(\Delta H_T^\circ)_{298}$	$(\Delta H_1^\circ)_{298}$	$(\Delta H_2^\circ)_{298}$	$(\Delta H_d^\circ)_{298}$
This study	42.53 \pm 0.1	44.10 \pm 0.1	45.26 \pm 0.1	43.51 \pm 0.1
Cosgarea	---	41.7	47.9	35.8
Yoshiyama	51.5	(60.0)	(50.0)	70.6
O'Donnell	51.7 \pm 0.6	---	---	---
Granovskaya and Lubimov	42.61	---	---	---
Ko	81.1 \pm 1.2	---	---	---
Leu	65.1 \pm 26.7	---	---	---

A comparison of the values of the total vapor pressure of antimony taken in this study with the recent work of Rosenblatt and Birchenall⁽²⁵⁾ and the earlier work of Niwa and Yoshiyama⁽³³⁾ is shown in Figure 31. The agreement of the values is excellent.

The data of Niwa and Yoshiyama on antimony agrees well with the values from this study whereas the data of Yoshiyama on bismuth does not, even though the same apparatus was used. The difference could be due to some changes made in the

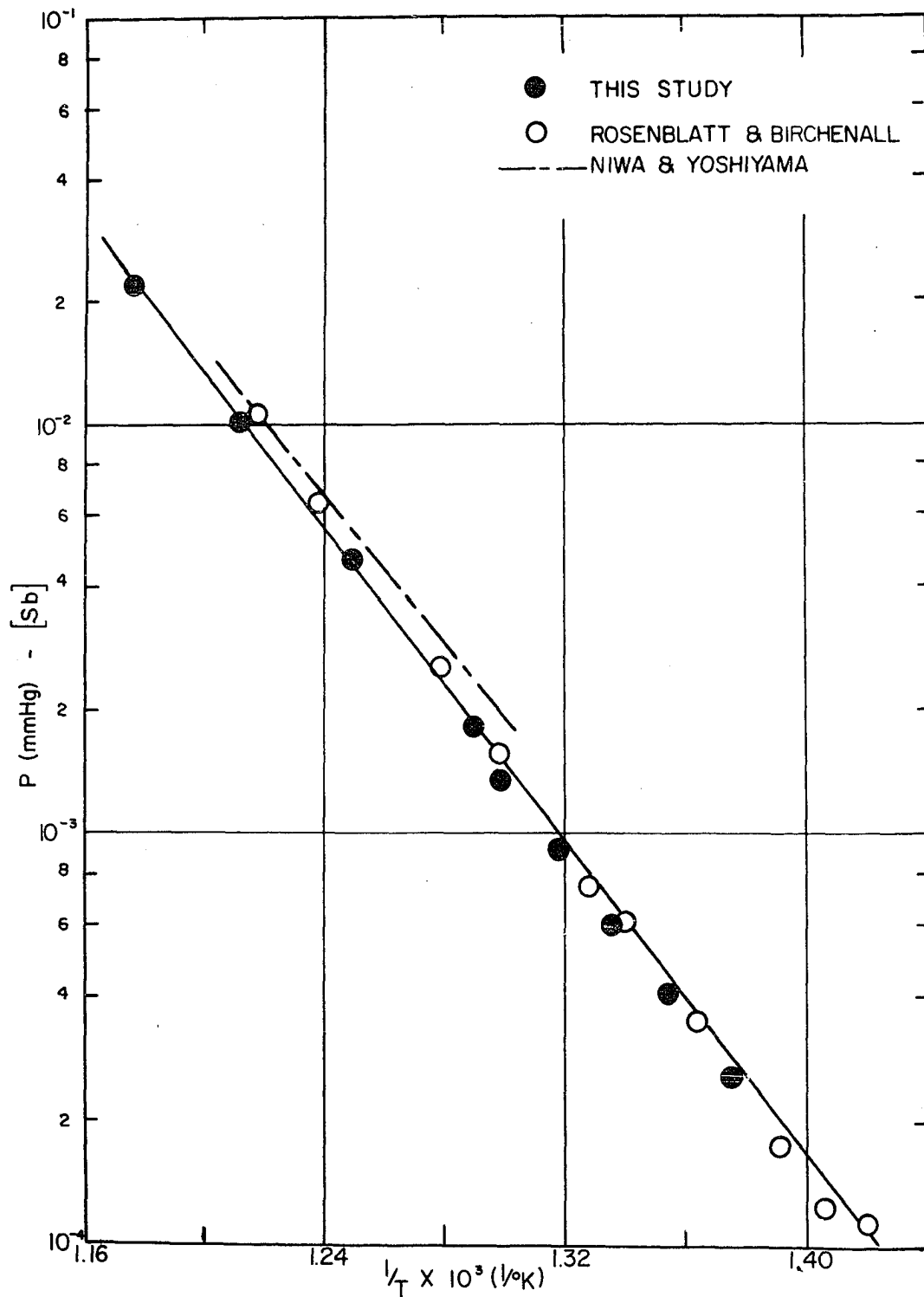


Figure 31. Comparison of Antimony Vapor Pressures

apparatus. It is known that a platinum torsion fiber was used for bismuth. There may have been other differences not mentioned.

The experimental data on antimony yield values of the total heat of vaporization, the heats of vaporization of Sb_2 and Sb_4 , and the heat of dissociation of Sb_4 . Table VI gives a comparison of the values obtained in this study for the heat of vaporization of Sb_4 and the heat of dissociation of Sb_4 with those previously reported.

TABLE VI

Heats of Vaporization and Dissociation of Antimony

<u>Investigator</u>	<u>$(\Delta H_4^\circ)_{298}$</u>	<u>$(\Delta H_d^\circ)_{298}$</u>
This Study	47.75 \pm 0.1	64.68 \pm 0.1
Niwa and Yoshiyama	49.04	57.40
Rosenblatt and Birchenall	49.45 \pm 0.09	---

The total vapor pressure of lead determined in this study is compared with the previously reported data by Egerton⁽⁹⁾ and Aldred and Pratt⁽¹⁾ in Figure 32. Only the least squares representation of the vapor pressure data was obtainable. The values of the other investigators lie slightly below those of this study. The difference in the values might be due to the presence of lead oxide on the samples since lead will oxidize considerably in a short period of exposure unless careful precautions are taken. Neither of the previous investigators mentioned precautions for cleaning the surface of the

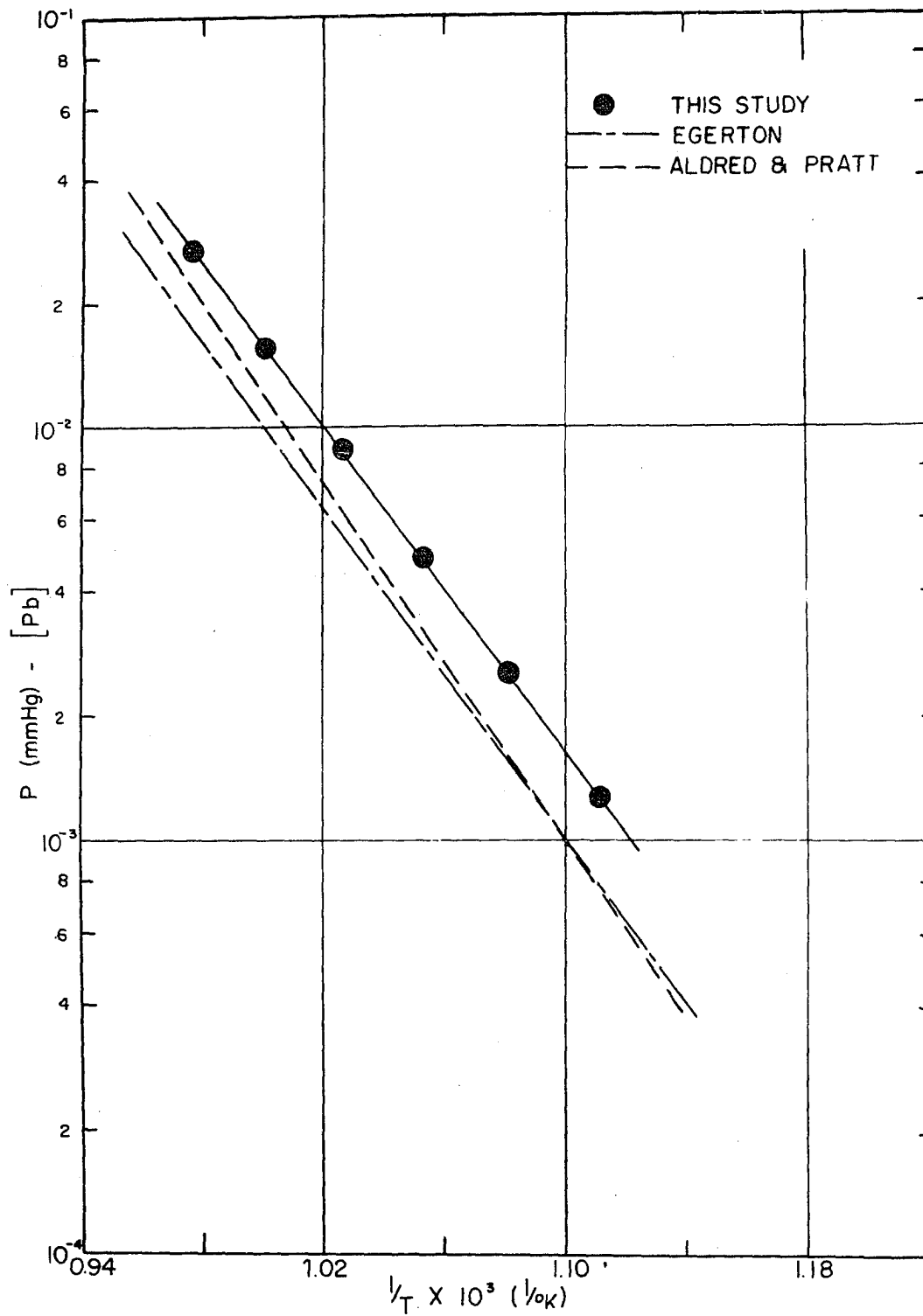


Figure 32. Comparison of Lead Vapor Pressures

samples to remove oxide. The experimental data on lead yield only a value of total heat of vaporization. Table VII gives a comparison of the values obtained in this study for the heat of vaporization of Pb with those reported by the other investigators.

TABLE VII

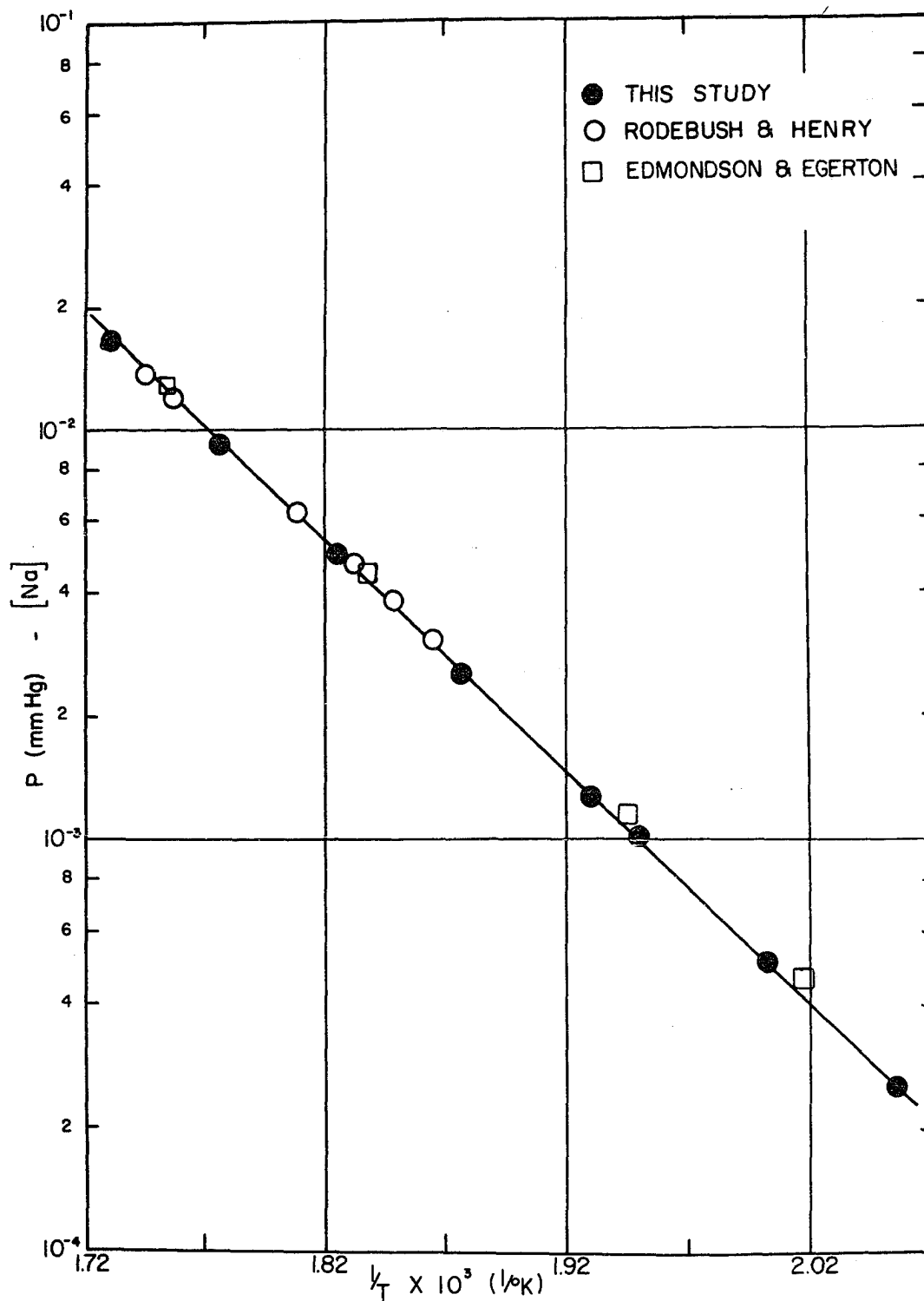
Heat of Vaporization of Lead

<u>Investigator</u>	<u>$(\Delta H_T^\circ)_{298}$</u>
This Study	46.94 \pm 0.10
Begerton	47.17 \pm 0.20
Aldred and Pratt	46.81 \pm 0.52

The values of the total vapor pressure of sodium measured in this study are compared with some values of previous investigators in Figure 33. The agreement is excellent.

From the experimental data on sodium values of the total heat of vaporization, the heats of vaporization of Na and Na₂, and the heat of dissociation of Na₂ were calculated. A comparison of the values of the heat of vaporization of Na and the heat of dissociation of Na₂ obtained in this study with the previously reported values is given in Table VIII.

A comparison of the values of the total vapor pressure of selenium determined in this study with some previously reported values is shown in Figure 34. The agreement of values is only fair. There seems to be no explanation for the difference since the methods used are basically the same.



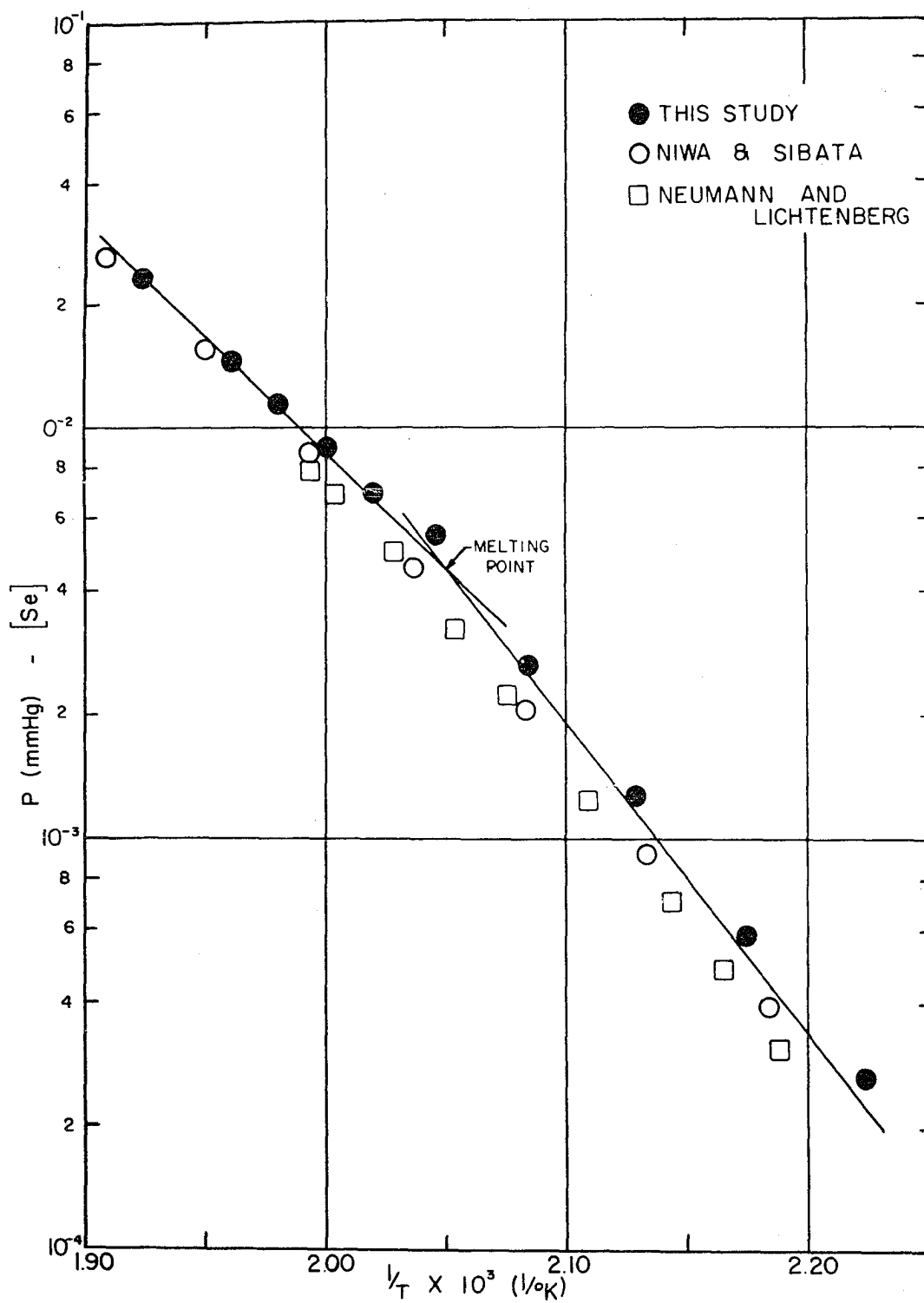


Figure 34. Comparison of Selenium Vapor Pressures

TABLE VIII

Heats of Vaporization and Dissociation of Sodium

<u>Investigator</u>	<u>$(\Delta H_1^\circ)_{298}$</u>	<u>$(\Delta H_d^\circ)_{298}$</u>
This Study	26.22 \pm 0.1	18.30 \pm 0.1
Rodebush and Henry	26.32	---
Edmondson and Egerton	26.30	---
Thomson and Garellis*	26.31	17.96

The experimental data on selenium yield values of the total heat of vaporization, the heats of vaporization of Se_2 and Se_6 , and the heat of dissociation of Se_6 . Table IX gives a comparison of the total heat of vaporization and the heat of dissociation of Se_6 determined in this study with the previously reported values.

TABLE IX

Heats of Vaporization and Dissociation of Selenium

<u>Investigator</u>		<u>**(ΔH_T°)</u>	<u>**(ΔH_d°)</u>
This Study	(Liquid)	24.12 \pm 0.1	56.27 \pm 0.1
	(Solid)	33.50 \pm 0.1	68.90 \pm 0.1
Neumann and Lichtenberg	(Liquid)	24.58	---
	(Solid)	33.92	---
Niwa and Sibata	(Liquid)	26.80 \pm 0.4	58.39 \pm 0.4
	(Solid)	33.22 \pm 0.4	67.87 \pm 0.4

*This work is a compilation of several investigator's data.

**These are values in the experimental range which is nearly identical in the three determinations.

The total vapor pressure of indium determined in this study is compared with some experimental values listed in "Selected Values for the Thermodynamic Properties of Metals and Alloys" in Figure 35. The agreement between the values is quite good. The data on indium yield a value of the total heat of vaporization at 298^oK of 59.77±0.1 kcal/gram mole compared to the value 58.01 kcal/gram mole listed in "Selected Values for the Thermodynamic Properties of Metals and Alloys."

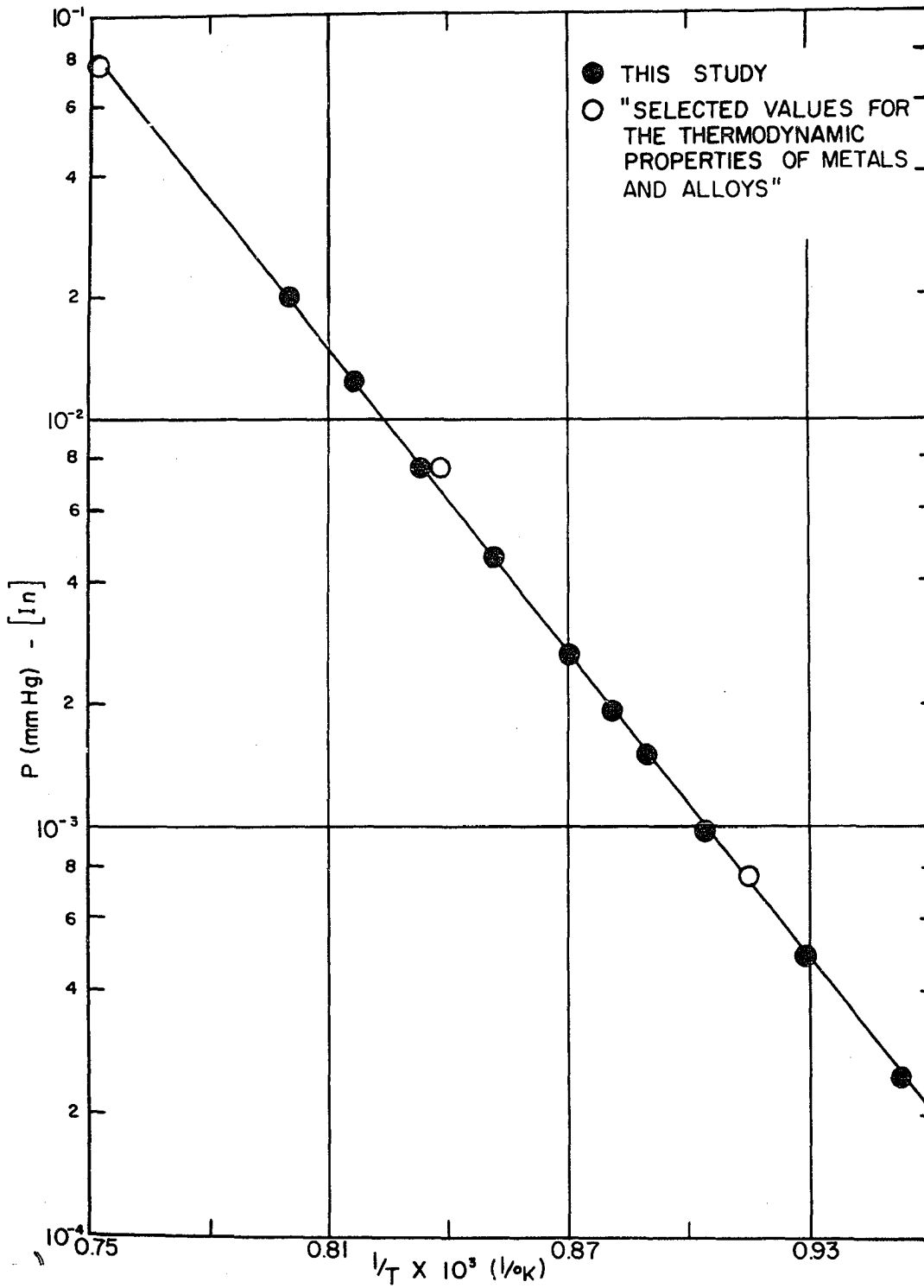


Figure 35. Comparison of Indium Vapor Pressures

CHAPTER VI

CONCLUSIONS

As a result of the experimental work done in this study the following is concluded:

(1) The combined torsion-effusion and mass loss apparatus used in this work permits accurate and precise experimental determination of vapor pressures.

(2) The thermodynamic quantities calculated from the experimental data are believed to be the best values available.

The values obtained for the heats of vaporization and heats of dissociation of the elements studied are:

Bismuth: (values at 298.1°K)

Total heat of vaporization	42.53±0.1 kcal/gram mole
Heat of vaporization of Bi	44.10±0.1 kcal/gram mole
Heat of vaporization of Bi ₂	45.26±0.1 kcal/gram mole
Heat of dissociation of Bi ₂	43.51±0.1 kcal/gram mole

Antimony: (values at 298.1°K)

Total heat of vaporization	47.79±0.1 kcal/gram mole
Heat of vaporization of Sb ₂	59.05±2.0 kcal/gram mole
Heat of vaporization of Sb ₄	47.75±0.1 kcal/gram mole
Heat of dissociation of Sb ₄	64.68±0.1 kcal/gram mole

Lead: (value at 298.1°K)

Total heat of vaporization 46.94±0.1 kcal/gram mole

Sodium: (Values at 298.1°K)

Total heat of vaporization 26.80±0.1 kcal/gram mole

Heat of vaporization of Na 26.22±0.1 kcal/gram mole

Heat of vaporization of Na₂ 34.19±0.1 kcal/gram mole

Heat of dissociation of Na₂ 18.30±0.1 kcal/gram mole

Selenium: (values at average temperature of 485°K)

Total heat of vaporization 24.12±0.1 kcal/gram mole

Total heat of sublimation 33.50±0.1 kcal/gram mole

Heat of vaporization of Se₂ 26.71±0.1 kcal/gram mole

Heat of sublimation of Se₂ 36.48±0.1 kcal/gram mole

Heat of vaporization of Se₆ 23.87±0.1 kcal/gram mole

Heat of sublimation of Se₆ 33.11±0.1 kcal/gram mole

Heat of dissociation of Se₆ 68.90±0.1 kcal/gram mole*
56.27±0.1 kcal/gram mole**

Indium: (value at 298.1°K)

Total heat of vaporization 59.77±0.1 kcal/gram mole

* (< 490°K)

** (> 490°K)

BIBLIOGRAPHY

1. Aldred, A.T. and Pratt, J.N. Trans. Faraday Soc., 57, p. 611 (1961).
2. Almy, G.M. and Sparks, F.M. Phys. Rev., 44, p. 365 (1933).
3. Brackett, E. and Brewer, L. "The Heat of Dissociation of Bi₂", UCRL - 3712, 5pp. (1957).
4. Brewer, L. "National Nuclear Energy Series" IV, vol. 19b, Paper #7, McGraw-Hill, New York (1950).
5. Clausing, P. Zeit. Phys., 66, p. 471 (1930).
6. Cosgarea, A. Jr. "Some Thermodynamic Properties of Uranium-Bismuth Alloys", Thesis, Univ. of Mich. (1959).
7. Edmondson, W. and Egerton, A.C. Proc. Roy. Soc. A, 113, p. 520 (1927).
8. Egerton, A.C. Phil. Mag., 33, p. 33 (1917).
9. Egerton, A.C. Proc. Roy. Soc. A., 103, p. 469 (1923).
10. Freeman, R.D. and Searcy, A.W. J. Chem. Phys., 22, p. 762 (1954).
11. Gaydon, A.G. "Dissociation Energies and Spectra of Diatomic Molecules", Wiley, New York (1947).
12. Goldfinger, P. and Drowart, J. "Vaporization of Compounds and Alloys at High Temperature", ASTIA Ad#148038 (1957).
13. Granovskaya, A. and Lubmiov, A. J. Phys. Chem. USSR, 22, p. 103 (1948).
14. Herzberg, G. "Atomic Spectra and Atomic Structure", Dover, New York, (1944).

15. Herzberg, G. "Spectra of Diatomic Molecules", Van Nostrand, New York, 2nd ed. (1950).
16. Ko, C.C. Journal Franklin Institute, 217, p. 173 (1934).
17. Mayer, H. Zeit. Phys., 67, p. 240 (1931).
18. Naude, S.M. South African J. Science, 32, p. 103 (1935).
19. Neumann, K. and Lichtenberg, E. Zeit. Phys. Chem. A., 184, p. 89 (1939).
20. Neumann, K. and Volker, E. Zeit. Phys. Chem. A, 161, p. 33 (1932).
21. Niwa, K. and Sibata, Z. J. Chem. Soc. Japan, 61, p. 667 (1940).
22. O'Donnell, T.A. Aust. J. Sciences, A-8, p. 493 (1955).
23. Richards, A.W. "The Vapor Pressures of Lead-Antimony Alloys and the Atomicity of Antimony Vapor", Physical Chemistry of Process Metallurgy - Part I, Interscience Publishers, N.Y. (1959).
24. Rodebush, W.H. and Henry, W.F. J. Amer. Chem. Soc., 52, p. 3159 (1930).
25. Rosenblatt, G.M. and Birchenall, C.E. J. Chem. Phys., 35, p. 788 (1961).
26. "Selected Values for the Thermodynamic Properties of Metals and Alloys", Inst. of Eng. Research, Univ. of Calif., Berkeley (July, 1959).
27. Stull, D.R. and Sinke, G.C. "Thermodynamic Properties of the Elements", Amer. Chem. Soc., Washington, D.C. (1956).
28. Thomson, G.W. and Garelis, E. "Physical and Thermodynamic Properties of Sodium", Ethyl Corp., Detroit, Mich. (1953).
29. Volmer, M. Zeit. Phys. Chem. Boden. Fest., p. 863 (1931).
30. Weber, A.H. and Kirsch, S.C. Phys. Rev., 57, p. 1042 (1940).
31. Whitman, C.I. J. Chem. Phys., 20, p. 161 (1952).
32. Yoshiyama, M. J. Chem. Soc. Japan, 62, p. 204 (1941).
33. Yoshiyama, M. and Niwa, K. J. Chem. Soc. Japan, 61, p. 1055 (1940).

APPENDIX A

Bismuth Data

$$\tau = 0.505 \text{ dyne-cm/rad}$$

$$a_1 = 4.40 \times 10^{-3} \text{ cm}^2$$

$$a_2 = 4.18 \times 10^{-3} \text{ cm}^2$$

$$q_1 = 0.472 \text{ cm}$$

$$q_2 = 0.490 \text{ cm}$$

$$f_1 = 0.676$$

$$f_2 = 0.617$$

<u>T (°K)</u>	<u>α (rad)</u>	<u>P (mmHg)</u>	<u>$\frac{G}{t} \frac{\text{gm}}{\text{sec}}$</u>	<u>M $\frac{\text{gm}}{\text{mole}}$</u>	<u>P (atm)</u>
850	0.0050	1.41×10^{-3}	6.40×10^{-7}	315.9	1.85×10^{-6}
875	0.0095	2.68×10^{-3}	1.20×10^{-6}	312.9	3.52×10^{-6}
900	0.0175	4.93×10^{-3}	2.20×10^{-6}	310.0	6.48×10^{-6}
925	0.0315	8.87×10^{-3}	3.90×10^{-6}	308.0	1.16×10^{-5}
950	0.0540	1.52×10^{-2}	6.40×10^{-6}	306.0	2.00×10^{-5}
975	0.0890	2.50×10^{-2}	1.04×10^{-5}	303.6	3.29×10^{-5}

<u>T (°K)</u>	<u>β</u>	<u>$\frac{\beta + 1}{\beta^2}$</u>	<u>K_p (atm⁻¹)</u>	<u>P_1 (mmHg)</u>	<u>P_2 (mmHg)</u>
850	0.803	2.795	1.51×10^6	6.32×10^{-4}	7.68×10^{-4}
875	0.851	2.556	7.26×10^5	1.25×10^{-3}	1.43×10^{-3}
900	0.900	2.346	3.62×10^5	2.34×10^{-3}	2.59×10^{-3}
925	0.939	2.214	1.89×10^5	4.27×10^{-3}	4.60×10^{-3}
950	0.980	2.094	1.03×10^5	7.46×10^{-3}	7.74×10^{-3}
975	1.035	1.900	5.76×10^4	1.26×10^{-2}	1.24×10^{-2}

Bismuth Data

$$\tau = 0.415 \text{ dyne-cm/rad}$$

$$a_1 = 9.33 \times 10^{-3} \qquad a_2 = 9.16 \times 10^{-3} \text{ cm}^2$$

$$q_1 = 0.998 \text{ cm} \qquad q_2 = 1.017 \text{ cm}$$

$$f_1 = 0.640 \qquad f_2 = 0.627$$

<u>T(°K)</u>	<u>α (rad)</u>	<u>P (mmHg)</u>	<u>$\frac{G}{t} \frac{\text{gm}}{\text{sec}}$</u>	<u>M $\frac{\text{gm}}{\text{mole}}$</u>	<u>P (atm)</u>
792	0.0050	2.64×10^{-4}	5.54×10^{-7}	324.1	3.47×10^{-7}
808	0.0080	4.22×10^{-4}	8.80×10^{-7}	321.6	5.57×10^{-7}
821	0.0120	6.33×10^{-4}	1.31×10^{-6}	319.9	8.35×10^{-7}
835	0.0180	9.49×10^{-4}	1.96×10^{-6}	318.3	1.25×10^{-6}

<u>T(°K)</u>	<u>β</u>	<u>$\frac{\beta + 1}{\beta^2}$</u>	<u>K_p (atm⁻¹)</u>	<u>p_1 (mmHg)</u>	<u>p_2 (mmHg)</u>
792	0.688	3.570	1.03×10^7	1.08×10^{-4}	1.56×10^{-4}
808	0.721	3.314	5.97×10^6	1.77×10^{-4}	2.45×10^{-4}
821	0.745	3.146	3.78×10^6	2.70×10^{-4}	3.63×10^{-4}
835	0.770	2.985	2.39×10^6	4.13×10^{-4}	5.36×10^{-4}

$$D_0 = 14,800 \text{ cm}^{-1} = 42.3 \text{ kcal/gm mole} \quad (15)*$$

$$v = 172.7 \text{ cm}^{-1} = 5.18 \times 10^{12} \text{ sec}^{-1} \quad (2)$$

$$\sigma = 2.85 \times 10^{-8} \text{ cm} \quad (2)$$

$${}^{\omega}\text{Bi}_2 = 1 \quad (15)$$

$${}^{\omega}\text{Bi} = 4 \quad (15)$$

* These numbers refer to references listed in the Bibliography.

APPENDIX B

Antimony Data

$$\tau = 0.505 \text{ dyne-cm/rad}$$

$$a_1 = 4.40 \times 10^{-3} \text{ cm}^2 \qquad a_2 = 4.18 \times 10^{-3} \text{ cm}^2$$

$$q_1 = 0.472 \text{ cm} \qquad q_2 = 0.490 \text{ cm}$$

$$f_1 = 0.676 \qquad f_2 = 0.617$$

<u>T(°K)</u>	<u>a (rad)</u>	<u>P (mmHg)</u>	<u>$\frac{G}{t} \frac{\text{gm}}{\text{sec}}$</u>	<u>M $\frac{\text{gm}}{\text{mole}}$</u>	<u>P (atm)</u>
775	0.0065	1.83×10^{-3}	1.20×10^{-6}	484.7	2.41×10^{-6}
800	0.00165	4.64×10^{-3}	2.90×10^{-6}	484.0	6.11×10^{-6}
825	0.0365	1.03×10^{-2}	6.40×10^{-6}	483.4	1.35×10^{-5}
850	0.0780	2.20×10^{-2}	1.33×10^{-5}	482.2	2.90×10^{-5}

<u>T(°K)</u>	<u>β</u>	<u>$\frac{\beta + 1}{\beta^2}$</u>	<u>$K_p (\text{atm}^{-1})$</u>	<u>$p_2 (\text{mmHg})$</u>	<u>$p_4 (\text{mmHg})$</u>
775	0.008	1.61×10^4	6.68×10^9	1.45×10^{-5}	1.82×10^{-3}
800	0.009	1.12×10^4	1.83×10^9	4.20×10^{-5}	4.60×10^{-3}
825	0.013	6.02×10^3	4.46×10^8	1.32×10^{-4}	1.02×10^{-2}
850	0.017	3.36×10^3	1.39×10^8	3.68×10^{-4}	2.16×10^{-2}

Antimony Data

$$\tau = 0.415 \text{ dyne-cm/rad}$$

$$a_1 = 9.33 \times 10^{-3} \text{ cm}^2 \qquad a_2 = 9.16 \times 10^{-3} \text{ cm}^2$$

$$q_1 = 0.998 \text{ cm} \qquad q_2 = 1.017 \text{ cm}$$

$$f_1 = 0.661 \qquad f_2 = 0.655$$

<u>T (°K)</u>	<u>α (rad)</u>	<u>P (mmHg)</u>	<u>$\frac{G}{t} \frac{\text{gm}}{\text{sec}}$</u>	<u>M $\frac{\text{gm}}{\text{mole}}$</u>	<u>P (atm)</u>
727	0.0050	2.54×10^{-4}	6.88×10^{-7}	486.3	3.33×10^{-7}
738.5	0.0080	4.06×10^{-4}	1.09×10^{-6}	486.0	5.34×10^{-7}
748.5	0.0120	6.09×10^{-4}	1.63×10^{-6}	485.8	8.01×10^{-7}
759	0.0180	9.14×10^{-4}	2.42×10^{-6}	485.4	1.20×10^{-6}
770	0.0270	1.37×10^{-3}	3.61×10^{-6}	485.0	1.80×10^{-6}

<u>T (°K)</u>	<u>β</u>	<u>$\frac{\beta + 1}{\beta^2}$</u>	<u>$K_p (\text{atm}^{-1})$</u>	<u>$p_2 (\text{mmHg})$</u>	<u>$p_4 (\text{mmHg})$</u>
727	4.5×10^{-3}	5.07×10^4	1.52×10^{11}	1.14×10^{-6}	2.53×10^{-4}
738.5	5.2×10^{-3}	3.79×10^4	7.10×10^{10}	2.10×10^{-6}	4.04×10^{-4}
748.5	5.9×10^{-3}	2.91×10^4	3.63×10^{10}	3.58×10^{-6}	6.06×10^{-4}
759	6.8×10^{-3}	2.16×10^4	1.80×10^{10}	6.17×10^{-6}	9.08×10^{-4}
770	7.7×10^{-3}	1.67×10^4	9.29×10^9	1.05×10^{-5}	1.36×10^{-3}

APPENDIX C

Lead Data

$$\tau = 0.453 \text{ dyne-cm/rad}$$

$$a_1 = 4.40 \times 10^{-3} \text{ cm}^2$$

$$a_2 = 4.18 \times 10^{-3} \text{ cm}^2$$

$$q_1 = 0.472 \text{ cm}$$

$$q_2 = 0.490 \text{ cm}$$

$$f_1 = 0.676$$

$$f_2 = 0.617$$

<u>T (°K)</u>	<u>α (rad)</u>	<u>P (mmHg)</u>	<u>$\frac{G}{\tau} \frac{\text{gm}}{\text{sec}}$</u>	<u>M $\frac{\text{gm}}{\text{mole}}$</u>	<u>P (atm)</u>
900	0.0050	1.27×10^{-3}	9.56×10^{-7}	207.0	1.67×10^{-6}
925	0.0100	2.53×10^{-3}	1.89×10^{-6}	207.2	3.33×10^{-6}
950	0.0190	4.82×10^{-3}	3.53×10^{-6}	207.2	6.33×10^{-6}
975	0.0350	8.87×10^{-3}	6.43×10^{-6}	207.3	1.17×10^{-5}
1000	0.0620	1.57×10^{-2}	1.12×10^{-5}	207.2	2.07×10^{-5}
1025	0.1075	2.72×10^{-2}	1.93×10^{-5}	207.3	3.51×10^{-5}

Lead Data

$$\tau = 0.415 \text{ dyne cm/rad}$$

$$a_1 = 9.33 \times 10^{-3} \text{ cm}^2$$

$$a_2 = 9.16 \times 10^{-3} \text{ cm}^2$$

$$q_1 = 0.998 \text{ cm}$$

$$q_2 = 1.017 \text{ cm}$$

$$f_1 = 0.683$$

$$f_2 = 0.685$$

<u>T (°K)</u>	<u>α (rad)</u>	<u>P (mmHg)</u>	<u>$\frac{G}{t} \frac{\text{gm}}{\text{sec}}$</u>	<u>M $\frac{\text{gm}}{\text{mole}}$</u>	<u>P (atm)</u>
845	0.0050	2.44×10^{-4}	4.01×10^{-7}	207.4	3.21×10^{-7}
867	0.0100	4.88×10^{-4}	7.91×10^{-7}	207.2	6.42×10^{-7}
891	0.0200	9.77×10^{-4}	1.56×10^{-6}	207.2	1.28×10^{-6}
900	0.0260	1.27×10^{-3}	2.02×10^{-6}	207.0	1.67×10^{-6}

APPENDIX D

Sodium Data

$$\tau = 0.453 \text{ dyne-cm/rad}$$

$$a_1 = 4.40 \times 10^{-3} \text{ cm}^2$$

$$a_2 = 4.18 \times 10^{-3} \text{ cm}^2$$

$$q_1 = 0.472 \text{ cm}$$

$$q_2 = 0.490 \text{ cm}$$

$$f_1 = 0.676$$

$$f_2 = 0.617$$

<u>T(°K)</u>	<u>α (rad)</u>	<u>P (mmHg)</u>	<u>$\frac{G}{t} \frac{\text{gm}}{\text{sec}}$</u>	<u>M $\frac{\text{gm}}{\text{mole}}$</u>	<u>P (atm)</u>
518	0.0050	1.27×10^{-3}	4.24×10^{-7}	23.23	1.67×10^{-6}
533	0.0100	2.53×10^{-3}	8.37×10^{-7}	23.29	3.33×10^{-6}
548	0.0195	4.94×10^{-3}	1.61×10^{-6}	23.35	6.50×10^{-6}
563	0.0360	9.12×10^{-3}	2.94×10^{-6}	23.40	1.20×10^{-5}
578	0.0650	1.65×10^{-2}	5.24×10^{-6}	23.47	2.17×10^{-5}

<u>T(°K)</u>	<u>β</u>	<u>$\frac{\beta + 1}{\beta^2}$</u>	<u>K_p (atm⁻¹)</u>	<u>p_1 (mmHg)</u>	<u>p_2 (mmHg)</u>
518	80	1.27×10^{-2}	7.58×10^3	1.25×10^{-3}	1.60×10^{-5}
533	64	1.59×10^{-2}	4.76×10^3	2.49×10^{-3}	3.90×10^{-5}
548	54	1.89×10^{-2}	2.90×10^3	4.85×10^{-3}	9.00×10^{-5}
563	46	2.22×10^{-2}	1.85×10^3	8.93×10^{-3}	1.94×10^{-4}
578	39	2.63×10^{-2}	1.21×10^3	1.61×10^{-2}	4.12×10^{-4}

Sodium Data

$$\tau = 0.415 \text{ dyne-cm/rad}$$

$$a_1 = 9.33 \times 10^{-3} \text{ cm}^2$$

$$a_2 = 9.16 \times 10^{-3} \text{ cm}^2$$

$$q_1 = 0.998 \text{ cm}$$

$$q_2 = 1.017 \text{ cm}$$

$$f_1 = 0.661$$

$$f_2 = 0.655$$

<u>T(°K)</u>	<u>α(rad)</u>	<u>P(mmHg)</u>	<u>$\frac{G}{t} \frac{\text{gm}}{\text{sec}}$</u>	<u>M $\frac{\text{gm}}{\text{mole}}$</u>	<u>P(atm)</u>
486.5	0.0050	2.54×10^{-4}	1.83×10^{-7}	23.07	3.33×10^{-7}
499.5	0.100	5.08×10^{-4}	3.62×10^{-7}	23.09	6.67×10^{-7}
513	0.0200	1.02×10^{-3}	7.16×10^{-7}	23.12	1.33×10^{-6}
518	0.0250	1.27×10^{-3}	8.91×10^{-7}	23.14	1.67×10^{-6}

<u>T(°K)</u>	<u>β</u>	<u>$\frac{\beta + 1}{\beta^2}$</u>	<u>$K_p(\text{atm}^{-1})$</u>	<u>$p_1(\text{mmHg})$</u>	<u>$p_2(\text{mmHg})$</u>
486.5	127	7.93×10^{-3}	2.38×10^4	2.52×10^{-4}	1.98×10^{-6}
499.5	104	9.74×10^{-3}	1.46×10^4	5.03×10^{-4}	4.84×10^{-6}
513	84	1.20×10^{-2}	8.98×10^3	1.01×10^{-3}	1.19×10^{-5}
518	79	1.28×10^{-2}	7.65×10^3	1.25×10^{-3}	1.59×10^{-5}

$$D_0 = 6,148 \text{ cm}^{-1} = 17,568 \text{ kcal/gm mole} \quad (11)$$

$$v = 159.23 \text{ cm}^{-1} = 4.78 \times 10^{12} \text{ sec}^{-1} \quad (15)$$

$$\sigma = 3.078 \times 10^{-8} \text{ cm} \quad (15)$$

$$\omega_{\text{Na}_2} = 1 \quad (15)$$

$$\omega_{\text{Na}} = 2 \quad (15)$$

APPENDIX E

Selenium Data

$$\tau = 0.453 \text{ dyne-cm/rad}$$

$$a_1 = 4.40 \times 10^{-3} \text{ cm}^2 \qquad a_2 = 4.18 \times 10^{-3} \text{ cm}^2$$

$$q_1 = 0.472 \text{ cm} \qquad q_2 = 0.490 \text{ cm}$$

$$f_1 = 0.676 \qquad f_2 = 0.617$$

<u>T (°K)</u>	<u>α (rad)</u>	<u>P (mmHg)</u>	<u>$\frac{G}{t} \frac{\text{gm}}{\text{sec}}$</u>	<u>M $\frac{\text{gm}}{\text{mole}}$</u>	<u>P (atm)</u>
470	0.0050	1.27×10^{-3}	1.90×10^{-6}	428.4	1.67×10^{-6}
480	0.0105	2.66×10^{-3}	3.95×10^{-6}	427.2	3.50×10^{-6}
490	0.0215	5.45×10^{-3}	7.99×10^{-6}	425.7	7.17×10^{-6}
500	0.0355	9.00×10^{-3}	1.30×10^{-5}	423.1	1.18×10^{-5}
510	0.0575	1.46×10^{-2}	2.07×10^{-5}	420.9	1.92×10^{-5}
520	0.0915	2.32×10^{-2}	3.26×10^{-5}	418.1	3.05×10^{-5}

<u>T (°K)</u>	<u>β</u>	<u>$\frac{(\beta + 1)^2}{\beta^3}$</u>	<u>K_p (atm⁻¹)</u>	<u>p_2 (mmHg)</u>	<u>p_6 (mmHg)</u>
470	0.131	5.69×10^2	2.05×10^{14}	1.47×10^{-4}	1.12×10^{-3}
480	0.135	5.24×10^2	4.27×10^{13}	3.16×10^{-4}	2.34×10^{-3}
490	0.139	4.83×10^2	9.41×10^{12}	6.65×10^{-4}	4.78×10^{-3}
500	0.147	4.14×10^2	2.96×10^{12}	1.15×10^{-3}	7.84×10^{-3}
510	0.155	3.58×10^2	9.75×10^{11}	1.96×10^{-3}	1.26×10^{-2}
520	0.163	3.12×10^2	3.36×10^{11}	3.25×10^{-3}	1.99×10^{-2}

Selenium Data

$$\tau = 0.453 \text{ dyne-cm/rad}$$

$$a_1 = 2.02 \times 10^{-3} \text{ cm}^2$$

$$a_2 = 2.04 \times 10^{-3} \text{ cm}^2$$

$$q_1 = 1.014 \text{ cm}$$

$$q_2 = 1.004 \text{ cm}$$

$$f_1 = 0.621$$

$$f_2 = 0.612$$

<u>T(°K)</u>	<u>α (rad)</u>	<u>P (mmHg)</u>	<u>$\frac{G}{t} \frac{\text{gm}}{\text{sec}}$</u>	<u>M $\frac{\text{gm}}{\text{mole}}$</u>	<u>P (atm)</u>
480	0.0100	2.68×10^{-3}	1.78×10^{-6}	427.1	3.52×10^{-6}
490	0.0205	5.49×10^{-3}	3.61×10^{-6}	426.1	7.22×10^{-6}
495	0.0260	6.98×10^{-3}	4.59×10^{-6}	424.8	9.18×10^{-6}
500	0.0335	8.99×10^{-3}	5.88×10^{-6}	423.8	1.18×10^{-5}
505	0.0425	1.14×10^{-2}	7.40×10^{-6}	422.4	1.50×10^{-5}

<u>T(°K)</u>	<u>β</u>	<u>$\frac{(\beta + 1)^2}{\beta^3}$</u>	<u>K_p (atm⁻¹)</u>	<u>p_2 (mmHg)</u>	<u>p_6 (mmHg)</u>
480	0.136	5.16×10^2	4.17×10^{13}	3.21×10^{-4}	2.36×10^{-3}
490	0.139	4.82×10^2	9.26×10^{12}	6.70×10^{-4}	4.82×10^{-3}
495	0.144	4.42×10^2	5.24×10^{12}	8.79×10^{-4}	6.10×10^{-3}
500	0.148	4.05×10^2	2.91×10^{12}	1.16×10^{-3}	7.83×10^{-3}
505	0.152	3.78×10^2	1.68×10^{12}	1.50×10^{-3}	9.90×10^{-3}

Selenium Data

$$\tau = 0.415 \text{ dyne-cm/rad}$$

$$a_1 = 9.33 \times 10^{-3} \text{ cm}^2$$

$$a_2 = 9.16 \times 10^{-3} \text{ cm}^2$$

$$q_1 = 0.998 \text{ cm}$$

$$q_2 = 1.017 \text{ cm}$$

$$f_1 = 0.640$$

$$f_2 = 0.627$$

<u>T(°K)</u>	<u>α (rad)</u>	<u>P (mmHg)</u>	<u>$\frac{G}{\tau} \frac{\text{gm}}{\text{sec}}$</u>	<u>M $\frac{\text{gm}}{\text{mole}}$</u>	<u>P (atm)</u>
450	0.0050	2.64×10^{-4}	8.52×10^{-7}	431.2	3.47×10^{-7}
460	0.0110	5.80×10^{-4}	1.86×10^{-6}	430.0	7.63×10^{-7}
470	0.0240	1.27×10^{-3}	4.01×10^{-6}	428.7	1.67×10^{-6}
480	0.0505	2.66×10^{-3}	8.33×10^{-6}	427.4	3.50×10^{-6}
490	0.1035	5.46×10^{-3}	1.69×10^{-5}	426.3	7.18×10^{-6}

<u>T(°K)</u>	<u>β</u>	<u>$\frac{(\beta + 1)^2}{\beta^3}$</u>	<u>K_p (atm⁻¹)</u>	<u>p_2 (mmHg)</u>	<u>p_6 (mmHg)</u>
450	0.122	7.01×10^2	5.82×10^{15}	2.87×10^{-5}	2.35×10^{-4}
460	0.126	6.11×10^2	1.05×10^{15}	6.49×10^{-5}	5.15×10^{-4}
470	0.131	5.69×10^2	2.05×10^{14}	1.47×10^{-4}	1.12×10^{-3}
480	0.135	5.24×10^2	4.27×10^{13}	3.17×10^{-4}	2.35×10^{-3}
490	0.139	4.83×10^2	9.40×10^{12}	6.66×10^{-4}	4.79×10^{-3}

APPENDIX F

Indium Data

$$\tau = 0.453 \text{ dyne-cm/rad}$$

$$a_1 = 4.40 \times 10^{-3} \text{ cm}^2 \qquad a_2 = 4.18 \times 10^{-3} \text{ cm}^2$$

$$q_1 = 0.472 \text{ cm} \qquad q_2 = 0.490 \text{ cm}$$

$$f_1 = 0.676 \qquad f_2 = 0.617$$

<u>T (°K)</u>	<u>α (rad)</u>	<u>P (mmHg)</u>	<u>$\frac{G}{v} \frac{\text{gm}}{\text{sec}}$</u>	<u>M $\frac{\text{gm}}{\text{mole}}$</u>	<u>P (atm)</u>
1125	0.0060	1.52×10^{-3}	7.64×10^{-7}	114.6	2.00×10^{-6}
1150	0.0105	2.66×10^{-3}	1.32×10^{-6}	114.8	3.50×10^{-6}
1175	0.0180	4.56×10^{-3}	2.24×10^{-6}	114.7	6.00×10^{-6}
1200	0.0300	7.60×10^{-3}	3.70×10^{-6}	114.8	1.00×10^{-5}
1225	0.0490	1.24×10^{-2}	5.97×10^{-6}	114.6	1.63×10^{-5}
1250	0.0790	2.00×10^{-2}	9.54×10^{-6}	114.8	2.63×10^{-5}

Indium Data

$$\tau = 0.415 \text{ dyne-cm/rad}$$

$$a_1 = 9.33 \times 10^{-3} \text{ cm}^2$$

$$a_2 = 9.16 \times 10^{-3} \text{ cm}^2$$

$$q_1 = 0.998 \text{ cm}$$

$$q_2 = 1.017 \text{ cm}$$

$$f_1 = 0.683$$

$$f_2 = 0.685$$

<u>T (°K)</u>	<u>α (rad)</u>	<u>P (mmHg)</u>	<u>$\frac{G}{t} \frac{\text{gm}}{\text{sec}}$</u>	<u>M $\frac{\text{gm}}{\text{mole}}$</u>	<u>P (atm)</u>
1050	0.0050	2.44×10^{-4}	2.68×10^{-7}	114.8	3.21×10^{-7}
1077	0.0100	4.88×10^{-4}	5.30×10^{-7}	114.7	6.42×10^{-7}
1106	0.0200	9.77×10^{-4}	1.04×10^{-6}	114.8	1.28×10^{-6}
1136	0.0400	1.95×10^{-3}	---	---	2.57×10^{-6}

APPENDIX G

The validity of the plots of $\log P$ vs $1/T$ and $\log K_p$ vs $1/T$ in determining the heat of vaporization and heat of dissociation, respectively, depends on a set of conditions which must be satisfied in the system being studied. The conditions are:

- (1) The system is in equilibrium; that is the vapor phase and the condensed phase are in equilibrium with each other so that $\Delta F = 0$.
- (2) The vapor phase behaves as an ideal gas so that $f = P$ (or $f_1 = p_1$, etc.).
- (3) The molal volume of the condensed phase is negligible compared to the molal volume of the vapor phase so that $V = V_v$ (the molal volume of the vapor).
- (4) The heat of vaporization and heat of dissociation are constant with respect to temperature.

The validity of condition (4) above for the systems in this study is due to the fact that the calculated change of the heats of vaporization and dissociation is less than 1.5% over the experimental measuring range.

In the case of the heat of vaporization the relation may be derived by considering the condition of equilibrium between

two phases:

$$F_v = F_L \quad (1)$$

(v and L refer to vapor and liquid), moreover if any change occurs and equilibrium is maintained it is required that

$$dF_v = dF_L \quad (2)$$

The two phases are completely determined by the system variables P and T. Thus the following relations are valid,

$$dF_v = \left[\frac{\partial F_v}{\partial P} \right]_T dP + \left[\frac{\partial F_v}{\partial T} \right]_P dT ; dF_L = \left[\frac{\partial F_L}{\partial P} \right]_T dP + \left[\frac{\partial F_L}{\partial T} \right]_P dT. \quad (3)$$

Then since,

$$\left[\frac{\partial F}{\partial P} \right]_T = V ; \quad \left[\frac{\partial F}{\partial T} \right]_T = -S \quad (4)$$

the relations in equation (4) can be substituted into the equations (3) and combined with equation (2) to give,

$$\left[(V dP)_v - (S dT)_v \right]_{F_v = F_L} = \left[(V dP)_L - (S dT)_L \right]_{F_v = F_L} \quad (5)$$

Since the system is at equilibrium,

$$dP_v = dP_L \text{ and } dT_v = dT_L \quad (6)$$

then equation (5) is rearranged to give,

$$\frac{dP}{dT} = \frac{S_v - S_L}{V_v - V_L} = \frac{\Delta S}{\Delta V} = \frac{\Delta H}{T \Delta V} \quad (7)$$

(since $\Delta S = \frac{\Delta H}{T}$ for a phase change at equilibrium).

If equation (7) is rearranged then:

$$\frac{d(\ln P)}{d(1/T)} = \frac{-(\Delta H)T}{P \Delta V} \quad (8)$$

if condition (3) is applied then:

$$\frac{d(\ln P)}{d(1/T)} = \frac{-(\Delta H)T}{P V} \quad (9)$$

and since the vapor behaves as an ideal gas then equation (6) becomes:

$$\frac{d(\ln P)}{d(1/T)} = \frac{-\Delta H}{R} \quad (10)$$

thus the slope of a plot of $\ln P$ (or $\log P$) vs $1/T$ is a constant, if condition (4) is applied, and from this constant the heat of vaporization (ΔH) may be calculated.

In the case of the heat of dissociation the relation may be derived by starting with the fundamental relation for a system at equilibrium:

$$\Delta F^\circ = -RT \ln K_a \quad (11)$$

By defining the standard state of the vapor as the state where the fugacity $f^\circ = 1$ at each temperature, the activity $a = f$ and since $f = P$ in these systems, $a = P$ and $K_a = K_p$.

For a process which occurs isothermally and at constant pressure (an equilibrium process) the following relation is valid:

$$\frac{d(\Delta F^\circ / T)}{d(1/T)} = \Delta H_d^\circ \quad (12)$$

where ΔH_d° is the heat of dissociation for the standard states of the reactants and products. If equation (11) is now rearranged and differentiated it becomes:

$$\frac{d(\Delta F^\circ / T)}{d(1/T)} = -R \frac{d(\ln K_p)}{d(1/T)} \quad (13)$$

equations (12) and (13) can now be combined to give:

$$\frac{d(\ln K_p)}{d(1/T)} = \frac{-\Delta H^\circ}{R} \quad (14)$$

Thus the slope of a plot of $\ln K_p$ (or $\log K_p$) vs $1/T$ is a constant, if condition (4) is applied, and from this constant the heat of dissociation can be calculated.

APPENDIX H

Errors in Experimental Measurements

The general procedure used in estimating the maximum experimental errors in the measurements is illustrated by the following examples:

(1) The maximum error due to the angle of deflection α will occur when reading the smallest angle of deflection which is 5 scale divisions; the scale can be read to one-half of a division; therefore, the error in reading is one-fourth of a division, thus the maximum error is

$$\frac{\Delta\alpha}{\alpha} = \frac{(1/4)}{5} = 0.05 = 5\%$$

(2) The maximum error due to the torsion constant τ can be estimated from the relation for τ which is

$$\tau = \frac{2\pi^2 m r^2}{t^2};$$

the maximum error for τ is thus,

$$\frac{\Delta\tau}{\tau} = + 2\frac{\Delta r}{r} + 2\frac{\Delta t}{t}$$

(the error in m the mass is insignificant compared to the other quantities); again the maximum occurs at the smallest value of each quantity involved and in this case, the smallest r is 0.508

cm and the maximum error in this value is 0.001 cm thus,

$$\frac{\Delta r}{r} = \frac{0.001}{0.508} = 0.002 \quad ;$$

the smallest t is 7.1 sec and the maximum error in this value is 0.1 sec so that,

$$\frac{\Delta t}{t} = \frac{0.1}{7.1} = 0.0141 \quad .$$

Thus,

$$\Delta T = 0.004 + 0.0282 = 0.0322 = 3.22 \% \quad .$$

(3) The maximum error due to the area of the holes, distance between the suspension point and the holes, and the orifice coefficient is

$$\frac{\Delta(a_1 q_1 f_1 + a_2 q_2 f_2)}{a_1 q_1 f_1 + a_2 q_2 f_2} \quad .$$

The value of this quantity is estimated by calculating the value of $\Delta(a_1 q_1 f_1 + a_2 q_2 f_2)$ using the estimated maximum errors of measurement for each factor in the expression:

$$\begin{aligned} \Delta a_1 &= 1.0 \times 10^{-5} \text{ cm}^2 & , & & \Delta a_2 &= 1.0 \times 10^{-5} \text{ cm}^2 \\ \Delta q_1 &= 1.0 \times 10^{-3} \text{ cm} & , & & \Delta q_2 &= 1.0 \times 10^{-3} \text{ cm} \\ \Delta f_1 &= 0.005 & , & & \Delta f_2 &= 0.005 \quad . \end{aligned}$$

Since $a_1 \approx a_2$, $q_1 \approx q_2$, $f_1 \approx f_2$:

$$\Delta(a_1 q_1 f_1 + a_2 q_2 f_2) \approx (q_1 f_1 + q_2 f_2) \Delta a + (a_1 f_1 + a_2 f_2) \Delta q + (a_1 q_1 + a_2 q_2) \Delta f$$

$$\begin{aligned} \Delta(a_1 q_1 f_1 + a_2 q_2 f_2) &= [(1.014)(0.621) + (1.004)(0.612)](10^{-5}) + \\ &\quad [(2.02 \times 10^{-3})(0.621) + (2.04 \times 10^{-3})(0.612)](10^{-3}) + \\ &\quad [(2.02 \times 10^{-3})(1.014) + (2.04 \times 10^{-3})(1.004)](0.005) \end{aligned}$$

$$\Delta(a_1 q_1 f_1 + a_2 q_2 f_2) = 3.44 \times 10^{-5} \quad .$$

then since the smallest value of $(a_1q_1f_1 + a_2q_2f_2)$ is $2.53 \times 10^{-3} \text{ cm}^3$,

$$\frac{\Delta(a_1q_1f_1 + a_2q_2f_2)}{a_1q_1f_1 + a_2q_2f_2} = \frac{3.44 \times 10^{-5}}{2.53 \times 10^{-3}} = 1.36 \times 10^{-2} = 1.36 \% .$$

(4) The maximum error due to the area of the holes, and the orifice coefficient is calculated in same manner as (3), and

$$\Delta(a_1f_1 + a_2f_2) \simeq (f_1 + f_2)\Delta a + (a_1 + a_2)\Delta f$$

$$\Delta(a_1f_1 + a_2f_2) = (0.621 + 0.612)(10^{-5}) + (2.02 \times 10^{-3} + 2.04 \times 10^{-3})(0.005)$$

$$\Delta(a_1f_1 + a_2f_2) = 3.26 \times 10^{-5}$$

then since the smallest value of $(a_1f_1 + a_2f_2)$ is $2.50 \times 10^{-3} \text{ cm}^2$

$$\frac{\Delta(a_1f_1 + a_2f_2)}{a_1f_1 + a_2f_2} = \frac{3.26 \times 10^{-5}}{2.50 \times 10^{-3}} = 1.30 \times 10^{-2} = 1.30 \% .$$

(5) The maximum error due to the mass effusion rate is

$$\frac{\Delta(G/t)}{G/t} = + \frac{\Delta G}{G} + \frac{\Delta t}{t} .$$

The value of $\Delta G/G$ is obtained from the calibration of the microbalance system,

$$\frac{\Delta G}{G} \simeq 1.32 \% .$$

The values of t (time for full scale deflection of the recorder in the microbalance system) ranged from 100 to 17,700 sec. The maximum error in t is 0.5 sec, thus

$$\frac{\Delta t}{t} = \frac{0.5}{100} = 0.005 = 0.5\%$$

and,

$$\frac{\Delta(G/t)}{G/t} = [(0.0132)^2 + (0.005)^2] = 0.0182 = 1.82 \% .$$

(6) The maximum error due to the temperature is estimated as the sum of instrument error and the errors due to correction of the instrument reading from the calibration curves. The maximum instrument error is 0.1% and the calibration correction error is $\leq 0.1\%$ of the instrument reading, therefore:

$$\frac{\Delta T}{T} \simeq 0.2\% .$$

APPENDIX I

CORRELATION OF K_p VALUES

In the case of bismuth the equilibrium constant K_p is for the equilibrium $2\text{Bi} \rightleftharpoons \text{Bi}_2$, and:

$$\Delta H_d = 2(H)_{\text{Bi}(g)} - (H)_{\text{Bi}_2(g)}$$

but since ΔH_d is a function of temperature,

$$\Delta H_d = (\Delta H_d)_{298} + \int_{298}^T \Delta C_p dT$$

$$\Delta C_p = 2(C_p)_{\text{Bi}(g)} - (C_p)_{\text{Bi}_2(g)} \quad .$$

The specific heats (C_p) of the gases are usually expressed by an equation of the form:

$$C_p = a + bT - cT^{-2}$$

but for gases in this study under the conditions of the system, the temperature dependence of the C_p 's is negligible and $C_p = a$. Thus:

$$\Delta C_p = \Delta a = 2a_{\text{Bi}} - a_{\text{Bi}_2} = 2(4.97) - 8.94 = 1.0 \quad .$$

(The C_p data used here is taken from reference 26.) ΔH_d can now be evaluated:

$$\Delta H_d = (\Delta H_d^\circ)_{298} + \int_{298}^T (1.0) dT = (\Delta H_d^\circ)_{298} + T - 298 \quad .$$

An expression relating K_p to $(\Delta H_d^\circ)_{298}$ can now be derived using the following relations:

$$\left[\frac{d \ln K_p}{dT} \right]_P = \frac{\Delta H_d}{RT^2} = \frac{(\Delta H_d^\circ)_{298} + T - 298}{RT^2}$$

$$R \int d \ln K_p = \int \left[\frac{(\Delta H_d^\circ)_{298}}{T^2} + \frac{1}{T} - \frac{298}{T^2} \right] dT$$

$$R \ln K_p = \frac{-[(\Delta H_d^\circ)_{298} - 298]}{T} + \ln T + C$$

$$R \ln K_p - \ln T = \frac{-[(\Delta H_d^\circ)_{298} - 298]}{T} + C \quad .$$

Similar relations apply to the other elements:

for antimony,

$$\Delta C_p = \Delta a = 2a_{\text{Sb}_2(\text{g})} - a_{\text{Sb}_4(\text{g})} = 2(8.94) - 19.88 = -2.0$$

for sodium,

$$\Delta C_p = \Delta a = 2a_{\text{Na}(\text{g})} - a_{\text{Na}_2(\text{g})} = 2(4.97) - 8.94 = 1.0 \quad .$$

APPENDIX J

SAMPLE CALCULATION OF K_p FOR BISMUTH

The expression for K is:

$$K = \frac{\sigma^2 (4\pi)^{\frac{1}{2}} h}{(m_A k_B T)^{\frac{3}{2}}} \frac{\omega_{Bi_2}}{\omega_{Bi}^2} \frac{e^{D_0/RT}}{(1 - e^{-hv/k_B T})} \quad (8)$$

when the values of the quantities are substituted into equation (8), using a temperature of 850°K:

$$K = \frac{(2.85 \times 10^{-8})^2 (12.56)^{\frac{1}{2}} (6.62 \times 10^{-27})}{[(3.47 \times 10^{-22})(1.38 \times 10^{-16})(850)]^{\frac{3}{2}}} \frac{1}{16} \frac{e^{25.74}}{(1 - e^{-0.292})}$$

$$K = 1.85 \times 10^{-13} \text{ cm}^3$$

The value of K is converted to a K_p value by the relationship:

$$K_p = \frac{K}{k_B T} = \frac{1.85 \times 10^{-13}}{(1.38 \times 10^{-16})(850)} = 1.58 \frac{\text{cm}^2}{\text{dyne}}$$

$$K_p = (1.58 \frac{\text{cm}^2}{\text{dyne}})(1.013 \times 10^6 \frac{\text{dyne}}{\text{cm}^2 - \text{atm}}) = 1.60 \times 10^6 \text{ atm}^{-1}$$